

PRATT AND WHITNEY AIRCRAFT GROUP WEST PALM BEACH FL 0--ETC F/G 21/2  
AUGMENTOR STABILITY MANAGEMENT PROGRAM USER'S MANUAL. (U)

F33615-79-C-2059

PWA-FR-15323

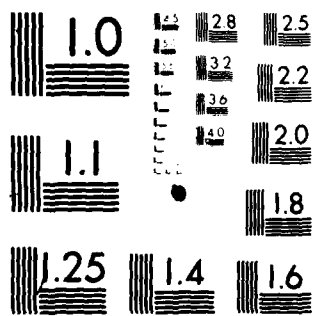
AFWAL-TR-81-2113

NL

$$1 + \frac{2}{\Delta_1 + \Delta_2}$$

■

ADA  
1774



MICROCOPY RESOLUTION TEST CHART  
NATIONAL BUREAU OF STANDARDS-1963-A

12



AFWAL-TR-81-2113

AP A 11 7 749

# **AUGMENTOR STABILITY MANAGEMENT PROGRAM USER'S MANUAL**

**R. Ernst  
Pratt & Whitney Aircraft Group  
Government Products Division  
Division of United Technologies Corporation  
P.O. Box 2691, West Palm Beach, Florida 33402**

**November 1981**

**Final Report for Period 1 September 1979 Through 1 September 1981**

**Approved for Public Release; Distribution Unlimited**

DTIC FILE COPY

**Air Force Aero Propulsion Laboratory  
Air Force Wright Aeronautical Laboratories  
Air Force Systems Command  
Wright-Patterson Air Force Base, Ohio 45433**

**DTIC  
ELECTE  
S AUG 0 3 1982  
E**

**82 08 03 014**

## NOTICE

When Government drawings, specifications, or other data are used for any purpose other than in connection with a definitely related Government procurement operation, the United States Government thereby incurs no responsibility nor any obligation whatsoever; and the fact that the government may have formulated, furnished, or in any way supplied the said drawings, specifications, or other data, is not to be regarded by implication or otherwise as in any manner licensing the holder or any other person or corporation, or conveying any rights or permission to manufacture use, or sell any patented invention that may in any way be related thereto.

This report has been reviewed by the Officer of Public Affairs (ASD/PA) and is releasable to the National Technical Information Service (NTIS). At NTIS, it will be available to the general public, including foreign nations.

This technical report has been reviewed and is approved for publication.

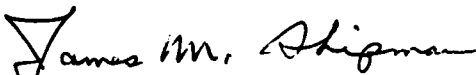


RUTH L. SIKORSKI  
Project Engineer



JACK RICHENS  
Acting Chief, Components Branch  
Turbine Engine Division

FOR THE COMMANDER



JAMES M. SHIPMAN, Major, USAF  
Deputy Director  
Turbine Engine Division  
Aero Propulsion Laboratory

"If your address has changed, if you wish to be removed from our mailing list, or if the addressee is no longer employed by your organization please notify AFWAL/POTC, W-PAFB, OH 45433 to help us maintain a current mailing list."

Copies of this report should not be returned unless return is required by security considerations, contractual obligations, or notice on a specific document.

## UNCLASSIFIED

SECURITY CLASSIFICATION OF THIS PAGE (When Data Entered)

REPORT DOCUMENTATION PAGE		READ INSTRUCTIONS BEFORE COMPLETING FORM
1. Report Number AFWAL-TR-81-2113	2. Govt Accession No. AD-A117749	3. Recipient's Catalog Number
4. Title (and Subtitle) AUGMENTOR STABILITY MANAGEMENT PROGRAM USER'S MANUAL		5. Type of Report & Period Covered User's Manual 1 Sept 1979 to 1 Sept 1981
		6. Performing Org. Report Number FR-15323
7. Author(s) R. C. Ernst		8. Contract or Grant Number(s) F33615-79-C-2059
9. Performing Organization Name and Address United Technologies Corporation Pratt & Whitney Aircraft Group Government Products Division P.O. Box 2691, West Palm Beach, FL 33402		10. Program Element, Project, Task Area & Work Unit Numbers P. E. 62203F, 30660530, 30660535
11. Controlling Office Name and Address Air Force Wright Aeronautical Laboratories AFAPL/TBC, WPAFB Ohio 45433		12. Report Date November 1981
14. Monitoring Agency Name & Address (if different from Controlling Office) Air Force Aero Propulsion Laboratory (AFAPL/TBC) Wright-Patterson AFB, Ohio 45433		13. Number of Pages 105
		15. Security Class. (of this report) UNCLASSIFIED
		15a. Declassification/Downgrading Schedule
16. Distribution Statement (of this Report)  APPROVED FOR PUBLIC RELEASE; DISTRIBUTION UNLIMITED.		
17. Distribution Statement (of the abstract entered in Block 20, if different from Report)		
18. Supplementary Notes		
19. Key Words (Continue on reverse side if necessary and identify by block number) Flameholder Combustion Stability Augmentors Afterburner Combustion Efficiency Turbofan		
20. Abstract (Continue on reverse side if necessary and identify by block number) This report describes the computer code and the models used to form the computer code used to analyze low frequency augmentor instability (rumble). Rumble occurs mainly at high fuel-air ratios and at flight Mach numbers and altitudes where low duct inlet air temperatures and pressures exist. Complete description of the models and the program responsible for their development is contained in AFWAL-TR-81-2113.		

DD FORM 1 JAN 73 1473

EDITION OF 1 NOV 65 IS OBSOLETE

UNCLASSIFIED

SECURITY CLASSIFICATION OF THIS PAGE (When Data Entered)

## FOREWORD

This report was prepared in accordance with Contract F33615-79-C-2059, Project Number 3066, titled Augmentor Stability Management Program. The work was conducted under the direction of Lt. D.J. Bess and Ms. R.L. Sikorski, Project Engineers, POTC of the Air Force Wright Aeronautical Laboratories. This report presents the User's Manual for the augmentor stability digital computer program developed by Pratt & Whitney Aircraft Group, Government Products Division of United Technologies Corporation, P.O. Box 2691, West Palm Beach, Florida, 33402. The contents were performed during the period 1 September 1979 through 1 August 1981 and were submitted for approval 1 September 1981. The principal contributors were E.A. Petrino, T.W. Miller and M.R. Glickstein, under the direction of R.C. Ernst, Program Manager for the Pratt & Whitney Aircraft Group.

Accession For	
NTIS GRA&I	<input checked="" type="checkbox"/>
DTIC TAB	<input type="checkbox"/>
Unannounced	<input type="checkbox"/>
Justification	
By	
Distribution/	
Availability Codes	
Dist	Avail and/or Special
A	



## TABLE OF CONTENTS

<i>Section</i>	<i>Page</i>
I INTRODUCTION.....	1
II TECHNICAL DISCUSSION.....	3
1. Augmentor Description.....	3
2. Rumble Model Program Description.....	4
3. Flameholder Combustion Model Program Description.....	8
4. Sprayring Model Program Description.....	18
5. Program Setup.....	27
6. Program Performance Options.....	29
7. Input.....	31
8. Output.....	47
9. Program Messages and Limits.....	56
10. Program Listings.....	65
11. Test Cases.....	66
12. Program Identification and Revision Procedure.....	67
APPENDIX A — Development of Rumble Model Equations.....	69
APPENDIX B — Development of Flameholder Combustion Model Equations.....	89

## ILLUSTRATIONS

<i>Figure</i>		<i>Page</i>
1	Combined Model Overview.....	1
2	V-Gutter Augmentor.....	3
3	Rumble Model Flow Diagram.....	6
4	Rumble Model Plotted Computer Output.....	7
5	"Feedback Loop" Visualization of Rumble Model.....	8
6	Location of a Core Streamtube in a Turbofan Engine Augmentor.....	10
7	Single Streamtube Logic Map.....	10
8	Duct Stream Flameholder Wake Solution.....	13
9	Location of Typical Fan Duct Streamtube.....	14
10	Single Streamtube Geometry and Flow Inputs — Fan.....	15
11	External Heat Addition to Fan Duct Gutters.....	16
12	Schematic of Spraybar Showing Fluid Regimes.....	19
13	Flow Logic for Augmentor Fuel System Model.....	21
14	Schematic of Sprayring.....	22
15	Sprayring Pressure vs. Time.....	23
16	Comparison of Fuel Flow Into and Out of Sprayring.....	23
17	Location of Fuel/Air Interface in Sprayring.....	24
18	Distribution Valve Schematic.....	25
19	Zone Flowrate Schedule.....	26
20	Sprayring — Flameholder Geometric Compatibility.....	27
21	Flameholder and Sprayring Relationship.....	28
22	Combined Model Input Requirements Attachment.....	32
23	Inputs Required for Various Run Options.....	33
24	Rumble Model Geometry Identification.....	34
25	Flameholder Combustion Model Geometry Schematic.....	35



26	Combined Rumble Model Input Setup.....	44
27	Parameter Identification Numbers.....	45
28	Computer Simulation Change Notice.....	68
29	Rumble Model Station Identification.....	70
30	Steps in Augmentor Combustion Process.....	82
31	Ideal Temperature Rise for Constant Pressure Combustion of Hydrocarbon Fuels.....	86
32	Location of a Core Streamtube in a Turbofan Engine Augmentor.....	90
33	Variation in Activation Energy with Inlet Temperature and Equivalence Ratio.....	95
34	External Heat Addition to Fan Duct Gutters.....	96
35	Schematic of Flame Spreading Analysis.....	98
36	Flame Speed for Monodisperse Tetralin Spray.....	100
37	Fictitious Temperature Rise vs. Main Burner Fuel-Air Ratio.....	104

# LIST OF SYMBOLS

<u>English Symbol</u>	<u>Definition</u>	<u>Typical Units</u>
A	Area	in. <sup>2</sup>
A	Stirred reactor mass loading	gm-mole/sec
A	Dummy variable in eqn. (128)	d'less
a	Reaction index in eqn. (111)	d'less
As	Surface area	sq in.
BPR	Bypass ratio	d'less
B/D	Wake width per unit flameholder	d'less
C	Activation energy constant in eqn. (111)	°K
c	Sonic velocity	in/sec
C <sub>d</sub>	Drag coefficient	d'less
C <sub>p</sub>	Specific heat at constant pressure	Btu/lbm/°R
C <sub>v</sub>	Specific heat at constant volume	Btu/lbm/°R
C <sub>v</sub>	Wake shape factor	litre/in. <sup>2</sup>
C <sub>1</sub>	Dummy variable in eqn. (85)	d'less
d	Diameter	in.
D <sub>v</sub>	Diffusion coefficient	in. <sup>2</sup> /sec
FA	Fuel-air ratio	d'less
H	Enthalpy	Btu/lbm
h <sub>f</sub>	Film coefficient	Btu/in. <sup>2</sup> /sec/°R
k	Reaction rate in eqn. (107)	d'less
k	Thermal conductivity in eqn. (91)	Btu/in./sec°R
K	Dummy variable in eqn. (71)	d'less
K <sub>1</sub>	Recirculation coefficient	d'less
L/D	Wake length per unit flameholder width	d'less
m	Mass	lbm
m	Mass flowrate	lbm/sec
M	Mach number	d'less
MW	Molecular weight	lbm/lb-mole
n	Reaction order in eqn. (107)	d'less
N	Flameholder width	in.
Nu	Nusselt number	d'less
p	Pressure	lbf/in. <sup>2</sup>
Δp	Pressure drop	lbf/in. <sup>2</sup>
PFSR	Sprayring fuel pressure	lbf/in. <sup>2</sup>
Pr	Prandtl number	d'less
q	Volumetric heat release rate	Btu/sec/in. <sup>3</sup>
q	Heat flux	Btu/in. <sup>2</sup> sec
R	Gas constant	ft-lbf/lbm/°R
Re	Reynold's number	d'less
S	Entropy	Btu/lbm/°R
St	Turbulent flame speed	ft/sec
S <sub>1</sub>	Laminar flame speed	ft/sec
T	Temperature	°F, °R, °K
T <sub>i</sub>	Ideal temperature	°R
t	Time	sec
TFSR	Sprayring fuel temperature	°F
U	Flameholder lip velocity	ft/sec
u	Internal energy	Btu/lbm/°R
u	RMS turbulence velocity fluctuation	ft/sec

## LIST OF SYMBOLS (CONTINUED)

<u>English Symbol</u>	<u>Definition</u>	<u>Typical Units</u>
V	Velocity	ft/sec
V <sub>0</sub>	Wake volume	litre
W	Duct width	in.
W	Mass flowrate	lbm/sec
WCOOL	Liner cooling flow/total engine flow	d'less
X	Axial distance	in.
$\Delta x$	Distance	in.
y	Stoichiometry factor in eqn. (108)	d'less
$\Delta y$	Flame penetration distance	in.
z	Defined in eqn. (76)	d'less
Z	Defined in eqn. (125)	d'less

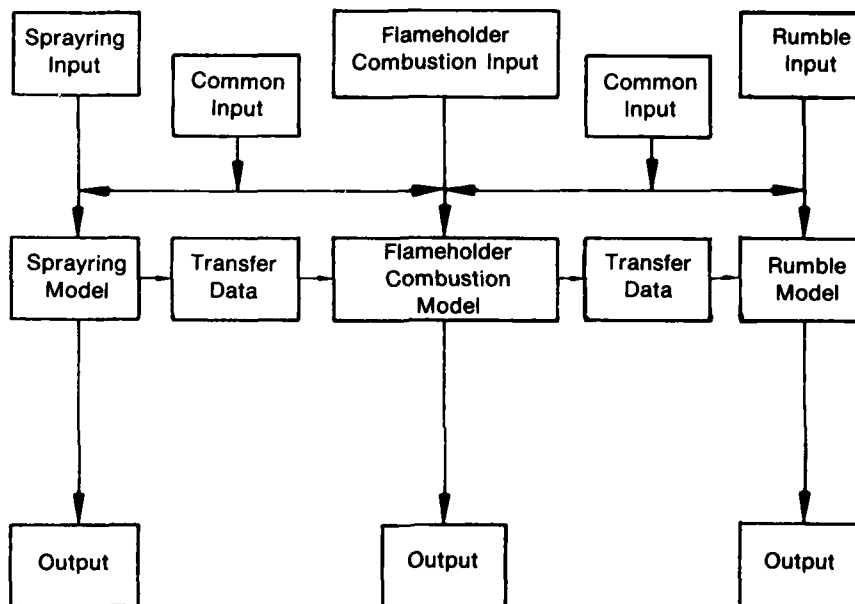
<u>Greek Symbol</u>	<u>Definition</u>	<u>Typical Units</u>
$\alpha$	Flameholder apex angle	deg
$\beta$	Defined in eqn. (75)	d'less
$\beta_1$	Droplet vaporization coefficient	d'less
$\beta_2$	Droplet collective coefficient	d'less
$\beta_3$	Surface vaporization coefficient	d'less
$\Gamma$	Blockage ratio	d'less
$\gamma$	Ratio of specific heats	d'less
$\epsilon$	Wake reaction efficiency	d'less
$\epsilon_0$	Turbulence intensity	d'less
$\eta$	Efficiency	d'less
$\lambda$	Latent heat or vaporization	Btu/lbm
$\mu$	Viscosity	lbf/in.
X <sub>o</sub>	Oxygen concentration	gm-mole/litre
X <sub>o2</sub>	Oxygen volume fraction	d'less
X <sub>f</sub>	Fuel concentration	gm-mole/litre
$\rho$	Density	lbm/in. <sup>3</sup>
$\tau$	Wake residence time	sec
$\tau'$	Normalized residence time	d'less
$l$	Axial length between stations	in.
$\delta$	Ratio of specific heats	d'less
$\tau$	Sonic travel time	sec

### Special Symbol:

$\Delta$	Finite difference
----------	-------------------

## SECTION I INTRODUCTION

Pratt & Whitney Aircraft Group Customer Computer Deck (CCD 1144-0.0) is a three-part program consisting of: (1) Spraying Model — an analytical model that will predict the fuel injection characteristics of turbofan sprayings or spraybars, (2) Flameholder Combustion Model — an analytical model that will predict the steady-state combustion field for a turbofan augmentor, and (3) Rumble Model a dynamic analytical model that will predict the rumble stability limits of turbofan augmentors. The models may be exercised independently of each other or sequentially to supply data from (1) to (2) to (3). The operating sequence is shown in Figure 1.



FD 223798

Figure 1. Combined Model Overview

The objective of the spraying model is to predict the fuel flowrate distribution from a specified fuel injector into the turbofan augmentor. It is capable of transient analysis to evaluate augmentor throttle excursions. The objective of the flameholder combustion model is to predict the augmentor heat release process for a specified geometry and operating point in a turbofan engine. The rumble model objective is to predict the conditions under which the specified turbofan augmentor will experience low frequency instability (rumble). Since the dynamic analysis is linear in nature, the models predict rumble onset but not amplitude.

The user may execute any one of the three models independently of the others. If the spraying model is not executed, the fuel-air ratio distribution must be user input to the combustion model. If the combustion model is not executed, then the combustion data must be user input to the rumble model.

2 -

The User's Manual describes the combined models and how to use the computer program to predict: (1) fuel system behavior, (2) augmentor combustion characteristics, and (3) turbofan engine low frequency instability (rumble) limits. To assist in checking out the CCD at the user facility, the following items are included:

- Program Listings
- Test Case Input
- Test Case Output

## SECTION II TECHNICAL DISCUSSION

### 1. AUGMENTOR DESCRIPTION

Afterburning is a method by which the maximum thrust capability of a basic engine may be augmented by an additional 50 percent, or more. Fundamentally, an augmentor (afterburner) is a ramjet engine attached to the turbine exhaust case of a turbojet or turbofan engine. The gases discharged from the turbine of the basic engine have sufficient velocity at the higher thrust settings to satisfy ramjet requirements, regardless of whether the aircraft is in a steep dive or standing still at the end of a runway.

The basic augmentor (V-gutter), Figure 2, consists of only four fundamental parts: the afterburner duct, the fuel nozzles or spraybars, the flameholders, and a two-position or variable area nozzle. Because the exhaust nozzle area requirements vary significantly depending on whether or not the augmentor is operating, a variable area exhaust nozzle is incorporated.

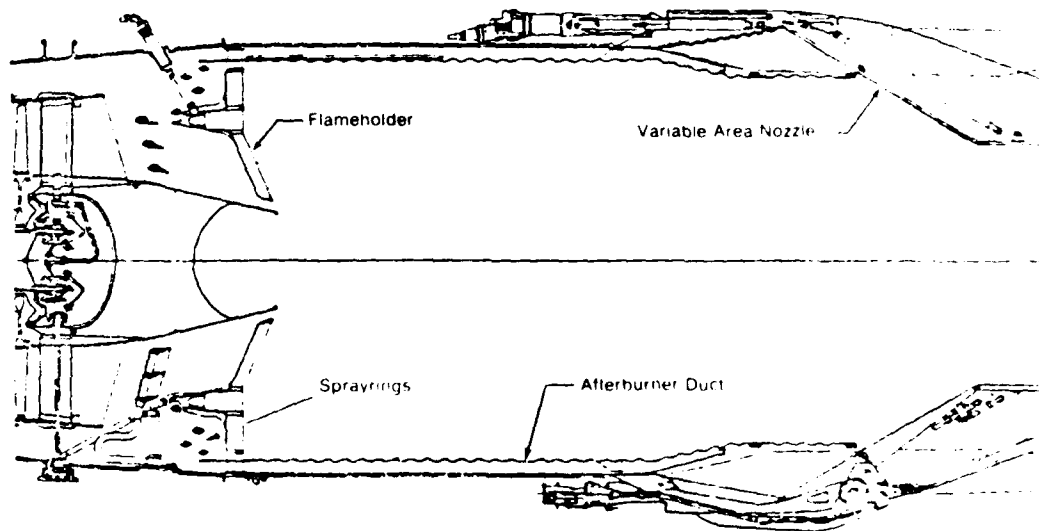


Figure 2. V-gutter Augmentor

Thrust modulation in the afterburning mode is accomplished by varying the flow of fuel to the augmentor. However, in order to maintain good combustion efficiency in the augmentor over a wide range of fuel-air ratios, the augmentor is separated into fuel supply "zones" or segments, for best fuel distribution.

The afterburner duct must be of such proportion that stable combustion can be maintained during augmentor operation. This requires a burning section of sufficient cross-sectional area to ensure that the gas velocity through the augmentor does not exceed the rate of flame propagation. Otherwise, the flame would not be able to establish a firm foothold because the onrushing turbine exhaust gases would push the burning mixture right out of the exhaust nozzle. Fuel is introduced through a series of perforated spraybars located inside the forward section of the afterburner duct. Not far aft of these, flameholders are provided to help

create local turbulence and to reduce the gas velocity in the vicinity of the flame. The flameholders may take the form of concentric rings or radial arms of an angular "V" cross section, hence the name V-gutter augmentor.

## **2. RUMBLE MODEL PROGRAM DESCRIPTION**

### **a. General**

The augmentor math model consists of a set of time dependent equations describing the longitudinal dynamics of the flowing airstream and the axially distributed combustion process in the augmentor, coupled with a solution technique for determining stability. These equations are linearized, through the assumption of small perturbations, and transformed from the time domain to the Laplace transform "S" domain. The solution technique is based upon the Nyquist stability criterion and consists of determining whether the time response of the system to a small disturbance would display oscillatory behavior with a growing amplitude. The result is a determination of stability at a given operating point, regions of operation which will cause rumble, and changes to the augmentor to make it rumble-free.

### **b. Modeling Approach**

Since rumble has long been associated with the relatively low-frequency longitudinal, or axial, modes of vibration of the air column in the augmentor, the model was formulated to take only the longitudinal dimension into account. Accordingly, each station in the model was considered to represent a plane over which the value of any parameter (such as velocity, pressure or density) could be considered as uniform at any instant in time.

Motion pictures of rumble have shown a change in color of the burning gas during a cycle of oscillation, indicating that alternate hotter and cooler combustion products were being produced. These hot and cold combustion products could be seen drifting from the flameholder to the exhaust nozzle in a time span which matched, or was a multiple of, the period of oscillation of the rumble. Since flowrate out through the nozzle is dependent upon the temperature of the entering gas, it was important that the model treat the traveling combustion products, which were mathematically identified as traveling entropy waves.

The equations developed for describing rumble can be classified into two types. First, there are the momentum, continuity and energy equations, together with the boundary conditions, which describe how each parameter at any station in the augmentor responds to a disturbance in combustion heat release. These are referred to as the acoustic equations. Secondly, there are the combustion equations which describe how combustion heat release responds to variations in the system parameters such as velocity, pressure and density. Together, the acoustic equations and the combustion equations describe the rumble mechanism, by which a disturbance in combustion causes a disturbance in velocity, pressure and density throughout the augmentor which in turn causes a disturbance in combustion. A description of the equations, boundary conditions and assumptions is presented in Appendix A.

Since the purpose of the program was to develop an understanding of the rumble mechanism and demonstrate that the onset of rumble could be predicted, thereby defining the boundary between stable and unstable operating regions, it was necessary only to model the augmentor for the first few increments of time before the oscillation had built up into an appreciable amplitude. This allowed use of a small perturbation technique which led to linear equations and mathematical simplification. Linear equations can describe the system for small oscillation amplitudes and can predict whether the system initially at rest would begin to oscillate. Because the nonlinearities associated with large amplitude oscillations (which eventually stop the amplitude from growing) were ignored, the linear equations do not allow a prediction of the final limit-cycle amplitude.

### c. Model Description

The rumble model was designed for simple input-output and requires no intermediate engineering interpretation, Figure 3. The input requires engine geometry and pressures, temperatures and Mach numbers, obtained from engine steady-state cycle tables. The user may select to input augmentor fuel-air ratio and empirical combustion data or he may exercise the flameholder combustion model which calculates and supplies the required augmentor combustion data to the rumble model. An input option allows the user to specify the specific augmentor types (V-gutter, Vorbix or Swirl) to be used. No calculation or dynamic information is required. The user may select either tabular and plotted output or only plotted output, as shown in Figure 4. From the plot the user identifies the frequencies at which the phase is zero. He then checks the gain at each of the identified frequencies. If the gain is one or greater, the program has predicted that rumble will occur. If the gain is less than one, the program has predicted that the operating point is stable. For example, Figure 4 indicates rumble at 60 Hz and at 140 Hz. The user can then change geometry or operating point inputs and repeat the process to determine the effects of the change. This form of output was chosen because it facilitated development of the model, yielded a compact, easy to interpret answers, and made better use of computer time than a time-domain solution.

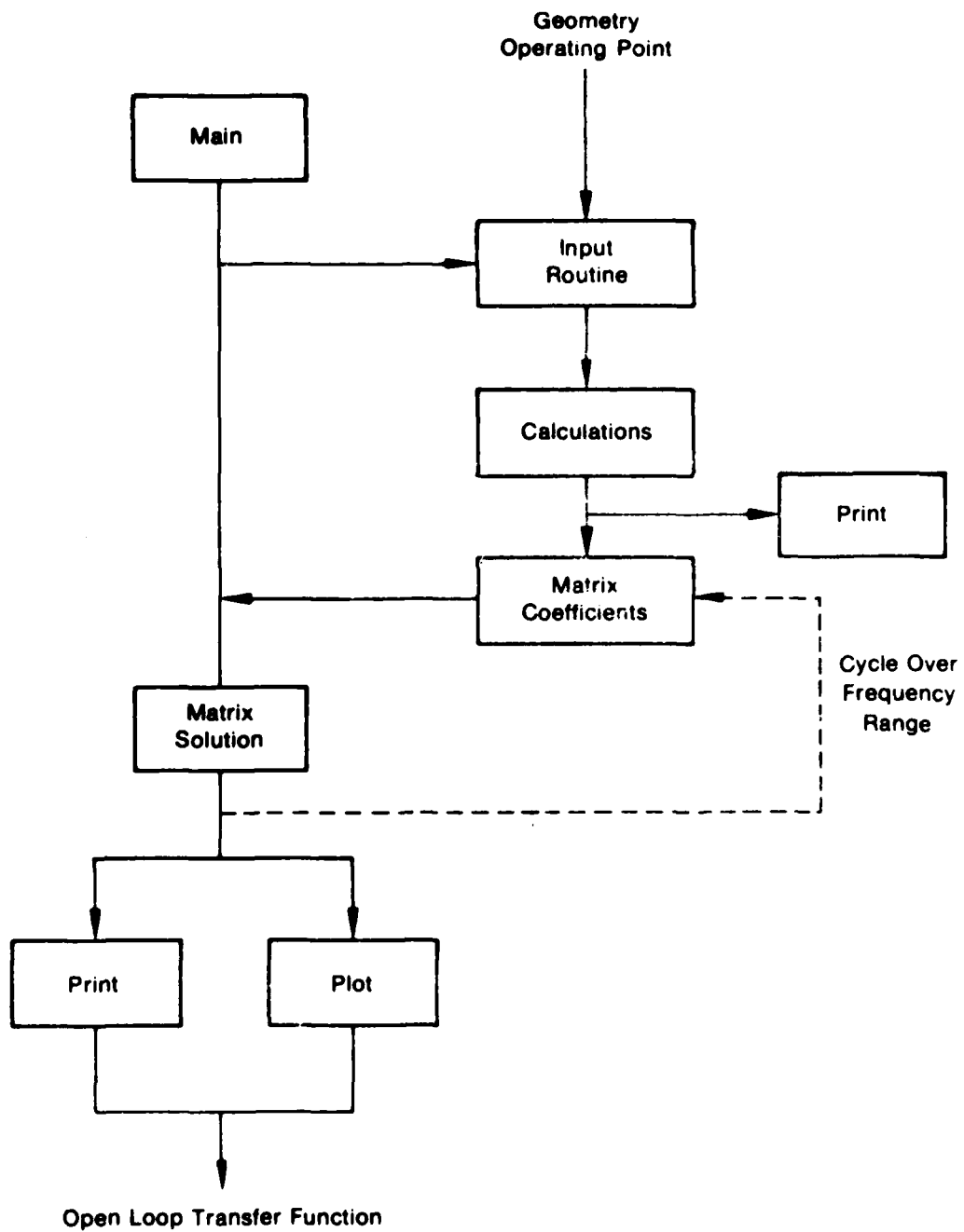
To model rumble required a transient description of the longitudinal dynamics of a turbofan engine. To computerize the formulation, the mathematical description was simplified by restricting the range of validity of the equations to small perturbations about a mean steady-state operating point. This allowed linearization of the equations to a form which correctly describes small scale transients, but in which the nonlinear terms which are important in large scale transients could be omitted. The resultant linearized equations describe the initial period of the time when rumble oscillations begin to grow and are valid to the point where the rumble amplitude reaches values at which the nonlinear terms become important. This is sufficient to determine whether an engine, if placed at a given operating point, will spontaneously bloom into rumble.

The model could have been made to yield solutions in the time-domain by programming the equations on an analog computer. The output would have been a time trace of any selected parameter (e.g., augmentor pressure). At a stable operating point the trace would be a straight line, whereas at an unstable operating point the trace would show a sinusoidal oscillation with an increasing amplitude. The amplitude would grow without bound for as long as the solution continued, because of the omission of the nonlinear terms.

The same information can be more easily obtained by a nontime-domain solution technique. Such a technique was chosen for the rumble model. Commonly called the Nyquist criterion, it is based upon the fact that the allowable forms of the time domain solution are known. This technique allows use of a matrix program which can quickly solve large numbers of simultaneous equations.

The Nyquist criterion is a procedure which makes use of the Laplace transform and conformal mapping to determine whether the transient solution would show unstable behavior. To apply the criterion, the time-domain equations are transformed into the Laplace "S" domain. The result is a square homogenous matrix. The determinant of the matrix coefficients is a function of "S", called the characteristic function, and contains all of the information needed to determine whether the system being described is stable or unstable. If all zeros of the characteristic function have negative real parts, the system is stable; if any zeros have positive real parts, the system is unstable. Conformal mapping is used to examine the characteristic function for the presence of zeros with positive real parts.





FD 146452

Figure 3. Rumble Model Flow Diagram

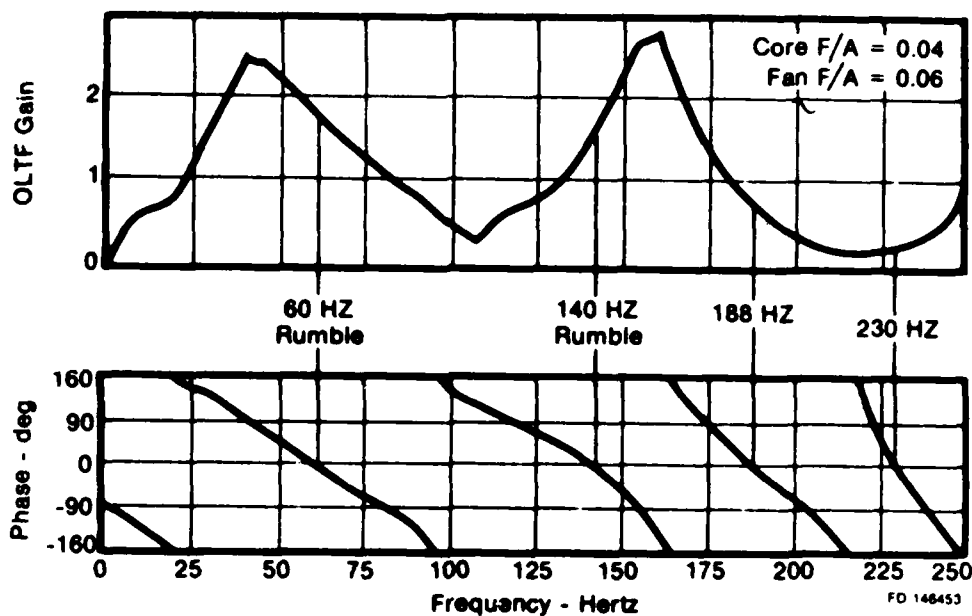
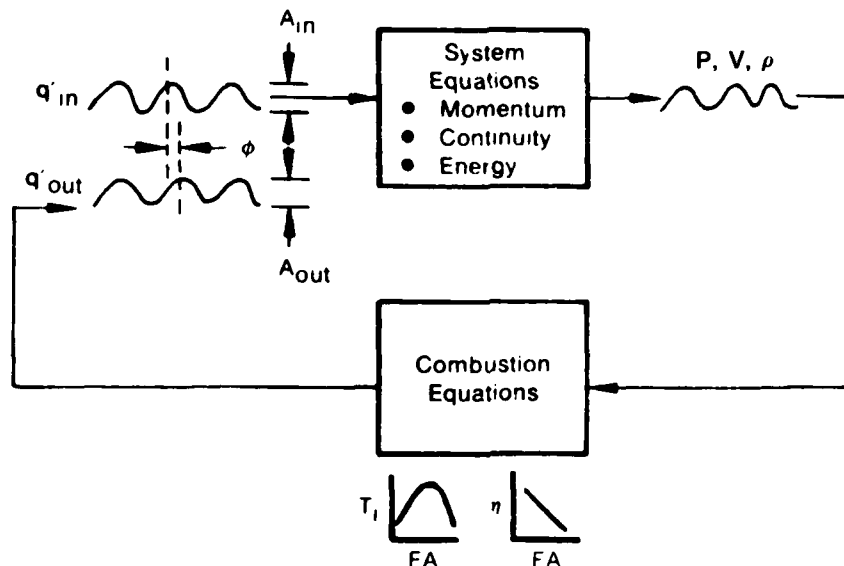


Figure 4. Rumble Model Plotted Computer Output

To accomplish the conformal mapping the equations which describe the augmentor were written to describe a "feedback loop." The feedback loop was formed for the rumble model by considering that the combustion rate, called  $q'_{in}$  was an "input" to the acoustic equations. This yielded as "output" the pressure, velocity and density at each station throughout the engine. The "output" was then considered to feedback through the combustion equations to form a "feedback" combustion heat release rate, called  $q'_{out}$ . The resultant "loop" is shown in Figure 5. Actually, only one heat release rate is present. The use of the two names  $q'_{in}$  and  $q'_{out}$  allows the formation of the ratio  $q'_{out}/q'_{in}$ , called the "Open Loop Transfer Function" (OLTF). Conformal mapping to examine the zeros of the characteristic function is carried out by using the OLTF.

Referring to Figure 5, the heuristic argument can be made that if a loop is subjected to an externally supplied sinusoidal input ( $q'_{in}$ ) and it returns a feedback ( $q'_{out}$ ) which is in phase with the input ( $\phi = 0$ ) and of equal amplitude (gain = 1), then the externally supplied input could be removed and the loop would continue to oscillate. A gain greater than one then implies that the loop would be driven to even higher amplitude, while a gain less than one implied that the oscillations would die out once the input was removed. The model determines whether the time solution, if calculated would display oscillatory behavior with a growing amplitude. It does this through a solution technique which is simpler and faster to apply than a solution in the time-domain.



• Unstable if at Some Frequency:  $A_{out} = A_{in}$  and  $\phi = 0$

5-114486-1

Figure 5. "Feedback Loop" Visualization of Rumble Model

### 3. FLAMEHOLDER COMBUSTION MODEL PROGRAM DESCRIPTION

#### a. General

The combustion model performs a multistreamtube analysis of the flame stabilization and propagation phenomena in a turbofan augmentor. The augmentor is divided into a multitude of equivalent two-dimensional streamtubes with a single flameholder element in each. The program evaluates each streamtube and then mass averages the results.

For each streamtube the program proceeds from the augmentor inlet towards the exhaust nozzle and evaluates each step in the stabilization and propagation of the augmentor process. The ultimate result is the level of combustion efficiency in that streamtube. The program then performs a small perturbation in velocity, pressure, inlet temperature and fuel-air ratio to evaluate the efficiency slopes.

The final outputs are the fan duct efficiency, the core stream efficiency and the efficiency slopes with respect to the four perturbed variables.

#### b. Modeling Approach

The approach taken for each streamtube is a step-by-step solution to the physical phenomena which determine the flame stability limits of the spraybar-flameholder configuration and the subsequent turbulent flame propagation rate. These phenomena include liquid fuel injection, droplet formation, vaporization, fuel impingement onto the flameholder, wake reaction kinetics and turbulent flame penetration.

The approach used is different for the fan duct streamtubes and the core streamtubes. The necessity for different approaches lies in the degree of liquid fuel vaporization between the spraybar and the flameholder. In the core streamtubes, the fuel is virtually totally vaporized in the first few inches by the hot turbine exhaust flow. In the fan duct stream, the much cooler airflow results in only a slight degree of vaporization in the four to six inches typical spraybar to flameholder distance.

The core stream analysis is thus done assuming that the fuel at the flameholder is in the vapor phase and the flameholder wake fuel-air ratio is the same as the total fuel-air ratio. This value is used in the kinetics analysis of the wake reaction to evaluate the stability limits.

In the fan duct streamtubes, however, the low level of droplet vaporization yields a vapor phase fuel-air ratio at the flameholder which is well below the lean limit for hydrocarbon fuels. Since the liquid fuel droplets are not capable of entering the flameholder recirculation wake due to their excessive momentum, there must be some other mechanism to provide the necessary wake vapor fuel for stable combustion.

This mechanism in the fan duct streamtubes is the collection of the liquid fuel droplets onto the surface of the flameholders and the vaporization of the resultant liquid film. This evolved vapor recirculates into the flameholder wake with a portion of the droplet evolved vapor fuel to generate the wake vapor fuel concentration.

The streamtube analyses compute the degree of wake reaction at the level of vapor fuel-air ratio appropriate to the streamtube type and approach conditions. For the fan duct cases, this requires a convergent solution between the wake kinetics and the surface vaporization.

Once the flameholder wake reaction is evaluated, the analysis computes the rate of flame penetration into the free-stream as a turbulent flame sheet. This rate is adjusted by the wake reaction level to account for the ignition response in the recirculation zone shear layers. The flame penetration rate is integrated over the available augmentor length to provide the level of streamtube efficiency.

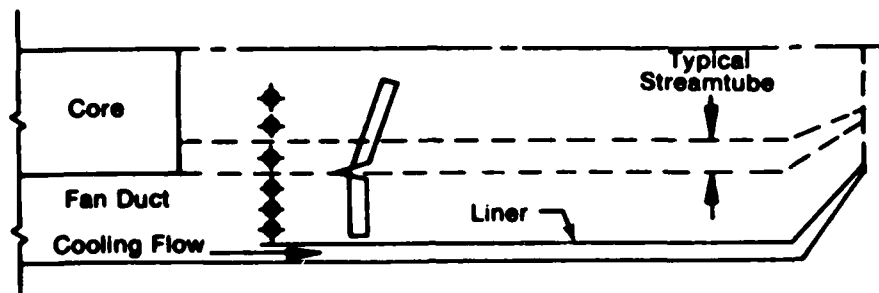
The program thus performs a quantitative evaluation of the phenomenological processes which occur in the turbofan augmentor. The individual calculations are a combination of analytical evaluations and empirical results as required to ensure quantitative accuracy.

### **c. Model Description**

The combustion model was designed as a complete unit. The program does not require on-line engineering interaction. The combustion model may be run as a separate entity or as a generator for subsequent stability analysis with the rumble model. When exercised alone, the combustion model is an augmentor analysis program and the output is a comprehensive description of the injection, stabilization and flame propagation processes. In this mode, the program is useful as a design tool for conventional turbofan augmentors. The effects of fuel system distribution and V-gutter flameholder tailoring may be determined.

When exercised in conjunction with the stability analysis, a less extensive output is given and the prime purpose of the program is to generate the response of augmentor efficiency to variations in fuel-air ratio and inlet velocity, pressure and temperature.

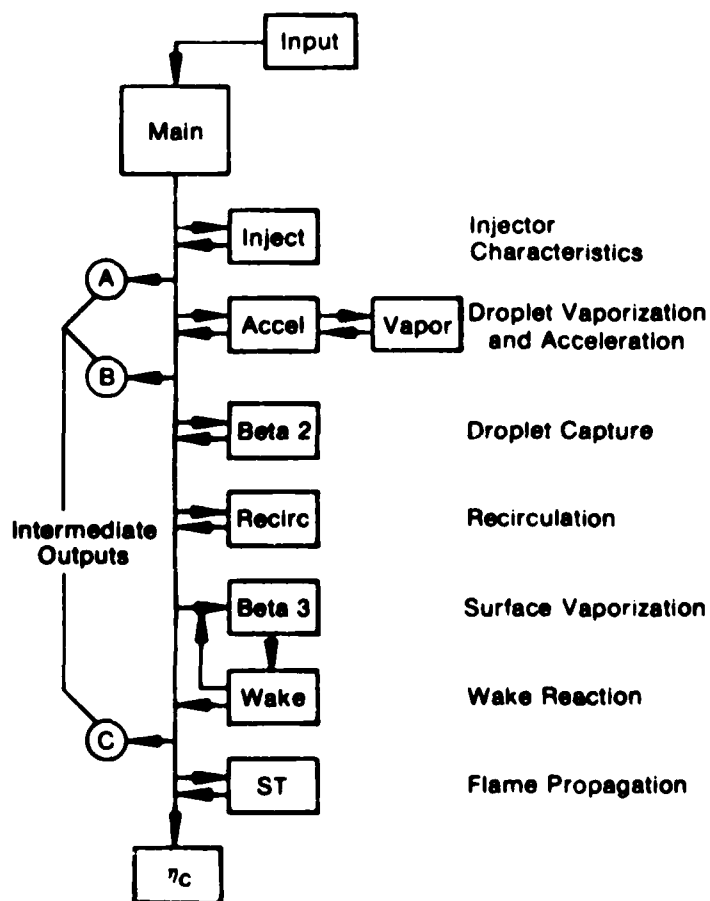
The augmentor breakdown and specific description of one-stream-tube is shown in Figure 6. For a single fan duct streamtube, the computer logic is shown in Figure 7. The identified subroutines each evaluate a specific portion of the overall combustion process.



$$BPR = W_{Duct}/W_{Core} \quad ; \quad W_{COOL} = W_{Cooling}/W_{Total}$$

FD 146488

Figure 6. Location of a Core Streamtube in a Turbopan Engine Augmentor



FD 151084

Figure 7. Single Streamtube Logic Map

The input requirements for a fan duct streamtube are those to fully describe the approach flow field, geometry of the streamtube and flameholder, and the total fuel-air ratio. The execution of one streamtube proceeds as follows:

**(1) Inject**

This subroutine evaluates the droplet sizes formed by a variable area spraybar as a function of the injection pressure drop. Five droplet sizes are calculated which represent the cumulative volume versus pressure drop curve for this spraybar type.

This subroutine evaluates the amount of the liquid fuel which is flash-vaporized by the injection process. This evaluation is performed as an adiabatic expansion process from the high-pressure spraybar fuel condition to the low-pressure augmentor conditions. The appropriate fuel enthalpy chart is used, keyed by the fuel type input variable.

The liquid flowrate which remains is partitioned equally into the five size groups. The total flowrate is originally calculated from the total fuel-air ratio input and the airflow which is calculated from the streamtube geometry and flow conditions.

**(2) Accel**

This program subroutine evaluates the rate of droplet vaporization and acceleration which occurs between the spraybar and the downstream V-gutter flameholder.

The equations for acceleration assume a spherical liquid droplet which is accelerated by drag forces only. The drag coefficient is evaluated as a function of Reynold's number based on the relative air-liquid velocity.

Concurrently, the rate of liquid vaporization is evaluated as forced convection mass transfer utilizing a mass transfer Nusselt number correlation which is also based on the relative velocity Reynold's number. The requirement to simultaneously solve the vaporization and acceleration equations was met by a finite difference solution. A small time increment is selected and the acceleration solution performed to generate a velocity increase for the liquid droplet. Using the average velocity over this time increment, a vaporization rate is calculated and a vaporized fraction evaluated. This sets a new droplet size for the next time interval. The average velocity over this time is also used to calculate a distance travelled.

This procedure is repeated until either the liquid droplet reaches the flameholder or is fully vaporized. This analysis is repeated for each size group of the five initially set.

**(3) Collect**

At the flameholder plane, the program evaluates the rate of liquid deposition onto the surface of the V-gutter. This deposition occurs as the liquid droplets are unable to follow the divergent air flow streamlines around the leading edge of the flameholder.

The evaluation of the rate of deposition is performed as a correlative solution to the point where liquid droplets just hit the flameholder surface. The variables include flameholder geometry, droplet diameter and flow conditions. The correlation equations are based on calculations which were done externally to this program, where limit trajectories were established based on potential flow solutions to the flow field approaching the flameholder.

The program utilizes the droplet diameter which exists after the vaporization evaluation to calculate the percentage of the liquid flowrate in each size group which is deposited on the V-gutter surface. This is done for each of the five size groups. The collection mass flowrate is evaluated from each size group collection percentage and the liquid flowrate in each group at the flameholder.

#### **(4) *Recirc***

The gaseous recirculation rate into the flame holder wake is evaluated from a variety of literature sources which present recirculation zone volume and flowrate as a function of flameholder geometry and flow conditions. The program evaluates a "recirculation efficiency" which is the ratio of recirculated mass flow to the flowrate through the area blocked by the flameholder. This typically runs 15 to 25%.

The correlations cover a range of the variables which control the recirculation such as flameholder apex angle, blockage, approach Mach number, and temperature. The result of the subroutine is the recirculation zone. These are used in the analysis of the wake reaction efficiency.

#### **(5) *Wake***

The wake reaction is treated as if it occurred in a well-stirred reactor with volume and entry flowrate as evaluated in RECIRC. The kinetics are assumed to proceed as a single-step, second order conversion process. The kinetics utilize rate coefficients which simulate aircraft fuel behavior. The required inputs are wake volume, wake fuel-air ratio, recirculation rate and inlet conditions of pressure, temperature, etc. The output of the analysis is the wake reaction efficiency and mean wake temperature.

#### **(6) *Beta 3***

This subroutine evaluates the degree of vaporization of the liquid film which exists on the flameholder surface. The vaporization process is one forced convection from the surface into the trailing wake shear layer and heat transfer from the flameholder wake through the flameholder metal into the liquid film. The program utilizes a small element approach using 10 elements on each side of the flameholder. The mass flux and heat flux are evaluated for one-at-a-time starting at the flameholder leading edge. Any liquid left unvaporized is assumed to leave the trailing edge of the flameholder and traverse through the wake shear layers downstream.

The solution of WAKE and BETA 3 must be done simultaneously since BETA 3 requires wake temperature to find fuel vaporization and the vaporization influences WAKE through fuel-air ratio. The solution approach is described in Appendix B with a typical result shown here in Figure 8.

#### **(7) *Flame***

The turbulent flame propagation downstream of the flameholder uses a small step difference solution with axial profiles of turbulence, flow, etc. The procedure is described in Appendix B.

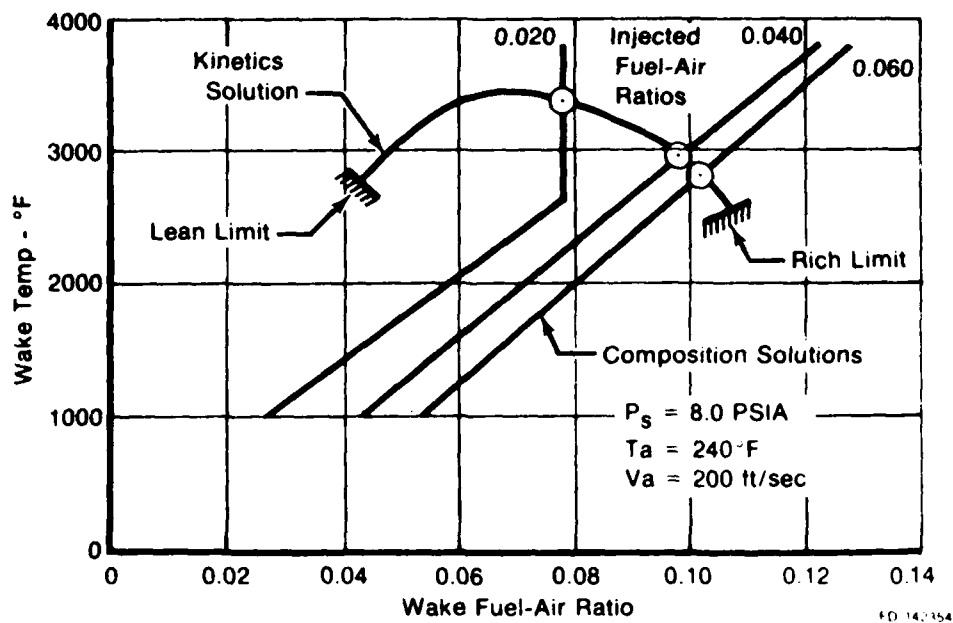


Figure 8. Duct Stream Flameholder Wake Solution

#### d. Input Requirements and Comments

The model requires as input the physical variables which describe the fan duct and core stream geometry and operating conditions. Since the model functions by repetitive analysis of single streamtubes, the input is required for each different type of streamtube. A different type is one with any input variable different.

The input requires the following values along with the input described in Section II.7.

BPR	Actual value. Default to 1.0 if run as a duct burner with no core engine and $W_{COOL} = 1/2 \times (\dot{m}_{cool}/\dot{m}_{duct})$
M6C	Inlet Mach numbers
M6H	
NTC	No. of types of fan duct streamtubes
NTH	No. of types of core streamtubes
PS6	Inlet static pressure, psia

Array input is required to describe each streamtube fully. These array values are aerodynamic and geometric. The array is the number of streamtube types in the fan (NTC) or core (NTH) and the number of stream flow tubes of each type identified in the fan (NSC) or core (NSH) sections. If three different types of fan streamtubes are used ( $NTC = 3$ ), with a total number of 28 fan streamtubes (18 of flameholder width (FWHC) = 1.0 in., 4 of flameholder width = 0.75 in. and 6 of flameholder width = 1.25 in.,  $NSC = 18, 4, 6$ ) and if the



first two types operate at the same fuel-air ratio (FAC), but different from the third, then the input to the model to describe this case would be:

δInput ....., NTC = 3, NSC = 18, 4, 6, FHWC = 1.0, 0.75, 1.25, FAC = 0.05, 0.05, 0.045,....

δEnd

The program as currently written assumes a unit depth streamtube, i.e., 1 inch depth. The mass flowrates will be based on this value. If true flow values are required, the number of each type (NSC or NSH) should be the number of 1 inch deep streamtubes of that type. This is shown in Figure 9.

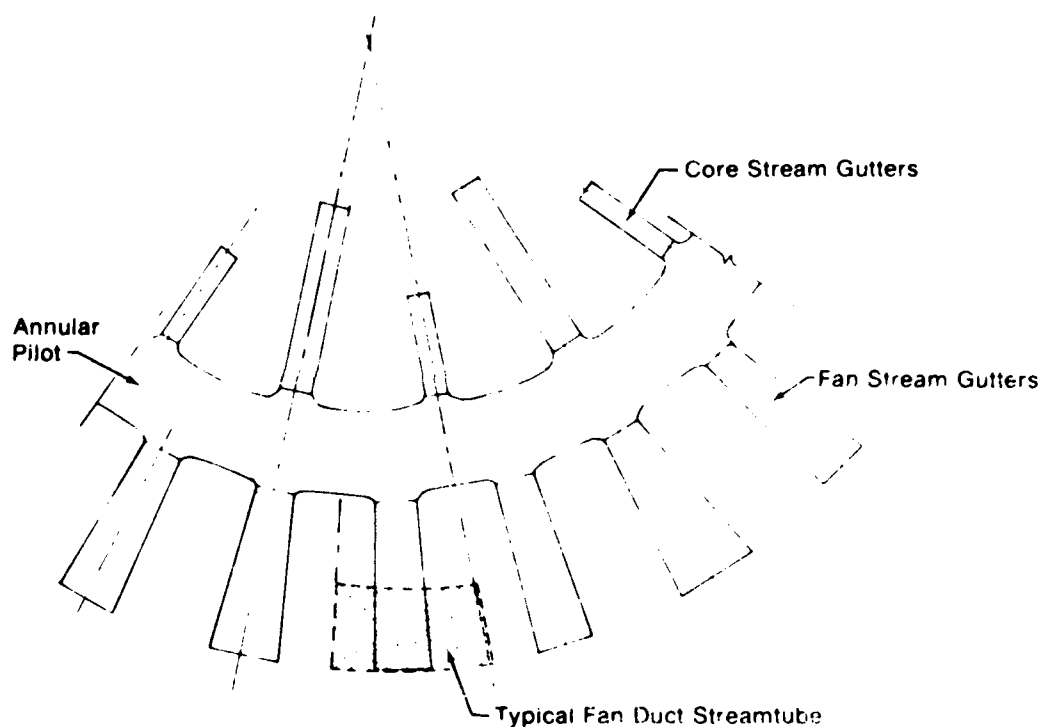


Figure 9. Location of Typical Fan Duct Streamtube

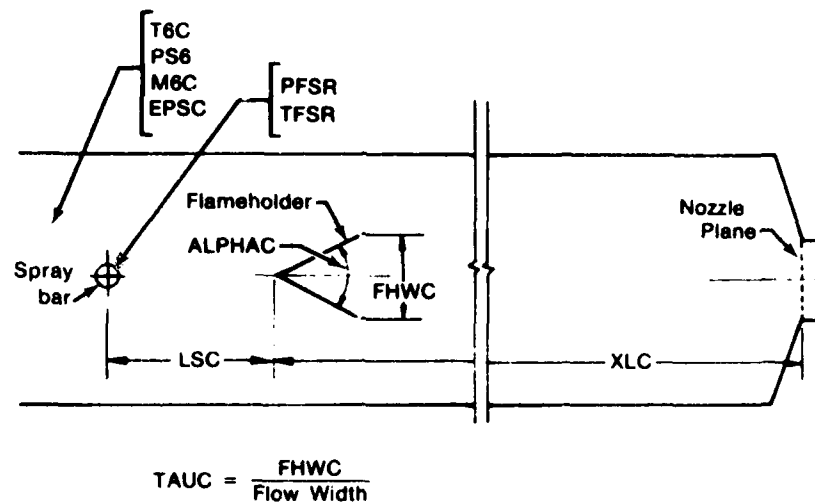
The geometric inputs required for a single streamtube are shown in Figure 10. The value of blockage is referenced to Figure 9. The input should reflect the ratio of flameholder width to the streamtube limits. This value of blockage sets the required flame penetration for 100% efficiency and must be input correctly.

The value of EPSC is the approach turbulence and will affect the flame speed. Unless specific data are available, use a value of 0.04 for a turbofan engine.

The input value for PFSR controls the mean droplet size from the spraying, which has data from a variable area orifice built in. If other values are desired, use the equation:

$$d_{50} = 795 - (PFSR - PS6) \cdot 4$$

to determine the input value of PFSR required to yield a desired mean droplet diameter, in microns. This is the only place where PFSR is used, so no disruption occurs if nontrue values are input.



FD 146486

Figure 10. Single Streamtube Geometry and Flow Inputs — Fan

For the aerodynamic inputs, also reference Figure 10, the required input is shown. As previously mentioned, PS6 is assumed to be uniform across the streamtubes.

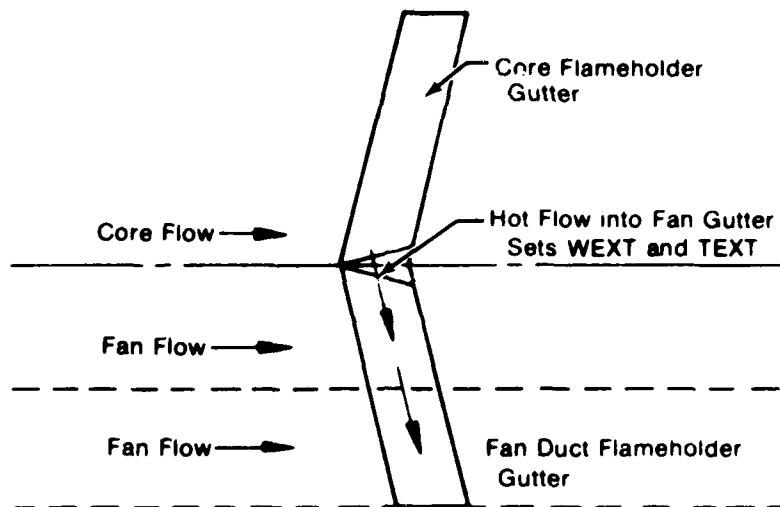
One input set requires external evaluation. This is the values assigned to WEXT and TEXT in the fan duct streamtubes. The purpose of this input is to account for the influence of hot gas migration down the wake region of the fan duct flameholders from either the core or from a pilot. WEXT is defined as the ratio of this "external" flowrate to the recirculated flowrate. To allow for flexibility in design selection, this input format was selected. The user must evaluate whatever flowrate is expected and calculate WEXT. For use in estimating the recirculated flowrate, assume  $K_1 = 0.25$  use:

$$\dot{m}_r = K_1 \cdot \rho_a \cdot V_a N$$

for recirculation rate per inch of flameholder length. Typical values of WEXT are 0.02 to 0.04. TEXT is the temperature of this "external" flowrate. These are shown in Figure 11.

The liner cooling airflow input, WCOOL, is the ratio of cooling liner air to total engine air. As such, the engine bypass ratio is required to evaluate the net available fan duct airflow. If no cooling air is taken from the fan duct or if input fuel-air ratios are based on the true net air available for combustion, input WCOOL = 0.0. If a duct burner is being analyzed and it does have a cooling liner, set a dummy valve of 1.0 for BPR and set WCOOL by:

$$WCOOL = \frac{\dot{m}_{cooling}}{\dot{m}_{duct\ burner}}$$



FD 146487

Figure 11. External Heat Addition to Fan Duct Gutters

#### e. Output

The program has two output formats, long and short. The long format presents detailed values for the processes which control the wake vapor-phase fuel-air ratio and flame penetration. The short format essentially presents the overall results. For both, the results are presented as a streamline-by-streamline analysis with fan and core summaries.

##### (1) Fan Streamtube

The long format presents the input data for each streamtube and two calculated values. These values are the effective streamtube fuel-air ratio and the effective recirculation temperature. The equations used for these are shown in Appendix B.

The output lists the calculated values for the injection process, mean droplet size and flash vaporization, and the influence coefficients,  $\beta_1$ ,  $\beta_2$ ,  $\beta_3$  and  $K_1$ , which control the wake fuel-air ratio. The importance of these values is explained earlier in this section and in Appendix B.

A word of caution is in order. If the output is preceded by the warning that the wake temperature iteration has failed, the situation is such that the wake has exceeded the rich limit at the input conditions. Although output is presented, it is not valid and merely represents the limits of the internal convergence search routine. For example, wake temperature will always be 5000°F for a failed case. If a single streamtube is being run, several other error messages will result as the program attempts to interpret zero efficiency. If multiple streamtubes are being run, the program will ignore the failed streamtube in all calculations.

The initial flame speed is the laminar flame speed at the appropriate inlet conditions. The turbulence level is the value induced by the flameholder.

In the stream efficiency section for each streamtube, the following comments are applicable:

- The ideal temperature use is based on the effective fuel-air ratio.
- The efficiency is the ratio of flame penetration to streamtube width at the exhaust nozzle.
- The actual temperature rise is based on the above conditions. The exit temperature is based on streamtube inlet plus this actual temperature rise.
- The flowrates are for a 1 inch deep streamtube. The fuel flowrate uses the effective fuel-air ratio.

The fan streamtube summary presents the major items from each streamtube and then the exit average results. The cooling air flowrate ratio is repeated here. Two more values of combustion efficiency are presented and two values of average exit temperature.

The average streamline exit temperature is the mass weighted average of the individual exit temperatures. The chemical combustion efficiency is based on this value for exit and an ideal temperature use based on the average effective fuel-air ratio and average inlet temperature.

The average duct exit temperature includes the mass weighted effect of the liner cooling air being added to the streamtubes at the exhaust nozzle inlet. The average thermal combustion efficiency is based on this exit temperature, the average inlet temperature and an ideal temperature rise is based on the average input fuel-air ratio.

Since engine analysis procedures generally base the fan duct fuel-air on the total duct airflow and use the thermal nozzle inlet averages, the value of thermal combustion efficiency is the one which is used for rumble prediction.

The total flowrate presented here includes the number of each type of streamtube as do all of the above-mentioned mass averaged values.

Also note that at no time are efficiencies ever mass averaged directly. All average efficiencies are based on comparison of the average results of individual streamtubes to the result of the average inlet. That is, the burn-then-mix process is compared to the ideal mix-then-burn process. Since curves of ideal temperature rise exhibit peak vs. fuel-air ratio, the average efficiency of two streamtubes, one lean and one rich, may very well be less than either streamtube separately.

## **(2) Core Streamtubes**

Due to the absence of droplet effects, the output is greatly simplified. The wake reaction results are presented as well as initial flame properties. Without liner cooling air, there is no fuel-air ratio shift and thus, only one efficiency definition. The process of evaluation of the ideal temperature rise is given in Appendix B. All of the comments in the fan stream apply here, except that thermal efficiency is not defined here due to the lack of liner cooling air.

If the message "Aerodynamic Loading exceeds Kinetic Capacity" occurs, the blowout limits were exceeded.

#### **4. SPRAYRING MODEL PROGRAM DESCRIPTION**

##### **a. General**

The spraying model is a transient analysis which solves the hydrodynamic and thermodynamic equations for fuel flow into and out of an augmentor fuel injection system. The type of fuel system may be either spraybars or sprayrings. Various options are available to specify the manner in which the fuel flowrate into the injection system is controlled. The model is capable of evaluating up to sixteen separate zones of fuel injection. The output consists of the fuel flowrate distribution at a specified transient time. The output is used to define the fuel-air ratio distribution for later use by the flameholder combustion model. The output may also be used directly to evaluate fuel injector designs by comparison of transient pressures and fuel distributions.

##### **b. Modeling Approach**

The augmentor combustion models which were available prior to the formulation of this injection model required that the user input the fuel-air ratio distribution. This value or values was then used in the combustion rate calculations. This requirement represented a restriction on the validity of the results in that the fuel injection system response was essentially assumed.

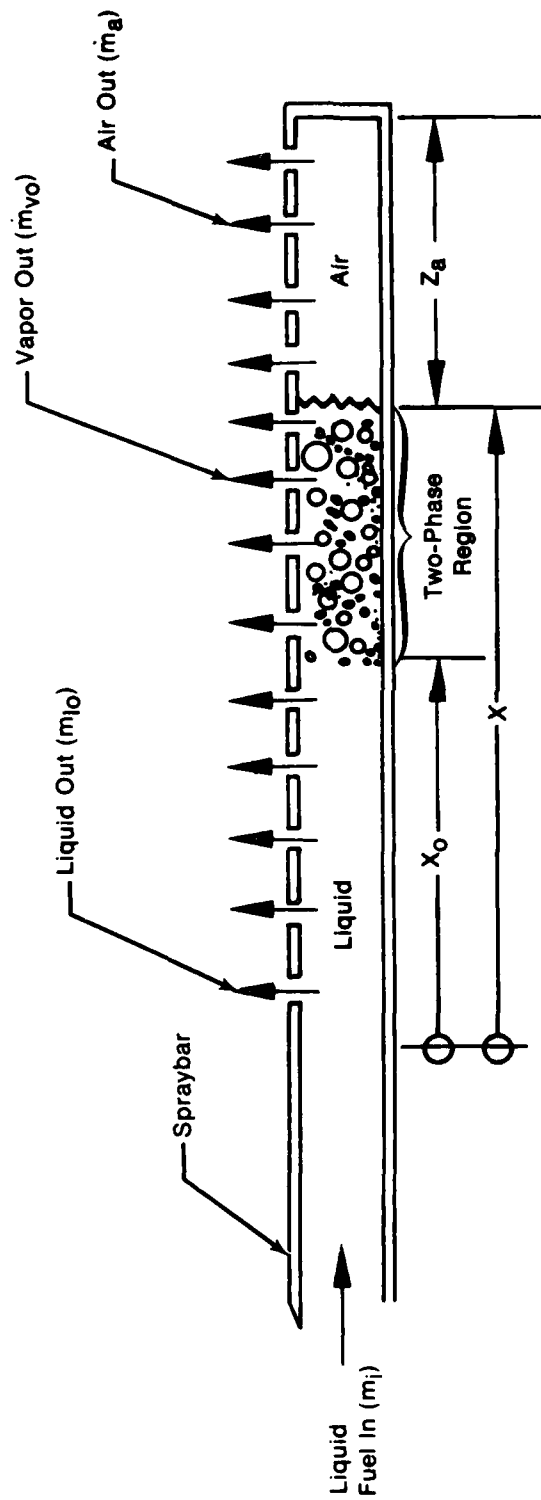
The major problem area with this approach was augmentor instabilities during transient operation as the augmentor fuel flowrate was increased towards maximum augmentation. There were numerous situations where rumble would occur on transients when the steady-state fuel flowrate was insufficient to cause rumble. Sometimes the rumble would disappear as steady-state operation was achieved and other times a rumble-induced blowout would occur. This indicated that a fuel maldistribution occurred which was significant enough to cause rumble during the transient operation of the fuel system.

The spraying model was formulated to evaluate this transient operation. The approach which was selected is to specify the manner in which fuel is introduced into the fuel injector system and then evaluate the response of this system to the flowrate. The model performs thermodynamic and hydrodynamic balances among the spraying fuel, the spraying wall material, and the specified control in order to predict the fuel outflow distribution from the injector at a specified time.

The type of allowed fuel control and the specified fuel sprayrings (or spraybars) was made as general as possible to analyze a wide selection of augmentor system designs.

##### **c. Model Description**

This model, based on the simplified physical model shown schematically in Figure 12, will handle sprayrings fed from either one or two locations or spraybars fed from one end. It will analyze the start transients in hot multiple zone systems with various zones started simultaneously, sequentially or in some combination of the two zones. The model accounts for the interaction between fuel flow, heat transfer, and fuel thermodynamic characteristics, predicting the instantaneous distribution of thermodynamic states throughout the fuel system and the fuel flowrate distribution into the augmentor. Evaluation of an augmentor start transient considers the fuel system initially hot and filled with air, and analyzes the fill process as air flows out of the system and the spraying cools down. The model simultaneously evaluates a set of continuity relations for air, liquid and gaseous fuel; a set of energy relations for the fuel and spraying, and calculates the flowrates, heat transfer and thermodynamic characteristics required for solution of these equations.



FD 165285

Figure 12. Schematic of Spraybar Showing Fluid Regimes

The continuity relations are developed by considering the mass rates of change of air, liquid, and fuel vapor in the system, assuming all three components/phases are at the same pressure, and solving the resulting equations simultaneously for the interdependent variables. The result is a set of rate equations defining the rates of change of system pressure, liquid volume, and vapor volume in the system. The resulting continuity set, written for a spraybar fed from one end, is:

$$\frac{dP}{dt} = \frac{\frac{\dot{m}_l}{\rho} - \frac{\dot{m}_{l0}}{\rho} + \left( \frac{1}{\rho_v} - \frac{1}{\rho} \right) \dot{m}_v - \frac{\dot{m}_{v0}}{\rho_v} - \frac{\dot{m}_a}{\rho_a}}{\frac{A Z_a}{\gamma P} + \frac{A \left( \frac{d\rho_v}{dP} \right)}{\rho_v}} \alpha (x - x_0)$$

$$\frac{d\alpha}{dt} (x - x_0) = \frac{\dot{m}_v - \dot{m}_{v0}}{A \rho_v} - \frac{\left( \frac{d\rho_v}{dP} \right) \alpha (x - x_0) \frac{dP}{dt}}{\rho_v}$$

$$\frac{dx}{dt} = \frac{d\alpha (x - x_0)}{dt} + \frac{\dot{m}_l - \dot{m}_{l0} - \dot{m}_v}{\rho A}$$

The dependent variables are system pressure (P), fuel-air interface location (x), two-phase interface ( $x_0$ ) and vapor void fraction ( $\alpha$ ). The relative flowrates are shown in Figure 17, and  $\dot{m}_v$  is the rate of vapor generation. Liquid, vapor and air density ( $\rho$ ,  $\rho_v$ ,  $\rho_a$ ), and cross-sectional area (A), and specific heat ratio for air ( $\gamma$ ) are the remaining independent variables. From the nature of this equation set, it is apparent that heat transfer and flow calculations must be performed prior to or simultaneously with the evaluation of the set, and are in turn dependent upon the results.

Figure 13 shows the logic flow developed to provide a satisfactory approximation to simultaneous solution of the system equations without the need for costly iteration.

Capability is incorporated in the model to account for several complex flow phenomena in the fuel, including two-phase choking flow, flow with boiling dryout, and instability with surging flow. Heat transfer models include capability for analysis of heat transfer from the hot gas stream to the sprayring and heat transfer from the sprayring to the fuel. Evaluation of heat transfer in the fuel as the initially hot sprayring is cooled considers all possible modes of boiling and convection, including film boiling with subcooled or saturated fluids, nucleate boiling with subcooled fuel, and convection. These models are integrated to allow evaluation of the thermodynamic change of state from the fuel entry condition until it is fully vaporized.

The model will analyze either single or multiple zone augmentor fuel systems with inlet condition specified as either flow control at the augmentor entry, or inlet pressure control with a variety of feedback parameters. Transient analysis of the fuel system provides instantaneous calculation of system pressure, temperature distributions in the fuel and sprayring, flow distributions into the augmentor and thermodynamic states of the fuel as it is injected, either in the vapor or liquid condition.

Figure 14 shows the arrangement of a sprayring with fuel supply at two locations. Figures 15 to 17 show the results of analysis of a start transient for a sprayring, with initial air-filled volume, for operation in a flow-controlled mode. Figure 15 illustrates how system pressure responds to the filling process and Figures 16 and 17 show the filling process and fuel discharge. These results can be used to determine the fuel distribution into the augmentor.

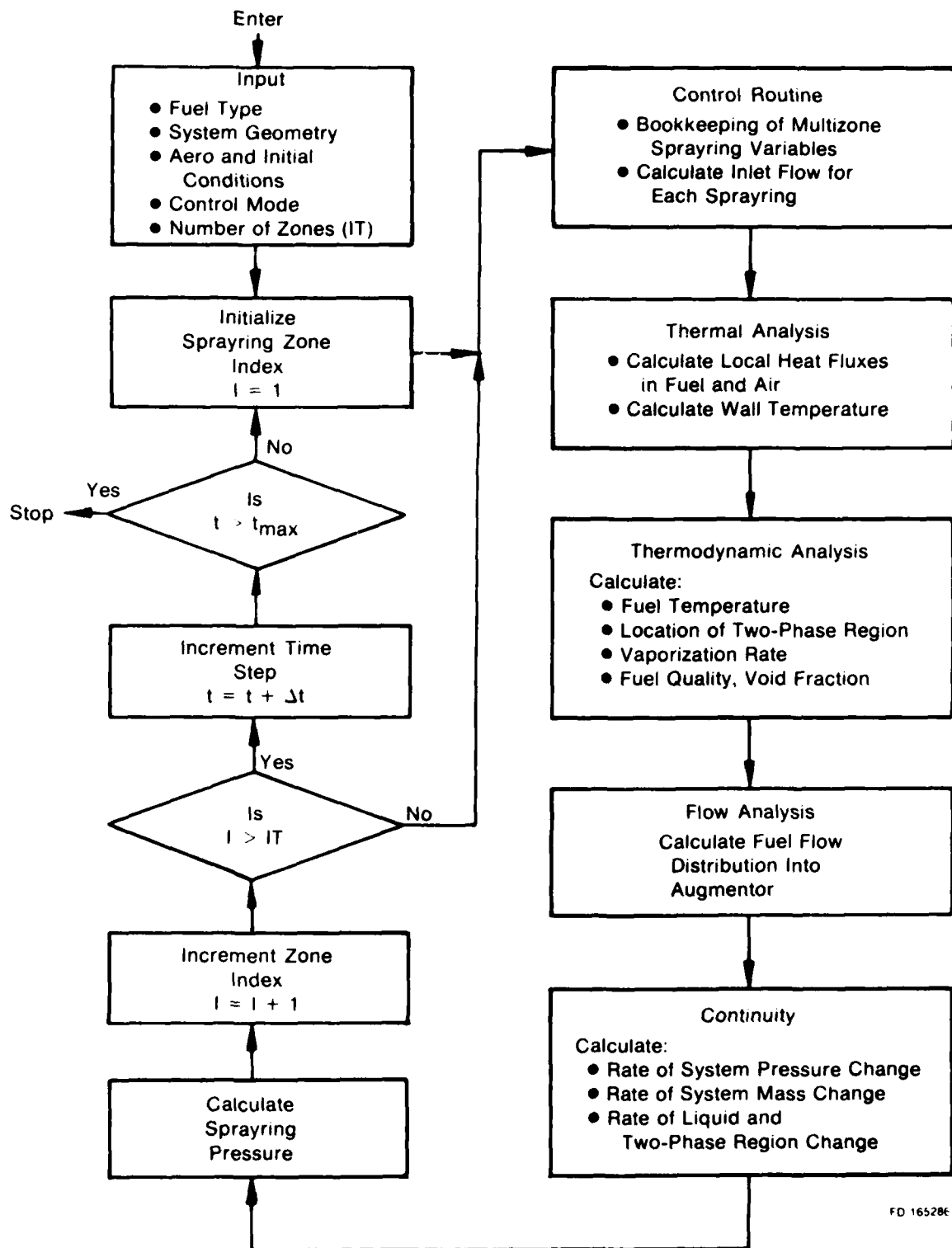
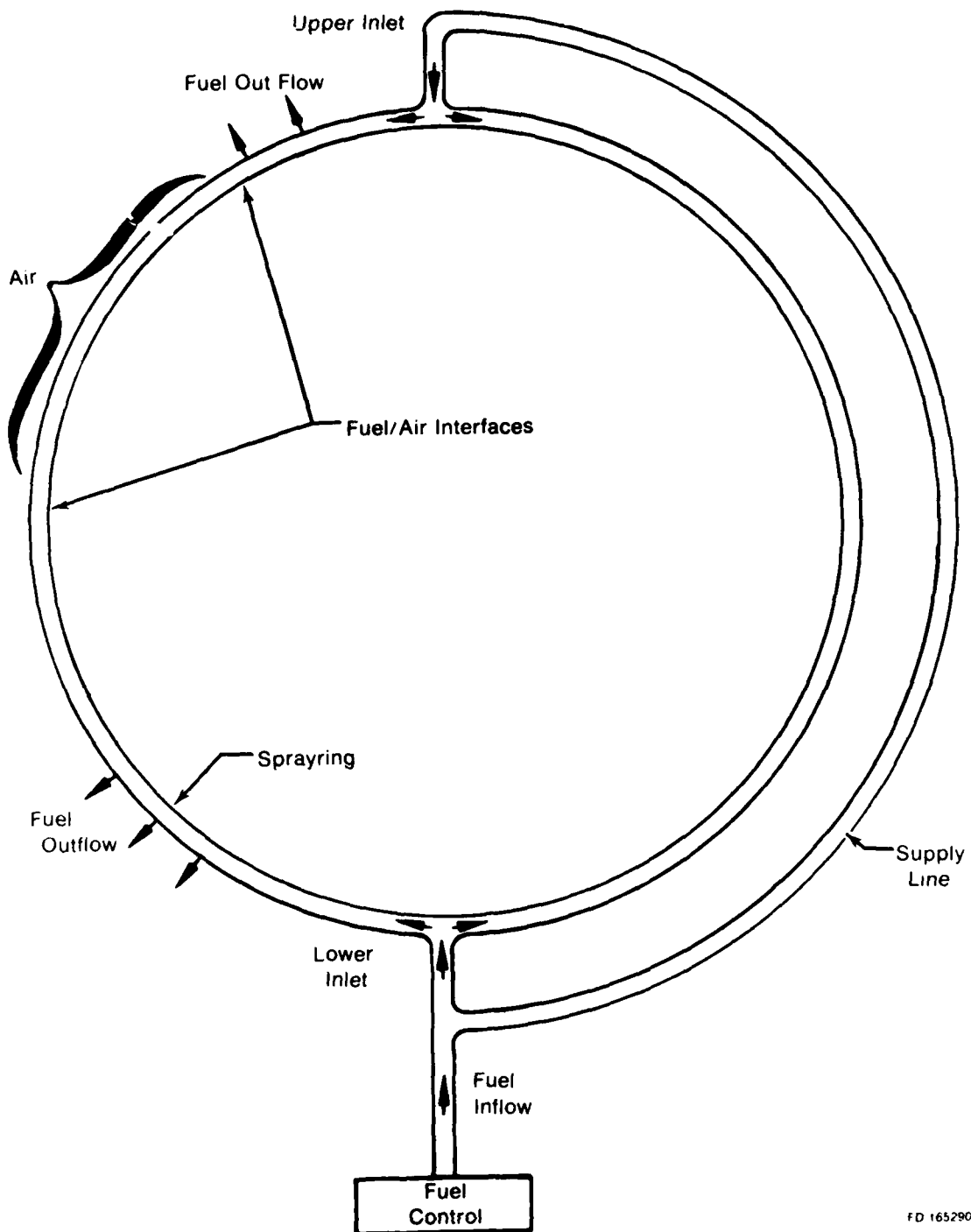


Figure 13. Flow Logic for Augmentor Fuel System Model





FD 165290

Figure 14. Schematic of Sprayring

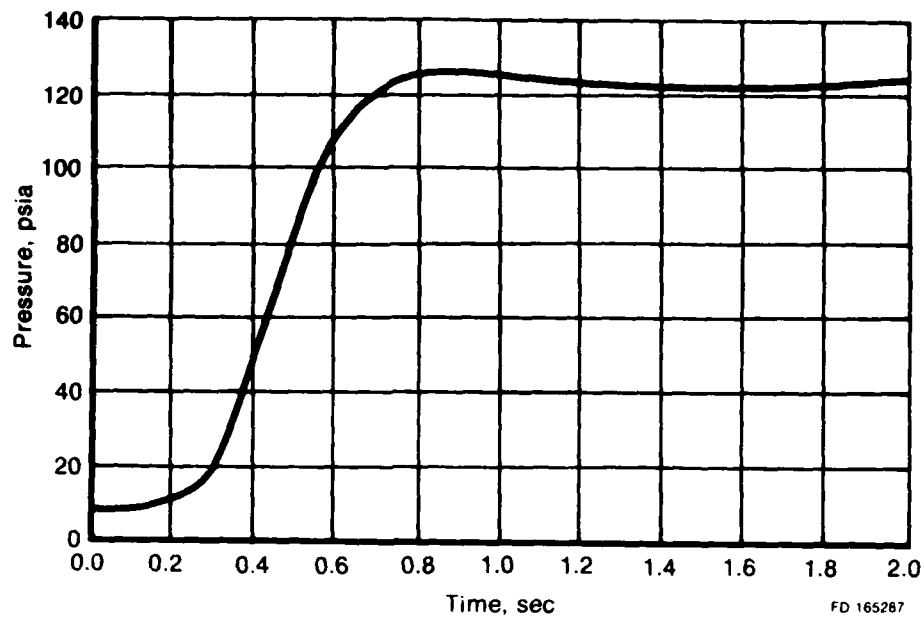


Figure 15. Spraying Pressure vs Time

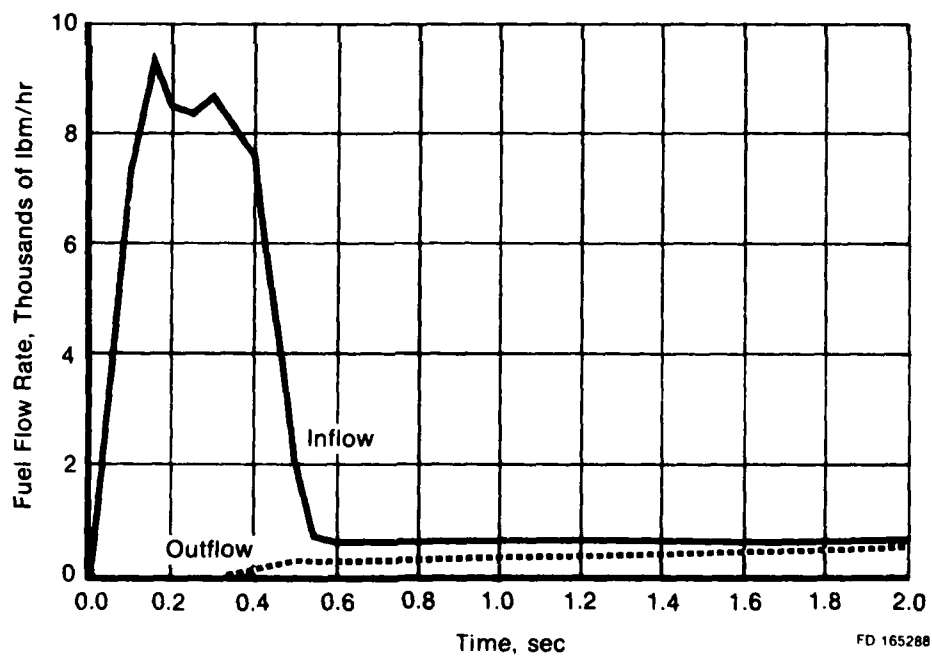


Figure 16. Comparison of Fuel Flow Into and Out of Spraying

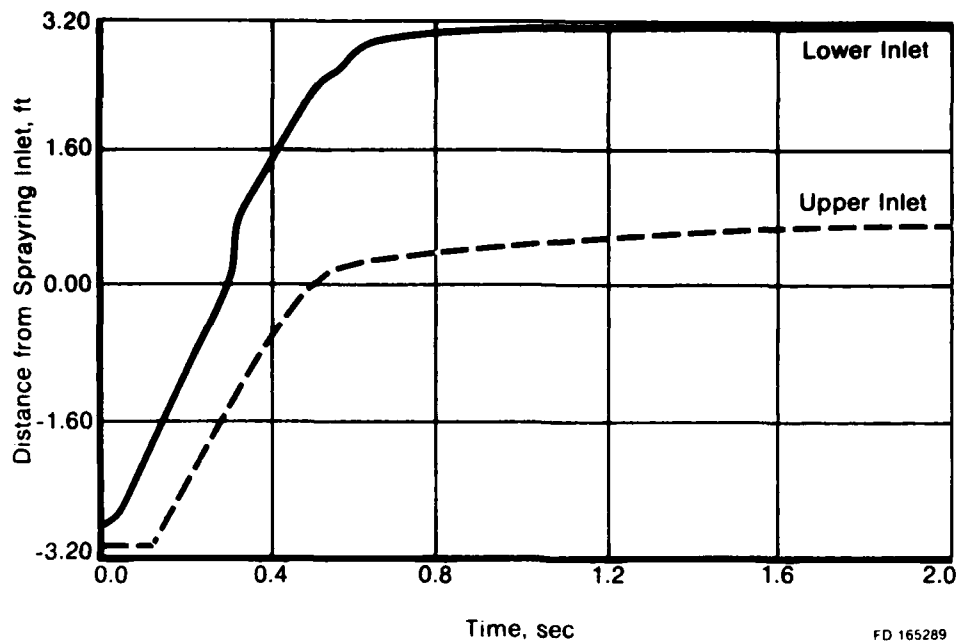
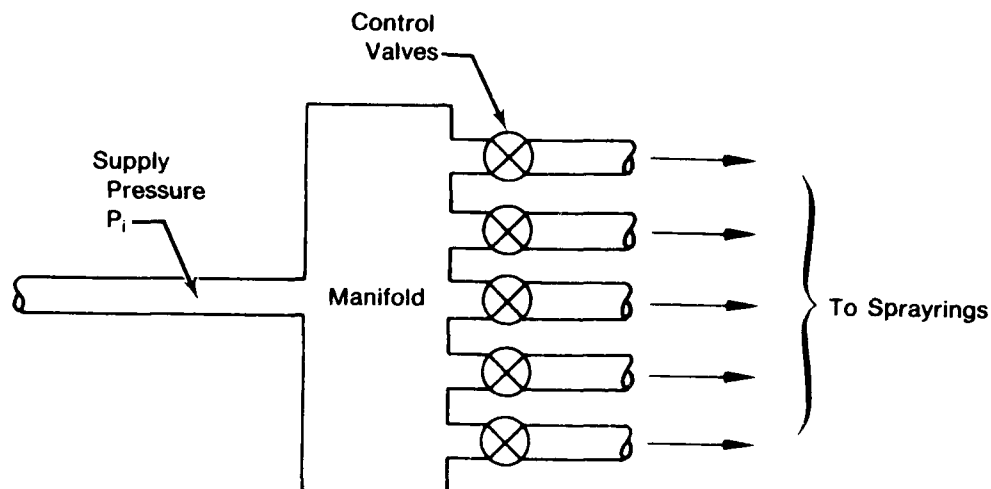


Figure 17. Location of Fuel/Air Interface in Spraying

The basic spraying model requires that the total inlet flow for a spraying is supplied to the analysis. The model then generates the spraying pressure and injected flowrate distribution as a function of time. Therefore, two options have been written to supply flow to the system.

One such control is a distribution valve. Such a valve, shown schematically in Figure 18, is used to sequentially open flow to each spraying as a function of time. The flow schedule is shown in Figure 19.



FD 217918

Figure 18. Distribution Valve Schematic

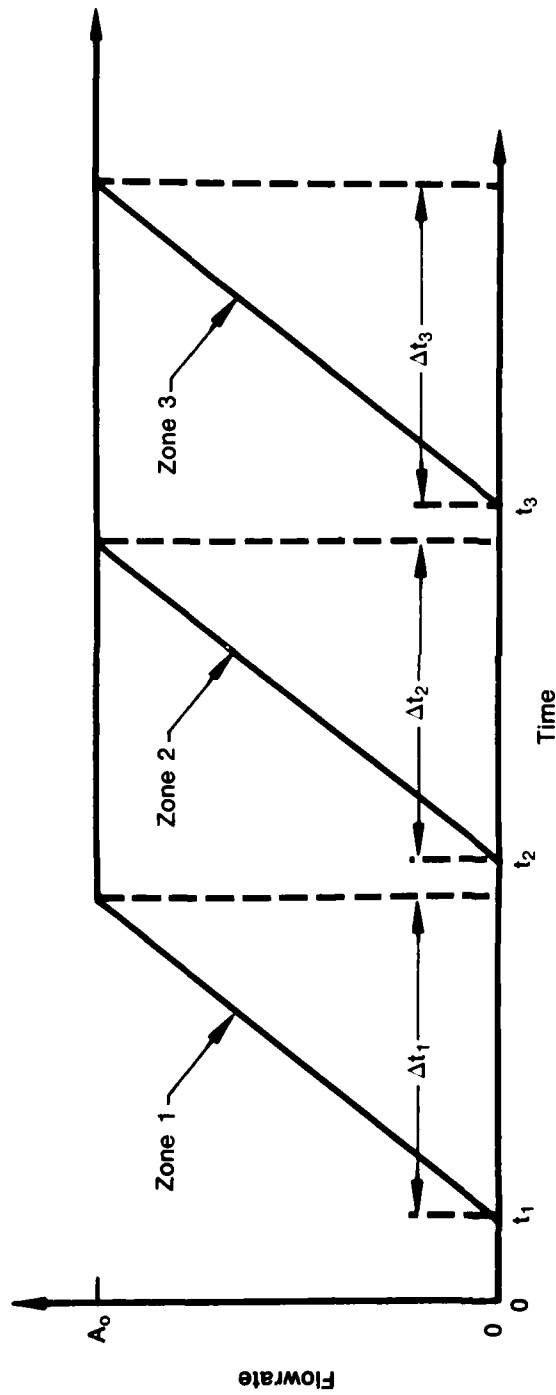
Rather than use a ramped flowrate, it also may be input directly. Either the total flowrate or individual spraying flowrates may be input as a function of time. If the total flowrate is used, the percentage which goes into each spraying must be specified.

The interface requirements between the spraying model and the flameholder combustion model are primarily those of geometric and aerodynamic consistency. The output from the analysis of a given spraying consists of fuel flowrate distribution around the circumference of the spraying. The spraying is analytically divided into a given number of segments, typically 20. Each segment has a calculated amount of injected fuel flowrate which occurs at the time specified by the user.

This fuel flowrate output is then divided among the streamtubes of the correct portion of the flameholder. This relationship is shown in Figure 20. The fuel-air ratio in this particular streamtube will be set by the amount of fuel flowrate from the spraying and the calculated airflow from the spraying and the calculated airflow from the flameholder description. For this reason, care must be taken to ensure that the input for the spraying and flameholder descriptions are consistent. For example, the combustion model may be successfully executed using only one streamtube each to describe the fan and core streams of the augmentor. If the spraying option is selected, however, all of the fuel from a given spraying would be placed into each single streamtube, resulting in a very rich fuel-air ratio.

The methodology by which the correct assignment is made is given in the following section.

The flameholder description is input as an array of description data. The first streamtube is the one at top dead center and proceeding clockwise around the flameholder (looking forward in the engine). Each spraying is told the index of the initial streamtube and the final streamtube which it feeds. The program will then calculate which section of the spraying feeds each streamtube and allocate the fuel from that section to the given streamtube. This is shown schematically in Figure 21.



$A_0$  = Zone Flowrate, lbm per hour  
 $t_n$  = Time to Start Opening Valve for Zone  $n$   
 $\Delta t_n$  = Time Required to Open Valve for Zone  $n$

Figure 19. Zone Flowrate Schedule

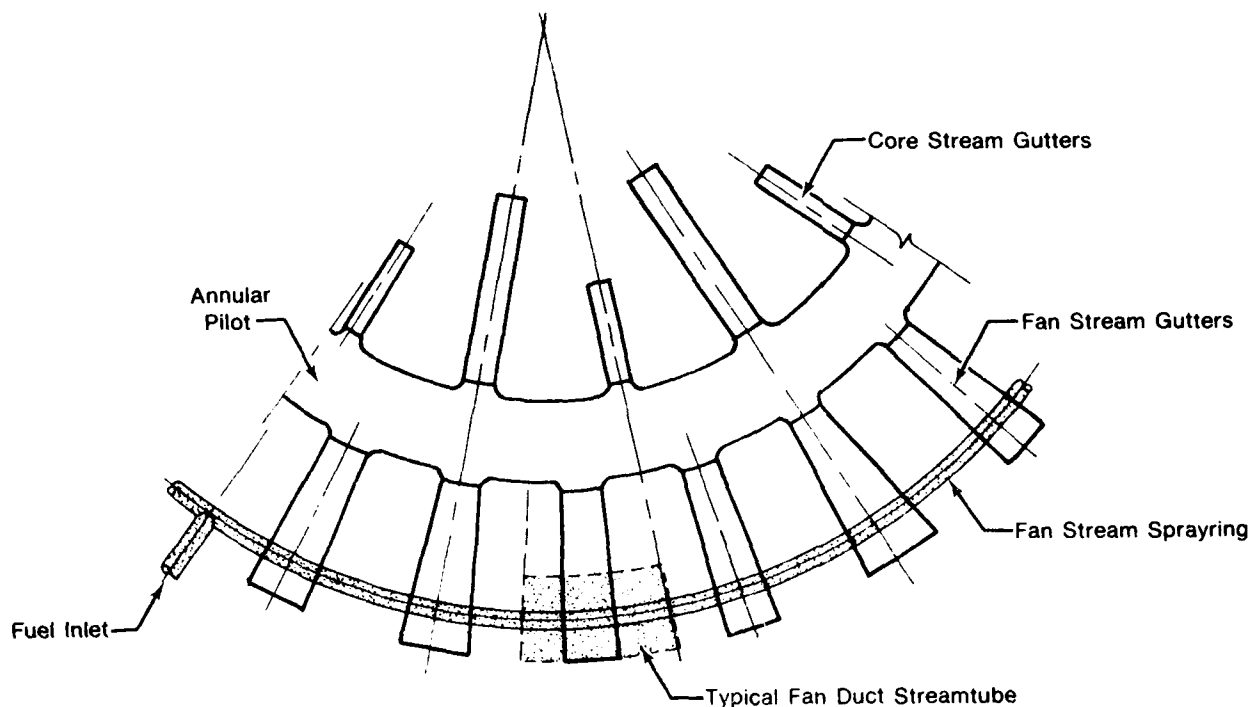


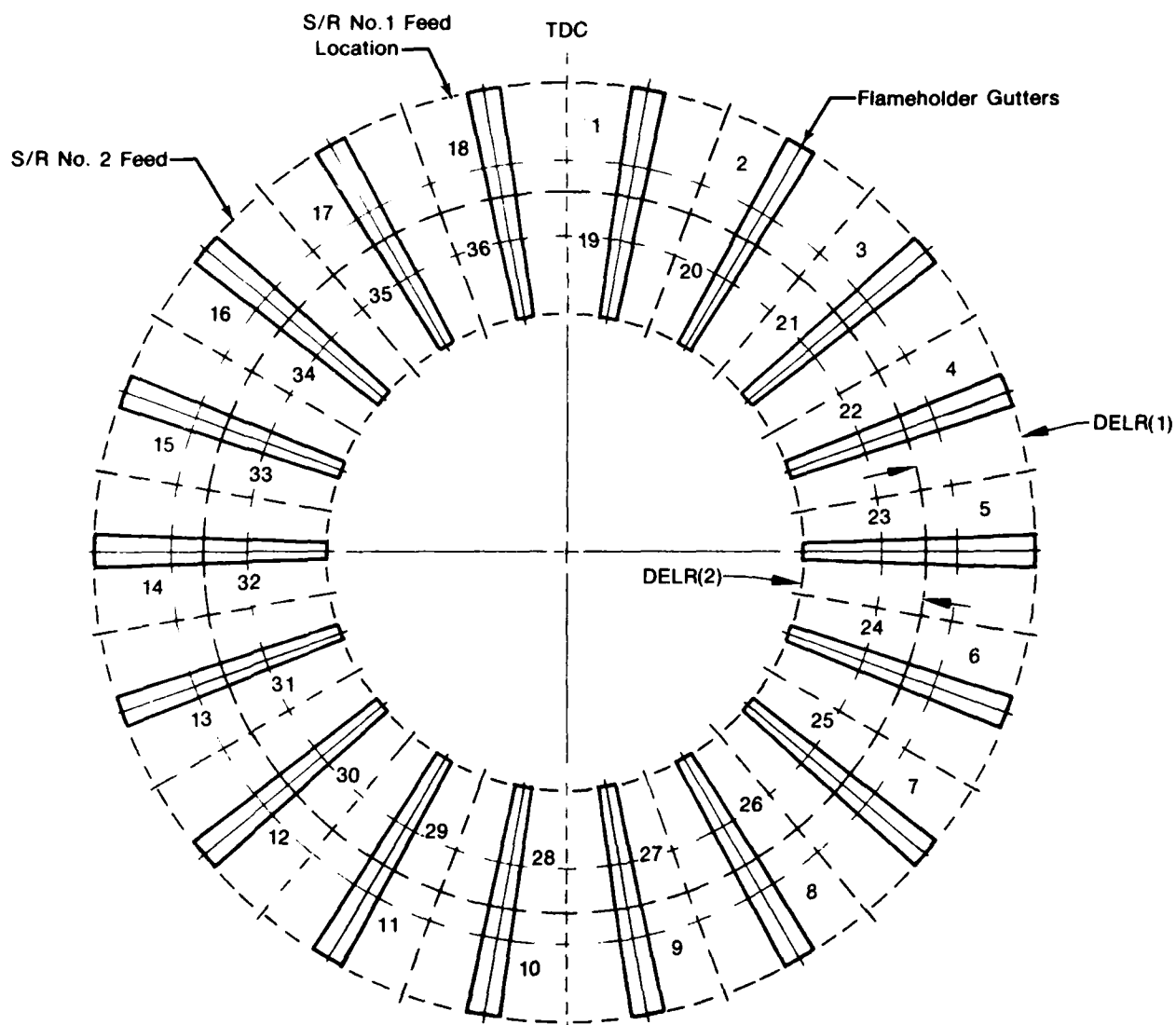
Figure 20. Spraying - Flameholder Geometric Compatibility

FD 217920

One final input is required to define the geometric compatibility. The fuel flowrates from the spraying are calculated referenced to the location of the only or primary feed location while the flameholder is referenced to top dead center. To finish the angular interface, the amount of counterclockwise offset of the feed from top dead center is input (see Figure 21). The fuel-air ratio for each streamtube is calculated from this amount of fuel flowrate and the airflow in the associated streamtube. The airflow calculation is based upon the inlet conditions to that streamtube, input in the arrays, and the delta radius which the appropriate spraying covers. These are shown as DELR(1) and DELR(2) in Figure 21. If the spraying and combustion models are run sequentially, the arrays NSC and NSH should be set to 1 to maintain airflow consistency in the program.

##### 5. PROGRAM SETUP

The combined spraying/rumble/flameholder combustion model program supplied by Pratt & Whitney Aircraft contains all the subroutines necessary to operate the programs with the exception of systems routines normally supplied by the computer manufacturer. The program is written in Fortran IV and runs on any large scale computer system with little or no modification required. Test case input and output are included to verify successful installation.



Spraying	Start Streamtube	Stop Streamtube	Offset Angle
1	1	18	15°
2	19	36	45°

FD 217921

Figure 21. Flameholder and Spraying Relationship

## 6. PROGRAM PERFORMANCE OPTIONS

The combined model computer program has options which control the models which are executed, as well as the type of spraying and control: the augmentor type, the fan splitter type, the combustion data source, fuel type and output format. These options are explained in the following sections:

### a. Run Option

The program is structured to permit execution of any one of the three major models or the following combinations of them:

<i>Input Symbol</i>	<i>Description</i>
IRUN	If IRUN = 1, the program executes the Spraying Model only.
	If IRUN = 2, the program executes the Flameholder Combustion Model only.
	If IRUN = 3, the program executes the Rumble Model only.
	If IRUN = 4, the program executes the Spraying Model and Flameholder Combustion Model in sequence.
	If IRUN = 5, the program executes the Flameholder Combustion Model and the Rumble Model in sequence.
	If IRUN = 6, the program executes all three models in sequence.

### b. Spraying Model Options

There are two options available which control the description of the augmentor fuel flowrate which are used in the execution of the program. This section describes the influence of these options.

<i>Control Option</i>	<i>Description</i>
ICAL	If ICAL = 1, the spraying model produces plots of pressure vs time and flowrate vs time.
	If ICAL = 0, no plots are generated.
IFLOW	If IFLOW = 1, the linear flowrate ramp is used for each spraying as shown in Figure 19.
	If IFLOW = 2, a single flowrate curve as a function of time is input using NTAB, TTAB, FTAB. The input variable PSPLIT can be used as a zone multiplier in this curve.



### **c. Rumble Model Options**

#### ***Augmentor Option***

The rumble model is designed to simulate three augmentor designs: V-gutter, Vorbix or Swirl.

<i>Input Symbol</i>	<i>Description</i>
NAUGOP	If NAUGOP = 1, the rumble model simulates a V-gutter flameholder augmentor.  If NAUGOP = 2, the rumble model simulates a Vorbix augmentor.  If NAUGOP = 3, the rumble model simulates a Swirl augmentor.

#### ***Splitter Option***

The rumble model is designed to simulate two fan splitter designs: proximate splitter or remote splitter.

<i>Input Symbol</i>	<i>Description</i>
NFSOP	If NFSOP = 1, the rumble model uses a proximate splitter assumption at fan discharge (Fan duct does not communicate with core at fan discharge).  If NFSOP = 2, the rumble model uses a remote splitter assumption at fan discharge (Fan duct communicates with core at fan discharge).

### **d. General Options**

#### ***Fuel Options***

The combined model is designed to operate with fuels of different lower heating values.

<i>Input Symbol</i>	<i>Descriptions</i>
JFUEL	If JFUEL = 1, the program uses values for JP-4 fuel.  If JFUEL = 2, the program uses values for JP-5 fuel.

### **Print Options**

The rumble model provides either tabular and plotted output or just plotted output. The flameholder combustion model provides either limited or full tabular output.

<i>Input Symbol</i>	<i>Description</i>
NPRNTR	If NPRNTR = 0, the program provides both tabular rumble model output and Open Loop Transfer Function plots.  If NPRNTR = 1, the program provides only Open Loop Transfer Function plots.
NPRNTF	If NPRNTF = 0, the program provides limited flameholder combustion model tabular output.  If NPRNTF = 1, the program provides full flameholder combustion model tabular output.
NPRINT	The input integer for NPRINT controls the number of time steps between printouts of the spraying model.

## **7. INPUT**

### **a. General**

The combined model uses various input parameters depending on which spraying, combustion and augmentor options have been selected from the previously described run options. An input data flow schematic is presented in Figure 22. The specific input blocks, which are required for each major run option selected, are shown in the chart in Figure 23. Figures 24 and 25 are schematics of the rumble model and the flameholder combustion model geometry identification. The user should note that not all input parameters are required for any given run option.

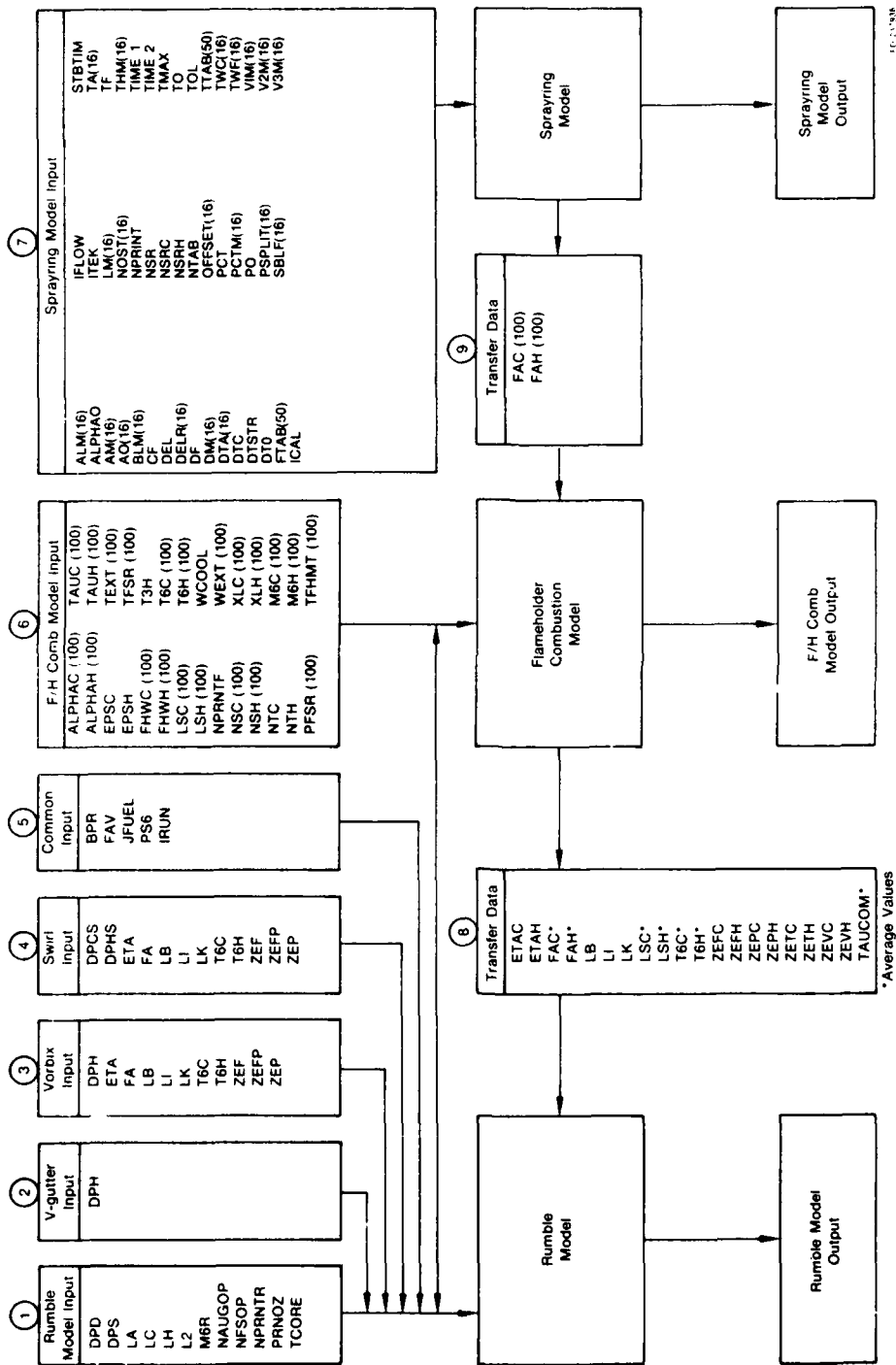


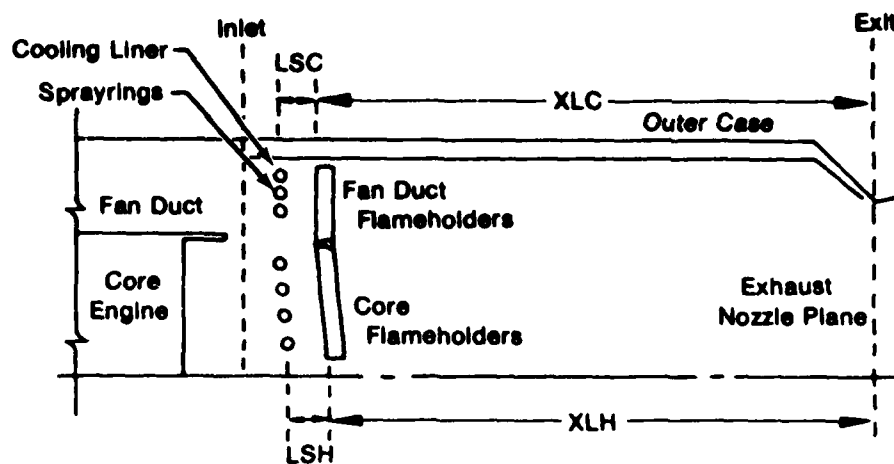
Figure 22. Combined Model Input Requirements Attachment

Augmentor Type	Models Executed			Run Option IRUN =	Augmentor Option NAUGOP =	Input Blocks Req'd
	Spraying Model	F/H Combustion Model	Rumble Model			
—	X	—	—	1	—	7
V-gutter F/H	X	X	—	4	—	5,6,7
V-gutter F/H	X	X	X	6	1	1,2,5,6,7
V-gutter F/H	—	X	X	5	1	1,2,5,6,9
V-gutter F/H	—	X	—	2	—	5,6,9
V-gutter F/H	—	—	X	3	1	1,2,5,8
Vorbix	—	—	X	3	2	1,3,5
Swirl	—	—	X	3	3	1,4,5

Figure 23. Inputs Required for Various Run Options

FD 217938





FD 151096

Figure 25. Flameholder Combustion Model Geometry Schematic

#### b. Input Description

The program uses "Namelist" input as defined in the applicable computer manual, i.e., for the IBM 370, the manual is IBM Systems 360/370 Fortran IV Language Manual, GC28-6515-10, pages 54-56. This section gives the "Namelist" names and a description for each input variable.

<u>Parameter Name</u>	<u>Description</u>
ALM(16)	Sprayring pintle area parameter
ALPHAC(100)	Fan stream flameholder apex angle, degrees
ALPHAH(100)	Core stream flameholder apex angle, degrees
ALPHAO	Maximum void fraction for 100% nucleate boiling in sprayring (must be <1.00)
AM(16)	Sprayring cross-sectional flow area, sq. ft.
AO(16)	Maximum flowrate ramped flow if IFLOW = 1
BLM(16)	Pintle flow area parameter, dimensionless

<u>Parameter Name</u>	<u>Description</u>
BPR	Bypass ratio, fan duct airflow/core air-flow, dimensionless
CF	Film coefficient multiplier for spraying heat transfer, dimensionless
DEL	Time increment for spraying model calculations, seconds
DELR(16)	Delta radius of augmentor into which fuel flow from each spraying flows, inches. Refer to Figure 21
DF	Film coefficient Reynolds number for spraying heat transfer, dimensionless
DM(16)	Spraying passage perimeter, feet
DPCS	Fan side vane pressure loss ( $\Delta P/P$ ) from mixing plane to ignition plane (STA 3 to STA4), dimensionless (Swirl augmentor only)
DPD	Fan duct pressure loss ( $\Delta P/P$ ) allocated to STA 2, dimensionless. Allocate remainder to STA 3; see DPS
DPH	Pressure loss ( $\Delta P/P$ ) from mixing plane to ignition plane (STA 3 to STA 4), dimensionless. For V-gutter augmentor this accounts for spraybar and flameholder pressure loss. For Vorbix augmentor this accounts for Vortex generator and pilot pressure loss (core and fan combined)
DPHS	Core side vane pressure loss ( $\Delta P/P$ ) from mixing plane to ignition plane (STA 3H to STA 4), dimensionless (Swirl augmentor only)
DPS	Fan duct pressure loss ( $\Delta P/P$ ) allocated to STA 3, dimensionless. Allocate remainder to STA 2; see DPD
DTA(16)	Delta time for control valve for each spraying to fully open, sec.
DTC	Maximum temperature difference for film boiling calculation in spraying, °R. ( $DTC = T_w - T_{sl}$ )
DTSTR	Maximum temperature difference for nucleate boiling in spraying, °R. ( $DTSTR = T_w - T_{sl}$ )
DTO	Minimum temperature difference for nucleate boiling, °R

<u>Parameter Name</u>	<u>Description</u>
EPSC	Fan stream turbulence factor, dimensionless
EPSH	Core stream turbulence factor, dimensionless
ETA	Augmentor overall combustion efficiency, actual temperature rise/ideal temperature rise, dimensionless
ETAC	Augmentor fan stream combustion efficiency, actual temperature rise/ideal temperature rise, dimensionless
ETAH	Augmentor core stream combustion efficiency, actual temperature rise/ideal temperature rise, dimensionless
FA	Augmentor overall fuel-air ratio, dimensionless. Defined as augmentor total fuel flow/fan stream air flow (STA 3) plus core stream air flow (STA 3H) plus primary engine fuel flow (STA 3H)
FAC	Augmentor fan stream fuel-air ratio, dimensionless. Defined as augmentor fan stream fuel flow/fan stream air flow (STA 3)
FAC(100)	Augmentor fuel-air ratio for each individual fan stream flow tube, dimensionless
FAH	Augmentor core stream fuel-air ratio, dimensionless. Defined as augmentor core stream fuel flow/core stream air flow (STA 3H) plus primary engine fuel flow (STA 3H)
FAH(100)	Augmentor fuel-air ratio for each individual core stream flow tube, dimensionless
FAV	Vitiated fuel-air ratio of core stream at entry to augmentor (STA 3H), dimensionless. Defined as primary engine fuel flow (STA 3H)/core stream air flow (STA 3H)
FHWC(100)	Individual flameholder widths in fan stream, inches
FHWH(100)	Individual flameholder widths in core stream, inches
FTAB(50)	Tabular flowrate values, lbm/hr
LA	Length of augmentor, mixing plane to nozzle (STA 3 to STA 11), inches
LB	Distance from ignition plane to nozzle (STA 4 to STA 11), inches
LC	Length of fan duct, fan discharge to mixing plane (STA 1 to STA 3), inches



<u>Parameter Name</u>	<u>Description</u>
LH	Distance from turbine discharge to mixing plane (STA 2H to STA 3H), inches
LI	Distance from ignition plane to beginning of combustion zone (STA 4 to STA 5), inches
LK	Distance from ignition plane to end of combustion zone (STA 4 to STA 10), inches
LM(16)	Spraying heated length, ft.
LSC	Distance from spraybar to flameholder in fan stream, inches
LSC(100)	Distance from spraybar to flameholder for each individual streamtube in the fan stream, inches
LSH	Distance from spraybar to flameholder in core stream, inches
LSH(100)	Distance from spraybar to flameholder for each individual streamtube in the core stream, inches
L2	Distance from fan duct pressure loss (DPD) to mixing plane (STA 2 to STA 3), inches
M6C	Fan stream Mach number at entry to augmentor (STA 3), dimensionless. (Must be $>0$ .)
M6H	Core stream Mach number at entry to augmentor (STA 3H), dimensionless. (Must be 0.)
M6R	Mach number of mixed augmentor stream flow prior to combustion (STA 4), dimensionless. (Must be 0.)
NOST(16)	Number of streamtubes fed by each spraying, integer (Must be $\geq 1$ .)
NSC(100)	Number of fan stream flow tubes of this type, integer
NSH(100)	Number of core stream flow tubes of this type, integer
NSR	Total number of sprayings, integer
NSRC	Total number of sprayings feeding fan air flow, integer
NSRH	Number of sprayings which feed the core stream air flow, integer
NTAB	Number of points in flowrate table
NTC	Number of streamtube types in the fan flow, integer

<u>Parameter Name</u>	<u>Description</u>
NTH	Number of streamtube types in the core flow, integer
OFFSET(16)	Angle of spraying feed line relative to top dead center of augmentor, degrees. Refer to Figure 21 for details
PCTM(16)	Length split between 4 and 4 directions of spraying relative to feed line, dimensionless (must be $\leq 1.0$ )
PFSR(100)	Individual spraybar fuel pressure for each fan flow tube, psia
PO	Initial spraying internal pressure prior to fuel flow. Generally equal to PS6, psia
PRNOZ	Exhaust nozzle pressure ratio (always $> 1.$ ), dimensionless. If nozzle is choked, any value greater than critical value required to choke nozzle (approximately 2.0) may be input. Exact value of PRNOZ is required only if nozzle is unchoked
PSPLIT(16)	Fraction of input total flowrate fed to a given spraying (must be $\leq 1.0$ ), dimensionless
PS6	Augmentor static pressure at entry to augmentor (STA 3), psia
SBLF(16)	Length of a spraybar which is exposed to fan airflow, feet
STBTIM	Time at which stability calculation is performed, sec
TA(16)	Time at which the control valve for a given spraying starts to open, seconds
TAUCOM	Average value of flameholder wake residence time, seconds
TAUC(100)	Individual streamtube blockage ratio for fan stream, dimensionless
TAUH(100)	Individual streamtube blockage ratio for core stream, dimensionless
TCORE	Core engine time constant, mass of air in core engine volume/mass flowrate of air through the core engine, sec
TEXT(100)	External flow temperature for individual flow tubes in the fan flow, °R

<u>Parameter Name</u>	<u>Description</u>
TF	Fuel temperature at inlet to control, °R
TFHMT(100)	Flameholder metal temperature for each streamtube in fan stream, °R
TFSR(100)	Sprayring fuel temperature for individual streamtubes in fan stream, °R
THM(16)	Sprayring wall thickness, feet
TIME1	First time for stability analysis of combined models, seconds
TIME2	Second time for stability analysis of combined models, seconds
TMAX	Maximum time for sprayring calculations, seconds
TO	Initial air temperature within sprayring, °R
TOL	Iteration between tolerance in sprayring model, dimensionless
TTAB(50)	Times for flowrate table, sec
TWC(16)	Initial wall temperature of portion of spraybar in core stream, °R
TWF(16)	Initial wall temperature of portion of spraybar in fan stream, °R
T3H	Main burner inlet temperature, °R
T6C(100)	Fan stream temperature at entry to augmentor (STA 3), °R
T6H(100)	Core stream temperature at entry to augmentor (STA 3H), for individual flow tubes, °R
V1M(16)	Volume of sprayring ahead of split in feed lines, cubic ft
WCOOL	Ratio of nozzle cooling air to total engine air flow, dimensionless
WEXT(100)	External flow ratio for individual flow tubes in the fan stream, dimensionless

<u>Parameter Name</u>	<u>Description</u>
XLC(100)	Distance from flameholder to nozzle for individual fan stream flow tubes, inches
XLH(100)	Distance from flameholder to nozzle for individual core stream flow tubes, inches
ZEF	Normalized slope, augmentor overall combustion efficiency vs overall fuel-air ratio, $\frac{FA}{ETA} \frac{\partial ETA}{\partial FA} , \text{ dimensionless}$
ZEFC	Normalized slope, augmentor fan stream combustion efficiency vs fan stream fuel-air ratio, $\frac{FAC}{ETAC} \frac{\partial ETAC}{\partial FAC} , \text{ dimensionless}$
ZEFH	Normalized slope, augmentor core stream combustion efficiency vs core stream fuel-air ratio, $\frac{FAH}{ETAH} \frac{\partial ETAH}{\partial FAH} , \text{ dimensionless}$
ZEFP	Normalized slope, augmentor overall combustion efficiency vs fuel-air ratio of the pilot burner, $\frac{FAP}{ETA} \frac{\partial ETA}{\partial FAP} , \text{ dimensionless}$
ZEP	Normalized slope, augmentor overall combustion efficiency vs pressure at ignition plane, $\frac{P}{ETA} \frac{\partial ETA}{\partial P} , \text{ dimensionless}$
ZEPC	Normalized slope, augmentor fan stream combustion efficiency vs pressure at ignition plane, $\frac{P}{ETAC} \frac{\partial ETAC}{\partial P} , \text{ dimensionless}$
ZEPH	Normalized slope, augmentor core stream combustion efficiency vs pressure at ignition plane, $\frac{P}{ETAH} \frac{\partial ETAH}{\partial P} , \text{ dimensionless}$

Parameter Name

Description

ZETC

Normalized slope, augmentor fan stream combustion efficiency vs fan stream entry temperature,

$$\frac{T6C}{ETAC} \frac{\partial ETAC}{\partial T6C}, \text{ dimensionless}$$

ZETH

Normalized slope, augmentor core stream combustion efficiency vs core stream entry temperature,

$$\frac{T6H}{ETAH} \frac{\partial ETAH}{\partial T6H}, \text{ dimensionless}$$

ZEVC

Normalized slope, augmentor fan stream combustion efficiency vs fan stream entry velocity,

$$\frac{V}{ETAC} \frac{\partial ETAC}{\partial V}, \text{ dimensionless}$$

ZEVH

Normalized slope, augmentor core stream combustion efficiency vs core stream entry velocity,

$$\frac{V}{ETAH} \frac{\partial ETAH}{\partial V}, \text{ dimensionless}$$

### c. Input Setup

In addition to the "Namelist" input, the program requires input for: (a) additional optional ratio calculations, (b) output plot selection and format, and (c) frequency range and increment selection. The input setup is shown in Figure 30 and is described below.

- (1) Each input case requires a title card. Column 1 for the first case must contain a 1. The "Namelist" input must be preceded by an & INPUT starting in column 2 and followed by an & END starting in column 2. The "Namelist" input (Columns 2-80) required for each case is presented in Figures 22 and 23. Each input must be separated by a comma (see Figure 26). The ratio calculations, plot setup and frequency selection must follow the first input case. For additional input cases, follow the frequency selection cards with a blank card and then the additional title cards and input cases. Only those parameters that differ from the previous case must be input. For the additional input cases, if column 1 of the title card contains a 1, the ratio calculations, plot setup and frequency selection will be the same as the preceding case. If column 1 of the title card contains a 1, new ratio calculations, plot setup and frequency selection may be input.
- (2) Additional ratio calculations may be performed by inputting the parameter identification numbers as indicated in Figure 26. Up to 40 ratios may be calculated and these ratios will automatically be included in the tabular output. The parameter identification numbers are presented in Figure 27. One blank field will terminate this type input. If columns 71-75 are used, a blank card must follow.
- (3) Calcomp plots of any rumble model output parameter may be obtained by inputting one card for each parameter as described below. A maximum of 10 plots may be requested for any case. A blank card must be input to terminate plot requests or if no plots are desired.

Column 1 - 3	— Output Parameter No., right adjusted (integer; no decimal)
Column 11 - 20	— Amplitude Option (decimal required)
Column 21 - 30	— Phase Option (decimal required)
Column 31 - 40	— Frequency Option (decimal required)
Column 41 - 50	— Amplitude Factor (decimal required)
Column 51 - 60	— Frequency Factor (decimal required)
Column 61 - 70	— XMIN (decimal required)
Column 71 - 80	— XMAX (decimal required)

# FORTRAN CODING FORM

ANALYST

ENGINEER

EXT

**ON BOARD**

COST CONTROL NO

C	NO.	X	PORTMAN STATEMENT	LABEL
1	2	3	4	5
6	7	8	9	10
11	12	13	14	15
16	17	18	19	20
21	22	23	24	25
26	27	28	29	30
31	32	33	34	35
36	37	38	39	40
41	42	43	44	45
46	47	48	49	50
51	52	53	54	55
56	57	58	59	60
61	62	63	64	65
66	67	68	69	70
71	72	73	74	75
76	77	78	79	80
81	82	83	84	85
86	87	88	89	90
91	92	93	94	95
96	97	98	99	100

Title Card  
 RUN CALC FLOW  
 INPUT  
 Namelist Input, Col's 2 Thru 80, as Req'd (See Fig 15)  
 log BPR = 59, DPD = 064, LA = 72, etc  
 S1/S2, S1/S2, S1/S2, etc  
 END  
 Additional Ratio Calculations, S1 and S2 are the Parameter Identification Numbers of the  
 Calculated Parameters (See Fig 19). Maximum Number of Ratio Calculations is 40 (5 Cards).  
 Input Must Be in the First 5 Columns of Each Field of 10. One Blank Field Will Terminate this Type Input.  
 If Columns 71-75 Are Used, a Blank Card Must Follow.  
 Par No. Amplitude Option Phase Option Frequency Option Amplitude Factor Frequency Factor XMin XMax  
 Plot Setup Cards (One Card for Each Parameter to be Plotted See Section II 6. c.3 for Details)  
 Blank Card  
 Max Freq Increment Max Freq Increment Max Freq Increment Frequency  
 Frequency Range and Increment Selection. Must be 3 Cards  
 Input Blank Cards if Required. Frequency and Increments Input in Hertz.  
 The Program Will Cycle Thru Each Frequency for Each Case  
 Frequency Etc  
 Additional Independent Frequencies for Each Case. Each Frequency Input in Fields of 10.  
 7 Field Per Card (500 Frequencies Max) A Field Containing -1 Will Terminate this Input  
 If Last Freq in Field 7, an Additional Card With -1 in Field 1 is Required

000,000

Figure 26. Combined Rumble Model Input Setup

Output Parameter Name	Parameter Identification Number
P1	1
V1	2
R1	3
P2	4
V2	5
R2	6
P3	7
V3	8
R3	9
P3H	10
V3H	11
R3H	12
P2H	13
V2H	14
R2H	15
QIN	16
W3	17
W3H	18
QOUT	19
P4	20
V4	21
R4	22
P5	23
V5	24
R5	25
P6	26
V6	27
R6	28
P7	29
V7	30
R7	31
P8	32
V8	33
R8	34
P9	35
V9	36
R9	37
P10	38
V10	39
R10	40
P11	41
V11	42
R11	43

Note:  $P1 = P1/Q_{IN} = (\Delta P_1/P_1)/(\Delta Q_{IN}/Q_{IN})$  Same for Other Output Parameters

Figure 27. Parameter Identification Numbers



- *Output Parameter No.*

A list of output parameter identification numbers is presented in Figure 31. If any of the additional ratio calculations (described above) are to be plotted, parameter identification numbers starting at 101 and incremented by 1 are used. The parameter identification numbers must be right adjusted in columns 1-3.

- *Amplitude Option*

If Amplitude Option = 0., Log (amplitude) will be plotted.  
If Amplitude Option = 1., Amplitude will be plotted.

- *Phase Option*

If Phase Option = 0., Phase angle of 0 to -360 will be plotted.  
If Phase Option = 1., Phase angle of 180 to -180 will be plotted.

- *Frequency Option*

If Frequency Option = 0., Log (Frequency) will be plotted.  
If Frequency Option = 1., Frequency will be plotted.

- *Amplitude Factor*

If Amplitude Option = 0., the Amplitude Factor must be input as a number which could be written as  $10^N$ , where  $N = (\pm)$  integer. Log (Amplitude Factor) will be added to the base Log amplitude scale, where the base Log amplitude scale ranges from -1.0 to 2.0.

If Amplitude Option = 1., the Amplitude Factor becomes a multiplier for the base amplitude scale, where the base amplitude scale ranges from 0. to 3.0.

- *Frequency Factor*

If Frequency Option = 0., the Frequency Factor must be input as a number which could be written as  $10^N$ , where  $N = (\pm)$  integer. Frequency factor will be a multiplier for the base frequency scale, where the base frequency scale ranges from .1 to 100.

If Frequency Option = 1., the Frequency Factor will be a multiplier for the base frequency scale, where the base frequency scale ranges from 0. to 100., unless XMIN and XMAX are input. XMIN is the minimum value for the frequency scale when Frequency Option = 1. XMAX is the maximum value for the frequency scale when Frequency Option = 1. If either Amplitude Factor or Frequency Factor is input at 0. when XMIN and XMAX are input, the program automatically sets Amplitude Factor or Frequency Factor to 1.

- (4) The frequencies used in the program calculations are input in two parts. First, there are three cards which contain the minimum frequency, increment and maximum frequency (see Figure 24). The increment is used to determine each frequency for the range defined. Additional independent frequencies (up to 500 values) may be input in fields of 10, 7 fields per card. A field containing -1. will terminate this input. If the 7th field of the last card is used, an additional card with -1. in the first field is required.
- (5) The rumble model has been set up to model a turbofan engine with a mixed flow augmentor. To model a turbojet (no fan), set BPR = 0 and NFSOP = 1. To model a fan duct augmentor (separate fan and core flows), set BPR =  $10^{10}$  and NFSOP = 1.

## **8. OUTPUT**

### **a. General**

This section is presented in three parts: (1) spraying model output, (2) combustion model output, and (3) rumble model output. The tabular or printed output for all output options is presented for the three models. The outputs are presented in the order in which they appear for a full-combined model run (IRUN = 6).

### **b. Output Description**

- (1) The first output is a full printing of the input for the case which is run. This is titled INPUT LISTING and is a direct repeat of all input values.
- (2) The second output is a printing of all default parameters. If a required input value has not been listed, the program will supply a reasonable value from an internal library. The user should check this listing to determine if the default value is appropriate to the particular problem being analyzed.
- (3) The third section prints all the namelist parameters in an expanded format for verification purposes. This list includes both input and default values and represents the actual parameter values used in the computer run.
- (4) The next section will write any check errors for erroneous input values. If an input error is detected, the program will terminate.

- (5) If the spraying and flameholder combustion model have both been executed (IRUN = 4 or 6), the next output section will print the results of the geometric compatibility subroutine. This subroutine (ASSOC) assigns a specific portion of one spraying to a given streamtube. Some of the output is an appropriate input listing. The new output parameters are:

<u>Parameter Name</u>	<u>Description</u>
SR	Spraying identification number
NOST	Number of streamtubes fed by this spraying
NFST	The number of the first streamtube fed by this spraying
NLST	The number of the last streamtube fed by this spraying
SUMDEG	Total degrees of spraying to be analyzed. Equal to 360 and OFFSET
SECDEG	Number of degrees in the repeating spraying sectors
TUBDEG	Number of degrees of spraying per streamtube
ST	Streamtube identification number
IBEGH IBEGC	Identification number of the first spraying sector feeding this streamtube in fan (IBEGC) or core (IBEGH).
IENDH IENDC	Identification number of the last spraying sector feeding this streamtube in fan (IENDC) or core (IENDH).
FRACBH FRACBC	The fraction of IBEGC/IBEGH which feeds this streamtube
FRACEH FRACEC	The fraction of IENDC/IENDH which feeds this streamtube
WIDTH	The width of this streamtube, inches.

(6) Sprayring Model Output

This section presents the results of the spraying model. A review of the appropriate input is printed first. Next follows a tabular listing of the model output as a function of time. The time between print steps is controlled by DEL and NPRINT inputs.

<u>Parameter Name</u>	<u>Description</u>
TIME	Time from the start of the flow calculations, seconds
N	Identification number of the spraying
A(N)	Distribution valve open area, ft <sup>2</sup>
P(I)	Supply pressure, psia
X	Axial location of the fluid fuel face in the x-direction, feet
X-XO	Length of the two-phase region in the x-direction, feet
Y	Axial location of the fluid fuel face in the y-direction, feet
Y-YO	Length of the two-phase region in the y-direction, feet
ALPX	Void fraction in the x two-phase region
ALPY	Void fraction in the y two-phase region
PRESS	Sprayring pressure, psia
FLOWIN	Fuel flowrate into the sprayring, lbm/hr
TW(I)	Wall temperature at sprayring inlet, °R
TW(E)	Wall temperature at sprayring exit, °R
TOTFLOW	Total fuel flow rate out of the sprayring into the streamtubes, lbm/hr
L FLOW	Liquid fuel flowrate out of the sprayring into the streamtubes, lbm/hr
AXMXO	Equals ALPX · (X-XO)
AYMXO	Equals ALPY · (Y-YO)

At the completion of the tabular output versus time, the calculated fuel flowrate and fuel-air ratio values are printed. The fuel flowrate is printed in lbm/sec units. Also printed are the fuel flowrates from each section of the sprayring (SRFUEL) in lbm/sec units.

(7) Flameholder combustion model full tabular output.

<u>Parameter(s)</u>	<u>Description</u>
Fan Stream	Identifies following sections as fan duct output
Streamtube type	Identifies for this set of input variables
No. of this type	The number of streamtubes with this set of input variables
Static Pressure (PS6)	Inlet static pressure, psia
Approach Temperature (T6C)	Inlet temperature, °R
Approach Mach No. (M6C)	Inlet flow Mach No., d'less
Input FA Ratio (FAC)	Inlet fuel-air ratio, d'less
Effective FA Ratio	Effective fuel-air ratio accounting for liner cooling air flow
F/H Width (FHWC)	Flameholder width, inches
Blockage Ratio (TAUC)	Ratio of flameholder width to stream tube width, d'less
F/H Apex Angle (ALPHAC)	V-gutter flameholder apex angle, degrees
S/R Fuel Temperature (TFSR)	Temperature of the fuel within spraying, °R
S/R Fuel Pressure (PFSR)	Pressure of the fuel within the spraying, psia
S/R to F/H Distance (LSC)	Axial separation distance between the spraying and the flameholder, inches
F/H to Nozzle Distance (XLC)	Axial distance from the flameholder to the exhaust nozzle throat, inches
Turbulence Level (EPSC)	Ratio of RMS turbulence velocity to the approach velocity at the inlet, d'less
Wake Flow Addition (WEXT)	Ratio of external wake flow to recirculated flow, d'less
Flow Source Temperature (TEXT)	Temperature of above flow, °R
Effective Inlet Temperature	Mass average of WEXT flow at TEXT and recirculated flow at T6C, °R

<u>Parameter(s)</u>	<u>Description</u>
Fuel Type (JFUEL)	Identifies for fuel 1 = JP-4 2 = JP-5
F/H Temperature	Flameholder metal temperature, °R
Mean droplet size	The mass median droplet size produced by the injector, microns
Flash vaporization	Fraction of the liquid fuel which is vaporized by injection from PFSR to PS6, d'less
Beta 1	Droplet vaporization fraction
Beta 2	Droplet collection fraction
Beta 3	Surface vaporization fraction
K1	Recirculation fraction
Wake FA	Flameholder wake vapor phase fuel-air ratio, d'less
Wake temperature	Reaction temperature in the flameholder, ft/sec
Initial speed	Laminar flame speed at the flameholder, ft/sec
Initial turbulence	Turbulence intensity at the flameholder, d'less
Ideal temperature rise	Ideal temperature rise for effective fuel-air ratio, °R
Efficiency	Streamtube combustion efficiency; ratio of flame penetration to streamtube width, d'less
Actual temperature rise	Efficiency times ideal temperature rise, °R
Exit temperature	Streamtube exit temperature without liner cooling air, °R
Flowrate — air	Air flowrate for this streamtube, lbm/sec
Flowrate — fuel	Fuel flowrate for this streamtube, lbm/sec
Cooling flow/total engine flow (WCOOL)	Ratio of liner cooling air flowrate to total engine flowrate, d'less

<u>Parameters</u>	<u>Description</u>
Chemical combustion efficiency	Average efficiency based on average streamtube exit temperature and average effective fuel-air ratio, d'less
Thermal combustion efficiency	Average efficiency based on streamtube average exit temperature plus cooling air and average input fuel-air ratio, d'less
Average cooling air temperature	Mass averaged inlet temperature used for cooling, °R
Average streamline exit temperature	Mass average of the streamtubes without cooling air, °R
Average duct exit temperature	Mass average of streamtubes plus cooling air, °R
Total flowrate	Total of each streamtube type times the number of each type, lbm/sec
Average fuel air-ratio	Mass average of the input fuel-air ratios
Core stream	Identified following sections as core stream output
Wake recirculation coefficient	Same as K1 in fan duct, d'less
Ideal temperature rise	Ideal temperature rise based on input fuel-air ratio and main burner fuel-air ratio. See Appendix B
M/B Fuel-air ratio	Fuel-air ratio of the vitiated air entering the core streamtubes
M/B Inlet temperature	Inlet temperature to the main burner, d'less
Average distance from spraybar to F/H	Average axial distance from the spraybars to the flameholders, inches

Note: Any core stream parameters which are not listed above have the same definition as their fan stream counterpart.

(4) Flameholder combustion model limited tabular output.

<u>Parameters</u>	<u>Description</u>
Fan stream	Identifies following as fan stream cases input and output
Inlet temperature (T6C)	Streamtube inlet temperature, °R
Fuel-air ratio (FAC)	Input fuel-air ratio, d'less.

<u>Parameter(s)</u>	<u>Description</u>
Average inlet temperature	Mass averaged inlet temperature, °R
Ideal temperature rise	Streamtube ideal temperature rise based on effective fuel-air ratio, °R
Combustion efficiency	Streamtube combustion efficiency, d'less
Exit temperature	Streamtube exit temperature based on effective fuel-air ratio, °R
Average ideal temperature rise	Ideal temperature rise based on average input fuel-air ratio, °R
Average combustion efficiency	Efficiency based on average ideal temperature rise with cooling air effect included, d'less
Average exit temperature	Exit temperature including cooling air, °R
Core stream	Identifies following as core stream section
Mach No.	Streamtube inlet flow Mach number, d'less
Average ideal temperature rise	Ideal temperature rise based on average input fuel-air ratio, °R
Average combustion efficiency	Efficiency based on average temperature rise and average ideal temperature rise, d'less
Average exit temperature	Exit temperature based on mass averaged actual temperature rise, °R

(8) Rumble model tabular output (listed in the order they appear):

<u>Parameter(s)</u>	<u>Description</u>
NAMelist INPUT	The "namelist" input parameters and the values input are listed for verification
KNOZ	A parameter that relates the influence of pressure at STA 11 on velocity at STA 11, dimensionless
FAAB	Augmentor overall fuel-air ratio, dimensionless
ETAAB	Augmentor overall efficiency, dimensionless
DTIAB	Augmentor overall ideal temperature rise, °R



<u>Parameter(s)</u>	<u>Description</u>
DTAB	Augmentor overall actual temperature rise, °R
T6M	Augmentor mixed temperature before combustion (STA 3), °R
TKC	Augmentor mixed exhaust temperature (STA 10), °R
XLHV	Lower heating value for the fuel selected, Btu/lbm
DTC	Fan stream temperature rise, °R
QCQT	Fraction of total heat release contributed to fan stream, dimensionless
DTIC	Fan stream ideal temperature rise, °R
TAUDC	Fan stream drift delay from spraybar to flameholder, sec
DTH	Core stream temperature rise, °R
QHQT	Fraction of total heat release contributed by core stream, dimensionless
DTIH	Core stream ideal temperature rise, °R
TAUDH	Core stream drift delay from spraybar to flameholder, sec
ZTFC	Normalized slope, augmentor fan stream ideal temperature rise vs fan stream fuel-air ratio, $\frac{FAC}{DTIC} \frac{\partial DTIC}{\partial FAC}$ , dimensionless.
	DTIC FAC
ZTFH	Normalized slope, augmentor core stream ideal temperature rise vs core stream fuel-air ratio $\frac{FAH}{DTIH} \frac{\partial DTIH}{\partial FAH}$ , dimensionless.
	DTIH ∂FAH
L (1-11)	Distance between model stations, in.
YL (1-11)	Station locations references to STA 1, inches

<u>Parameter(s)</u>	<u>Description</u>
C (1-11)	Velocity of sound at each station, in./sec
CH	Velocity of sound in core stream at STA 3H, in./sec
M (1-11)	Mach number at each station, dimensions
MH	Mach number in core stream at STA 3H, dimensionless
T (1-11)	Temperature at each station, °R
TH	Temperature in core stream at STA 3H, °R
PRHOT	Pressure drop through combustion zone (STA 5 - STA 10), psia
G (1-11)	Ratio of specific heats at each station, dimensionless
GH	Ratio of specific heats in a core stream at STA 3H, dimensionless
TAUF (1-11)	Time delays for downstream running sonic waves between stations, sec
TAUFH	Time delay for downstream running sonic wave between STA 2H and 3H, sec
TAUG (1-11)	Time delays for upstream running sonic waves between stations, sec
TAUGH	Time delay for upstream running sonic wave between STA 2H and 3H, sec
TAUE (1-11)	Time delays for downstream running entropy waves between stations, sec
TAUEH	Time delay for downstream running entropy wave between STA 2H and 3H, sec
QOP (1-11)	Ratio of volumetric heat release rate at each station to pressure at each station, 1/sec
(2) Rumble model Open Loop Transfer Function plots. Each plot consists of Open Loop Transfer Function Gain vs frequency and phase vs frequency for the parameters selected.	

## 9. PROGRAM MESSAGES AND LIMITS

### a. Input Checks

The program checks all inputs to see if the inputs are missing or equal the default values built into the deck. Missing inputs are set equal to the default values. A warning message (presented below) is printed to alert the user if default input values are identified. The program also checks specific inputs to ensure reasonable input data. If these data checks are not satisfied, the run will be canceled. These checks and corresponding print-out messages are presented below:

<u>Condition</u>	<u>Message</u>
Input value = default value or no input for certain parameter	WARNING — PARAMETER XXXXXX = YYY.Y is a default value
$LA < LB$ , where LK and LB are Rumble Model Inputs	INPUT ERROR 1 — LA must be greater than or equal to LB
$LK > LB$ , where LK and LB are Rumble Model Inputs	INPUT ERROR 2 — LB must be greater than or equal to LK
$LA < LCALC$ , where $LCALC = LB$ + MAX (LSC, LSH)	INPUT ERROR 3 — LA must be greater than or equal to the sum of LB plus the max of LSC or LSH. LA has been adjusted accordingly. Check input.
$LI \geq LK$	INPUT ERROR 4 — LI must be less than LK.
$LC < L2$	INPUT ERROR 5 — LC must be greater than or equal to L2.
$ETA < 0$ or $> 1$ .	INPUT ERROR 6 — ETA must be between 0 and 1.
$ETAC < 0$ or $> 1$ .	INPUT ERROR 7 — ETAC must be between 0 and 1.
$ETAH < 0$ or $> 1$ .	INPUT ERROR 8 — ETAH must be between 0 and 1.
$(FAC + FAH) = 0$	INPUT ERROR 9 — FAC and FAH cannot both be zero with augmentor on.

Condition

$$[FAV + (1 + FAV) FAH] \times$$

$$\left[ \frac{XLHV}{18500.} \right] \geq 0.09$$

$$\text{or if (FAC)} \left[ \frac{XLHV}{18500.} \right] \geq 0.09$$

$$NFSOP = 2 \text{ and } BPR = 0.$$

$$DPCS < 0 \text{ or } > 1.$$

$$DPD < 0 \text{ or } > 1.$$

$$DPH < 0 \text{ or } > 1.$$

$$DPHS < 0 \text{ or } > 1.$$

$$DPS < 0 \text{ or } > 1.$$

$$T3H \geq 2200.$$

$$BPR < 0.$$

$$FAV < 0.$$

$$NAUGOP \leq 0. \text{ or } > 3.$$

$$NFSOP \leq 0 \text{ or } > 2.$$

$$IRUN \leq 0 \text{ or } > 6.$$

$$JFUEL \leq 0 \text{ or } > 2.$$

Message

INPUT ERROR 10 -- Core or fan stream total fuel-air ratio exceeds limits of ideal temperature rise curve. Blowout likely.

INPUT ERROR 11 -- BPR cannot be zero when the remote flow splitter option is selected.

INPUT ERROR 12. -- DPCS must be between 0 and 1.

INPUT ERROR 13 -- DPD must be between 0 and 1.

INPUT ERROR 14 -- DPH must be between 0 and 1.

INPUT ERROR 15 -- DPHS must be between 0 and 1.

INPUT ERROR 16 -- DPS must be between 0 and 1.

INPUT ERROR 17 -- T3H exceeds limits of ideal temperature rise curve. T3H must be less than 2200°R.

INPUT ERROR 18 -- BPR must be equal to or greater than 0.

INPUT ERROR 19 -- FAV must be equal to or greater than 0.

INPUT ERROR 20 -- NAUGOP must be 1, 2 or 3.

INPUT ERROR 21 -- NFSOP must be 1 or 2.

INPUT ERROR 22 -- IRUN must be 1, 2, 3, 4, 5 or 6.

INPUT ERROR 23 -- JFUEL must be 1 or 2.

<u>Condition</u>	<u>Message</u>
$\text{NPRNTR} < 0 \text{ or } > 1.$	INPUT ERROR 24 — NPRNTR must be 0 or 1.
$\text{NPRNTF} < 0 \text{ or } > 1.$	INPUT ERROR 25 — NPRNTF must be 0 or 1.
$\text{M6C} \leq 0$	INPUT ERROR 26 — M6C must be greater than 0.
$\text{M6H} \leq 0$	INPUT ERROR 27 — M6H must be greater than 0.
$\text{M6R} \leq 0$	INPUT ERROR 28 — M6R must be greater than 0.
$\text{LI} < 0$	INPUT ERROR 29 — LI must be equal to or greater than 0.
$\text{LK} \leq 0$	INPUT ERROR 30 — LK must be greater than 0.
$\text{LA} \leq 0$	INPUT ERROR 31 — LA must be greater than 0.
$\text{LB} \leq 0$	INPUT ERROR 32 — LB must be greater than 0.
$\text{LC} \leq 0$	INPUT ERROR 33 — LC must be greater than 0.
$\text{LSC} \geq \text{LA}$	INPUT ERROR 34 — LSC must be less than LA.
$\text{LSH} \geq \text{LA}$	INPUT ERROR 35 — LSH must be less than LA.
$\text{LH} \leq 0$	INPUT ERROR 36 — LH must be greater than 0.
$\text{L2} < 0$	INPUT ERROR 37 — L2 must be greater than or equal to 0.
$\text{TCORE} < 0$	INPUT ERROR 38 — TCORE must be equal to or greater than 0.
$\text{PS6} \leq 0$	INPUT ERROR 39 — PS6 must be greater than 0.
$\text{T6C} \leq 0$	INPUT ERROR 40 — T6C must be greater than 0.

Condition

Message

$T6H \leq 0$

INPUT ERROR 41 — T6H must be greater than 0.

$T3H \leq 460.$

INPUT ERROR 42 — T3H must be greater than 460.

$FA < 0$

INPUT ERROR 43 — FA must be greater than or equal to 0.

$FAC < 0$

INPUT ERROR 44 — FAC must be greater than or equal to 0.

$FAH < 0$

INPUT ERROR 45 — FAH must be greater than or equal to 0.

$PRNOZ \leq 1$

INPUT ERROR 46 — PRNOZ must be greater than 1.

$ALPHAC (100) \leq 0 \text{ or } > 180$

INPUT ERROR 47 — ALPHAC must be greater than 0 and less than or equal to 180 deg.

$ALPHAH (100) \leq 0 \text{ or } > 180$

INPUT ERROR 48 — ALPHAH must be greater than 0 and less than or equal to 180 deg.

$ESPC < 0 \text{ or } > 1$

INPUT ERROR 49 — EPSC must be greater than or equal to 0 and less than or equal to 1.

$EPSH < 0 \text{ or } > 1$

INPUT ERROR 50 — EPSH must be greater than or equal to 0 and less than or equal to 1.

$FAC (100) \leq 0$

INPUT ERROR 51 — FAC must be greater than 0.

$FAH (100) \leq 0$

INPUT ERROR 52 — FAH must be greater than 0.

$FAV > 0.068$

INPUT ERROR 53 — FAV cannot exceed stoichiometric (0.068).

$FHWC (100) \leq 0$

INPUT ERROR 54 — FHWC must be greater than 0.

$FHWH (100) \leq 0$

INPUT ERROR 55 — FHWH must be greater than 0.

$LSC (100) \leq 0$

INPUT ERROR 56 — LSC must be greater than 0.

Condition

Message

LSH (100)  $\leq 0$

INPUT ERROR 57 -- LSH must be greater than 0.

$\frac{M6C}{1-TAUC (100)} > 1.$

INPUT ERROR 58 -- Flow is supersonic in fan stream at the flameholder plane.

$\frac{M6H}{1-TAUH (100)} > 1.$

INPUT ERROR 59 -- Flow is supersonic in core stream at the flameholder plane.

NSC (100)  $< 0$  or  $> 100.$

INPUT ERROR 60 -- NSC must be greater than or equal to 0 and less than or equal to 100.

NSH (100)  $< 0$  or  $> 100.$

INPUT ERROR 61 -- NSH must be greater than or equal to 0 and less than or equal to 100.

NTC  $< 0$  or  $> 100.$

INPUT ERROR 62 -- NTC must be greater than or equal to zero and less than or equal to 100.

NTH  $< 0$  or  $> 100$

INPUT ERROR 63 -- NTH must be greater than or equal to 0 and less than or equal to 100.

PFSR (100)  $\leq PS6$

INPUT ERROR 64 -- PFSR must be greater than PS6.

TAUC (100)  $\leq 0$  or  $\geq 1.$

INPUT ERROR 65 -- TAUC must be greater than 0 and less than 1.

TAUH (100)  $\leq 0$  or  $\geq 1.$

INPUT ERROR 66 -- TAUH must be greater than 0 and less than 1.

TEXT (100)  $< 460.$

INPUT ERROR 67 -- TEXT must be greater than or equal to 460.

TFSR (100)  $< 460.$

INPUT ERROR 68 -- TFSR must be greater than or equal to 460°R.

T6C (100)  $\leq 460.$

INPUT ERROR 69 -- T6C must be greater than 460.

T6H (100)  $\leq 460.$

INPUT ERROR 70 -- T6H must be greater than 460.

WEXT (100)  $< 0$

INPUT ERROR 71 -- WEXT must be greater than or equal to 0.

Condition

Message

$XLC(100) \leq 0$

INPUT ERROR 72 — XLC must be greater than 0.

$XLH(100) \leq 0$

INPUT ERROR 73 — XLH must be greater than 0.

$WCOOL < 0$  or  $\geq 1$ .

INPUT ERROR 74 — WCOOL must be greater than or equal to 0 and less than 1.

$ALM(16) \leq 0$

INPUT ERROR 75 — ALM must be greater than 0.

$ALPHAO < 0$  or  $\geq 1$

INPUT ERROR 76 — ALPHO must be greater than or equal to 0 and less than 1.

$AM(16) \leq 0$

INPUT ERROR 77 — AM must be greater than 0.

$AO(16) \leq 0$

INPUT ERROR 78 — AO must be greater than 0 if IFLOW = 1.

$BLM(16) < 0$

INPUT ERROR 79 — BLM must be greater than or equal to 0.

$CF \leq 0$

INPUT ERROR 80 — CF must be greater than 0.

$DEL \leq 0$

INPUT ERROR 81 — DEL must be greater than 0.

$DELR(16) \leq 0$

INPUT ERROR 82 — DELR must be greater than 0.

$DF < 0$

INPUT ERROR 83 — DF must be greater than or equal to 0.

$DM(16) \leq 0$

INPUT ERROR 84 — DM must be greater than 0.

If IFLOW = 1,  $DTA(16) < 0$

INPUT ERROR 87 — DTA must be greater than or equal to 0, if IFLOW = 1.



Condition

Message

If IFLOW = 1, DTA (16)  $\geq$  TMAX

INPUT ERROR 88 — DTA must be less than TMAX, if IFLOW = 1.

DTC  $\leq$  0

INPUT ERROR 89 — DTC must be greater than 0.

DTSTR  $\leq$  0

INPUT ERROR 90 — DTSTR must be greater than 0.

DTO  $\leq$  0

INPUT ERROR 91 — DTO must be greater than 0.

DTO  $\geq$  DTSTR

INPUT ERROR 92 — DTO must be less than DTSTR.

DTSTR  $\geq$  DTC

INPUT ERROR 93 — DTSTR must be less than DTC.

LM (16)  $\leq$  0

INPUT ERROR 95 — LM must be greater than 0.

NOST (16)  $<$  1

INPUT ERROR 96 — NOST must be greater than or equal to 1.

NSR  $<$  1

INPUT ERROR 97 — NSR must be greater than or equal to 1.

NSRC  $<$  0

INPUT ERROR 98 — NSRC must be greater than or equal to 0.

NSRH  $<$  0

INPUT ERROR 99 — NSRH must be greater than or equal to 0.

NSR = (NSRC + NSRH)

INPUT ERROR 100 — NSR must equal NSRC plus NSRH.

OFFSET (16)  $<$  0 or  $>$  180

INPUT ERROR 101 — OFFSET must be greater than or equal to 0 and less than or equal to 180.

PCTM (16)  $>$  1.0

INPUT ERROR 102 — PCTM must be less than or equal to 1.

Condition

Message

$PO \leq 0$

INPUT ERROR 105 — PO must be greater than 0.

$PSPLIT(16) < 0$

INPUT ERROR 106 — PSPLIT must be greater than or equal to 0.

$SBLF(16) \leq 0$

INPUT ERROR 109 — SBLF must be greater than 0.

$STBTIM \leq 0$  or  $> TMAX$

INPUT ERROR 110 — STBTIM must be greater than 0 and less than or equal to TMAX.

$TA(16) < 0$  or  $> TMAX$

INPUT ERROR 111 — TA must be greater than or equal to 0 and less than or equal to TMAX.

$TAUCOM < 0$

INPUT ERROR 112 — TAUCOM must be greater than or equal to 0.

$TF \leq 0$

INPUT ERROR 113 — TF must be greater than 0.

$TFSR(100) \leq 0$

INPUT ERROR 114 — TFSR must be greater than 0.

$THM(16) \leq 0$

INPUT ERROR 115 — THM must be greater than 0.

$TMAX \leq 0$

INPUT ERROR 116 — TMAX must be greater than 0.

$TO \leq 0$

INPUT ERROR 117 — TO must be greater than 0.

$TOL < 0$  or  $\geq TMAX$

INPUT ERROR 118 — TOL must be greater than or equal to 0 and less than TMAX.

$TWC(16) \leq 0$

INPUT ERROR 119 — TWC must be greater than 0.

$TWF(16) \leq 0$

INPUT ERROR 120 — TWF must be greater than 0.

Condition

Message

V1M (16)  $\leq 0$

INPUT ERROR 121 — V1M must be greater than 0.

V2M (16)  $\leq 0$

INPUT ERROR 122 — V2M must be greater than 0.

V3M (16)  $\leq 0$

INPUT ERROR 123 — V3M must be greater than 0.

If IFLOW = 2, NTAB  $\leq 0$  or  $> 50$

INPUT ERROR 129 — NTAB must be greater than 0 and less than or equal to 50 when IFLOW = 2.

IFLOW  $\neq 1$  or 2

INPUT ERROR 132 — IFLOW must be equal to 0 or 1.

Condition

Message

If IFLOW = 2, PSPLIT (16)  $\leq$  0

INPUT ERROR 136 — PSPLIT must be greater than 0 when IFLOW = 2.

NPRINT < 1

INPUT ERROR 138 — NPRINT must be equal to or greater than 1.

NPRINT > (TMAX/DEL)

INPUT ERROR 139 — NPRINT cannot exceed the number of time steps calculated (TMAX/DEL).

**b. Calculation Failure Messages for Flameholder Combustion Model**

The Flameholder Combustion Model program checks for specific calculation failures. The causes and corresponding messages are presented below:

Message

Cause

Warning \*\*\* wake temperature iteration failed for streamtube No. XX

The calculated value of the fan duct flameholder wake fuel-air ratio exceeds the rich limit at the inlet conditions for this streamtube. This streamtube case has failed.

Aerodynamic loading exceeds kinetic capacity

The inlet values of velocity, pressure, and temperature produce a wake loading which exceeds the reaction limit at this fuel-air ratio. This streamtube case has failed.

All fuel vaporized — terminate case

The injection process has resulted in only vapor fuel. Run this input as a core case if desired.

Overall fuel-air ratio below lean limit

The input fuel-air ratio is less than the calculated minimum value for flame propagation in the fan stream.

FAR outside flammability limit

The input fuel-air ratio is outside the limits of the data for laminar flame speed built into the program. Currently set at 0.027 lean and 0.120 rich limit fuel-air ratios.

**10. PROGRAM LISTINGS**

Complete listings of the computer program are provided in Appendix C.

## 11. TEST CASES

The test cases which follow are provided in Appendix D. These cases were selected to provide the prospective user with a broad range of the potential combinations of the various input options. All input parameters have been used, even if the value was the same as a default value. Prior to executing a new case, the user should become familiar with the appropriate test case.

<i>Test Case</i>	<i>Models Executed</i>			<i>IRUN</i>	<i>NAUGOP</i>	<i>Notes</i>
	<i>Sprayring</i>	<i>Combustion</i>	<i>Rumble</i>			
1	X	—	—	1	—	
2	—	X	—	2	—	
3	—	—	X	3	1	V-gutter F/H
4	—	—	X	3	2	Vorbix augmentor
5	—	—	X	3	3	Swirl augmentor
6	X	X	—	4	—	
7	—	X	X	5	1	
8	X	X	X	6	1	

All of these were executed with JP4 fuel, input fuel flowrates for the sprayring model and remote splitter for the rumble model. Full output was selected in all cases.

## **12. PROGRAM IDENTIFICATION AND REVISION PROCEDURE**

### **a. CCD Number**

Customer Computer Decks (CCD's) are identified by a CCD number and date. An example is CCD 1001=0.0 November 15, 1969.

The CCD number consists of:

- Basic number (first four digits)
- Dash (no change) number
- Decimal (or addition/correction) number.

#### **(1) Basic Number**

This four-digit number generally corresponds to a given program. If another method is developed or studied which does not replace or supersede the original, a new four-digit number is issued.

#### **(2) Dash Number**

Major changes in the program are reflected in different dash numbers. A change in techniques or mathematical methods would produce a new dash number provided the new techniques replace or change the old techniques. For more than nine changes, the dash number shifts to letters. The dash number of the original program is zero.

#### **(3) Decimal Number**

The decimal is used for all other program changes such as:

- Adding new optional routines
- A change to the FORTRAN source language due to computer differences
- Correcting a mistake in the program
- Input and output changes
- Adding unique customer oriented curves or initialization data.

In most cases a decimal number change is made and documented by writing an addendum to the user's manual without reprinting the user's manual. An errata or addendum to the user's manual is used in conjunction with a Computer Simulation Change Notice (Figure 28). This notice briefly describes the changes affecting the deck and manual.

Accompanying the notice is a new manual title page reflecting the new date and/or dash or decimal changes. The SCN also includes the change pages with black bars in the right-hand margin opposite data changed and a new date in the upper right-hand corner.

Programs revised by the user without written consent of the supplier are the responsibility of the user.

Engine or Component Designation \_\_\_\_\_ Date \_\_\_\_\_

User's Manual No. \_\_\_\_\_ Customer Computer Deck No. \_\_\_\_\_

Deck and User's Designation is Changed to: \_\_\_\_\_

Dated: \_\_\_\_\_

Change Nature: ☐ Errata ☐ Addendum Changes Effect: ☐ Deck ☐ Manual

Change: \_\_\_\_\_

Reason: \_\_\_\_\_

Detailed Reasons for Changes are Shown in Enclosure

Approval: \_\_\_\_\_

Program Office \_\_\_\_\_

Systems Stability and Control \_\_\_\_\_  
C. H. Borgmeyer

FD 151091

Figure 28. Computer Simulation Change Notice

## APPENDIX A

### DEVELOPMENT OF RUMBLE MODEL EQUATIONS

#### 1. DEVELOPMENT OF ACOUSTIC EQUATIONS

In this section equations are developed to describe how velocity, pressure and density at every point in the augmentor respond to a combustion disturbance, which is treated as a heat input to a flowing inviscid ideal gas stream. Knowing how these three parameters (velocity, pressure, density) respond allows calculation of any other parameter needed, such as mass flowrate or temperature. The first equations to be developed are the three longitudinal wave equations, which are applicable between boundaries and discontinuities. Then equations for the boundaries and discontinuities are developed. The wave equations plus the boundary and discontinuity equations are referred to as the "acoustic" equations. The "combustion" equations needed to complete the rumble model are developed in paragraph 2 of this appendix.

Symbols used below are defined in the list of symbols. For any section of augmentor with rigid walls and constant cross-sectional area, such as shown in Figure 29, through which an inviscid fluid (viscosity is zero) is flowing, the one-dimensional momentum, continuity and energy equations are:

$$\begin{aligned} \frac{\partial P}{\partial x} + \rho V \frac{\partial V}{\partial x} + \rho \frac{\partial V}{\partial t} &= 0 \\ \rho \frac{\partial V}{\partial x} + V \frac{\partial \rho}{\partial x} + \frac{\partial \rho}{\partial t} &= 0 \\ q + \frac{PV}{\rho} \frac{\partial \rho}{\partial x} + \frac{P}{\rho} \frac{\partial \rho}{\partial t} &= \rho V \frac{\partial u}{\partial x} + \rho \frac{\partial u}{\partial t} \end{aligned} \quad (1)$$

For an ideal gas, these equations reduce to the following non-linear wave equations:

$$\begin{aligned} (V+C) \left[ \frac{1}{P} \frac{\partial P}{\partial x} + \frac{\gamma}{C} \frac{\partial V}{\partial x} \right] + \left[ \frac{1}{P} \frac{\partial P}{\partial t} + \frac{\gamma}{C} \frac{\partial V}{\partial t} \right] &= (\gamma-1) \frac{q}{P} \\ (V-C) \left[ \frac{1}{P} \frac{\partial P}{\partial x} - \frac{\gamma}{C} \frac{\partial V}{\partial x} \right] + \left[ \frac{1}{P} \frac{\partial P}{\partial t} - \frac{\gamma}{C} \frac{\partial V}{\partial t} \right] &= (\gamma-1) \frac{q}{P} \\ V \left[ \frac{1}{P} \frac{\partial P}{\partial x} - \frac{\gamma}{\rho} \frac{\partial \rho}{\partial x} \right] + \left[ \frac{1}{P} \frac{\partial P}{\partial t} - \frac{\gamma}{\rho} \frac{\partial \rho}{\partial t} \right] &= (\gamma-1) \frac{q}{P} \end{aligned} \quad (2)$$

The wave equations are linearized by the small perturbation substitutions:

$$\begin{aligned} P(x,t) &= \bar{P}(x) + \Delta P(x,t) \\ \rho(x,t) &= \bar{\rho}(x) + \Delta \rho(x,t) \\ C(x,t) &= \bar{C}(x) + \Delta C(x,t) \\ V(x,t) &= \bar{V}(x) + \Delta V(x,t) \\ q(x,t) &= \bar{q}(x) + \Delta q(x,t) \end{aligned} \quad (3)$$

Second order terms are neglected in making the substitutions.



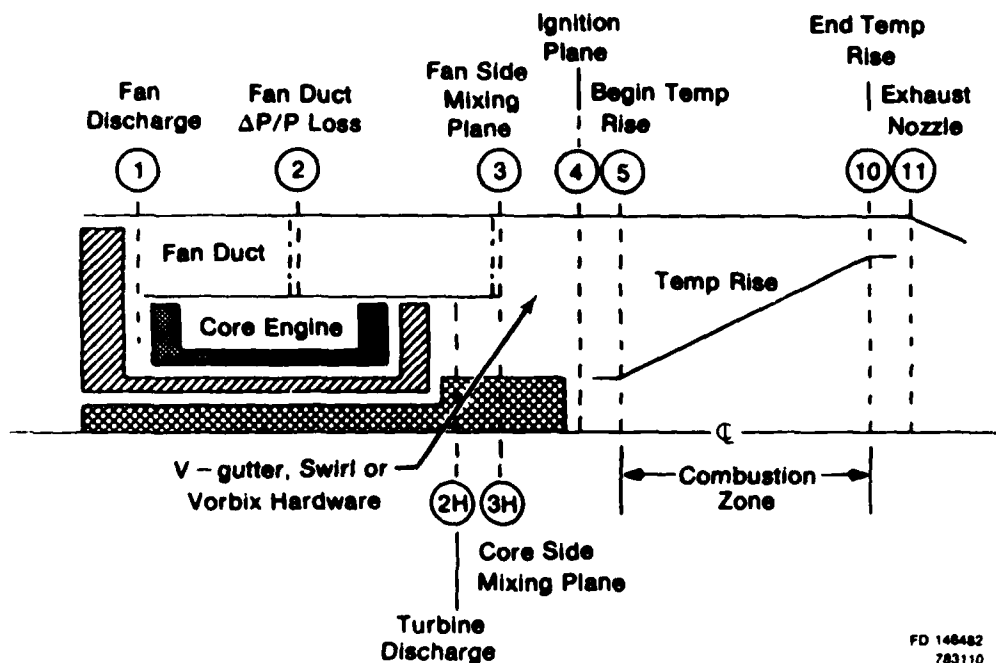


Figure 29. Rumble Model Station Identification

FD 148482  
783110  
012-788

To simplify notation, the following substitutions are made which normalize the change in each variable by its steady-state value:

$$P' = \frac{\Delta P}{\bar{P}}, V' = \frac{\Delta V}{\bar{V}}, \rho' = \frac{\Delta \rho}{\bar{\rho}}, q' = \frac{\Delta q}{\bar{q}} \quad (4)$$

The linearized version of equations (2) becomes:

$$\begin{aligned} (\bar{V} + \bar{C}) \frac{\partial}{\partial x} \left[ P' + \gamma \bar{M} V' \right] + \frac{\partial}{\partial t} \left[ P' + \gamma \bar{M} V' \right] + (\gamma - 1) \frac{\bar{q}}{\bar{P}} \beta_F &= (\gamma - 1) \frac{\bar{q}}{\bar{P}} q' \\ (\bar{V} - \bar{C}) \frac{\partial}{\partial x} \left[ P' - \gamma \bar{M} V' \right] + \frac{\partial}{\partial t} \left[ P' - \gamma \bar{M} V' \right] + (\gamma - 1) \frac{\bar{q}}{\bar{P}} \beta_G &= (\gamma - 1) \frac{\bar{q}}{\bar{P}} q' \\ \bar{V} \frac{\partial}{\partial x} \left[ P' - \gamma \rho' \right] + \frac{\partial}{\partial t} \left[ P' - \gamma \rho' \right] + (\gamma - 1) \frac{\bar{q}}{\bar{P}} \beta_E &= (\gamma - 1) \frac{\bar{q}}{\bar{P}} q' \end{aligned} \quad (5)$$

where:

$$\begin{aligned} \beta_F &= \frac{1}{(1 - \bar{M}^2)} \left[ P' (1 - \bar{M} - \bar{M}^2) + \rho \bar{M} + V \left\{ \frac{1}{2} + \frac{3}{2} \bar{M} - \bar{M}^2 [1 + (1 + \bar{M}) \frac{\gamma}{2}] \right\} \right] \\ \beta_G &= \frac{1}{(1 - \bar{M}^2)} \left[ P' (1 - \bar{M} - \bar{M}^2) + \rho \bar{M} + V \left\{ \frac{1}{2} + \frac{3}{2} \bar{M} - \bar{M}^2 [1 + (1 + \bar{M}) \frac{\gamma}{2}] \right\} \right] \end{aligned} \quad (6)$$

$$\beta_E = P - V'$$

Taking the Laplace transform with respect to time, with zero initial conditions, and letting subscripts 1 and 2 stand for the upstream and downstream stations respectively (see Figure 33), the general solution to equations (5) becomes:

$$\begin{aligned}
 [P'_2 + \gamma \bar{M}_2 V'_2] e^{\int_0^x \frac{dx}{V+C}} &= [P'_1 + \gamma \bar{M}_1 V'_1] + \frac{(\gamma-1)}{S} \int_0^x \frac{\bar{q}}{\bar{P}} \beta_F(x,s) \frac{d}{dx} e^{\int_0^x \frac{dx}{V+C}} dx \\
 &= \frac{(\gamma-1)}{S} \int_0^x \frac{\bar{q}}{\bar{P}} q'(x,s) \frac{d}{dx} e^{\int_0^x \frac{dx}{V+C}} dx \\
 [P'_2 - \gamma \bar{M}_2 V'_2] e^{\int_0^x \frac{dx}{V-C}} &= [P'_1 - \gamma \bar{M}_1 V'_1] + \frac{(\gamma-1)}{S} \int_0^x \frac{\bar{q}}{\bar{P}} \beta_G(x,s) \frac{d}{dx} e^{\int_0^x \frac{dx}{V-C}} dx \\
 &= \frac{(\gamma-1)}{S} \int_0^x \frac{\bar{q}}{\bar{P}} q'(x,s) \frac{d}{dx} e^{\int_0^x \frac{dx}{V-C}} dx \\
 [P'_2 - \gamma \rho'_2] e^{\int_0^x \frac{dx}{V}} &= [P'_1 - \gamma \rho'_1] + \frac{(\gamma-1)}{S} \int_0^x \frac{\bar{q}}{\bar{P}} \beta_E(x,s) \frac{d}{dx} e^{\int_0^x \frac{dx}{V}} dx \\
 &= \frac{(\gamma-1)}{S} \int_0^x \frac{\bar{q}}{\bar{P}} q'(x,s) \frac{d}{dx} e^{\int_0^x \frac{dx}{V}} dx
 \end{aligned} \tag{7}$$

In equations (7) the first equation describes downstream running sonic waves of the form  $P' + \gamma \bar{M} V'$ , traveling at sonic speed plus through-flow velocity. The second equation describes upstream running sonic waves of the form  $P' - \gamma \bar{M} V'$ , traveling at sonic speed minus through-flow velocity. The third equation describes entropy waves,  $P' - \gamma \rho'$ , drifting downstream at through-flow velocity.

The entropy waves become more apparent from the expression for the entropy of an ideal gas:

$$\frac{\Delta S}{C_v} = S' = P' - \gamma \rho' \tag{8}$$

The entropy waves are related to temperature by:

$$\gamma T' = S' + (\gamma-1) P' \tag{9}$$

It is through equation (9) that the drifting hot and cold combustion products, or entropy waves, are accounted for in the rumble model. Temperature changes produced as the entropy waves strike the exhaust nozzle create waves which then travel back upstream at sonic speed.

Equations (7) are not useful until the integrals are evaluated, which will require definitions of  $\bar{V}(x)$ ,  $\bar{C}(x)$ ,  $\bar{q}(x)$ ,  $\bar{P}(x)$  and some assumptions that will allow integration of  $q''(x, s)$ ,  $\beta_F(x, s)$ ,  $\beta_G(x, s)$  and  $\beta_E(x, s)$ . To complete the solution, the augmentor is divided into several "short" sections, each of length  $\ell$ , for each of which it can be assumed:

- (a)  $\frac{dP(x)}{dx} = 0$
- (b)  $\frac{dT(x)}{dx} = \text{constant}$
- (c)  $q''(x, t) = q''\left(0, t - \int_0^x \frac{dx}{V}\right)$
- (d)  $\frac{q(x)}{P(x)} = \text{constant}$

The small static pressure drop in an augmentor justifies assumption (a). A linear temperature rise throughout a section of length  $l$  is a good approximation, which justifies assumption (b). Assumption (c) is the equation for a "drifting burning particle" releasing heat at a constant volumetric rate as it drifts down the augmentor. A more detailed explanation of this assumption will be provided in part 2 (Development of Combustion Equations). To justify the constant steady-state heat release rate ( $\bar{q}$ ), consider the steady-state version of the energy equation (third in equations (2)).

$$V \left[ \frac{1}{P} \frac{dP}{dx} - \frac{\gamma}{\rho} \frac{d\rho}{dx} \right] = (\gamma - 1) \frac{\bar{q}}{P}$$

With appropriate substitutions, the equation reduces to:

$$\frac{\bar{q}}{P} = \left( \frac{\gamma}{\gamma - 1} \right) \frac{R}{P} \frac{W}{A} \frac{dT}{dx} - \frac{V}{P} \frac{dP}{dx}$$

Since  $\frac{dP}{dx} = 0$  and  $\frac{dT}{dx} = \text{constant}$ , then

$$\frac{\bar{q}}{P} = \text{constant} = \frac{\gamma}{\gamma - 1} \frac{\bar{C}_1 \bar{M}_1}{\ell} \left( \frac{T_2}{T_1} - 1 \right) \quad (10)$$

For a "short" section of length  $\ell$ , the integration of  $\beta_F(x, s)$  in equations (7) can be carried out as follows:

$$\begin{aligned} \int_0^x \frac{\bar{q}}{P} \beta_F(x, S) \frac{d}{dx} e^{s \int_0^x \frac{dx}{V+C}} dx &\approx \frac{\bar{q}}{P} \beta_F(0, S) \int_0^{\ell/2} \frac{d}{dx} e^{s \int_0^x \frac{dx}{V+C}} dx \\ &+ \frac{\bar{q}}{P} \beta_F(\ell, S) \int_{\ell/2}^{\ell} \frac{d}{dx} e^{s \int_0^x \frac{dx}{V-C}} dx \end{aligned}$$

Similar treatment allows integration of  $\beta_G(x, s)$  and  $\beta_E(x, s)$  in equation (7). To determine how "short" a section must be for the solution to be valid, the resulting rumble model was exercised repeatedly while decreasing the section length (by adding more stations in the combustion zone). As the section length decreases, the result will rapidly approach an exact solution. It was found that section lengths shorter than about 20 inches were unnecessary.

With the above assumptions, equation (7) becomes:

$$\begin{aligned} [P_2 + \gamma M_2 V_2] - [P_1 + \gamma M_1 V_1] e^{-\tau_E S} - (\gamma - 1) \frac{\bar{q}}{\bar{p}} \beta_{F_1} \left[ \frac{e^{-\tau_1 S} - e^{-\tau_2 S}}{S} \right] \\ + (\gamma - 1) \frac{\bar{q}}{\bar{p}} \beta_{F_2} \left[ \frac{1 - e^{-\tau_2 S}}{S} \right] = (\gamma - 1) \frac{\bar{q}}{\bar{p}} q_1 \left\{ M_1 \left[ \frac{e^{-\tau_1 S} - e^{-(\tau_1 + \tau_2) S}}{S} \right] \right. \\ \left. + M_2 \left[ \frac{e^{-(\tau_1 + \tau_2) S} - e^{-\tau_2 S}}{S} \right] \right\} \end{aligned} \quad (11)$$

$$\begin{aligned} [P_1 + \gamma M_1 V_1] - [P_2 + \gamma M_2 V_2] e^{-\tau_0 S} + (\gamma - 1) \frac{\bar{q}}{\bar{p}} \beta_{G_1} \left[ \frac{1 - e^{-\tau_0 S}}{S} \right] \\ + (\gamma - 1) \frac{\bar{q}}{\bar{p}} \beta_{G_2} \left[ \frac{e^{-\tau_0 S} - e^{-\tau_{G_1} S}}{S} \right] \\ = (\gamma - 1) \frac{\bar{q}}{\bar{p}} q_1 \left\{ M_1 \left[ \frac{1 - e^{-(\tau_{G_1} + \tau_E) S}}{S} \right] + M_2 \left[ \frac{e^{-(\tau_{G_1} + \tau_E) S} - e^{-(\tau_{G_1} + \tau_F) S}}{S} \right] \right\} \\ [P_2 + \gamma \rho_2] - [P_1 + \gamma \rho_1] e^{-\tau_E S} - (\gamma - 1) \frac{\bar{q}}{\bar{p}} \beta_{E_1} \left[ \frac{e^{-\tau_E S} - e^{-\tau_{E_2} S}}{S} \right] \\ + (\gamma - 1) \frac{\bar{q}}{\bar{p}} \beta_{E_2} \left[ \frac{1 - e^{-\tau_{E_2} S}}{S} \right] = (\gamma - 1) \frac{\bar{q}}{\bar{p}} q_1 \tau_E e^{-\tau_E S} \end{aligned}$$

where:

$$\tau_F \equiv \int_0^t \frac{dx}{V+C} \quad \tau_G \equiv - \int_0^t \frac{dx}{V-C} \quad \tau_E \equiv \int_0^t \frac{dx}{V}$$

$$\tau_{F1} \equiv \int_0^{t/2} \frac{dx}{V+C} \quad \tau_{G1} \equiv - \int_0^{t/2} \frac{dx}{V-C} \quad \tau_{E1} \equiv \int_0^{t/2} \frac{dx}{V}$$

(12)

$$\begin{aligned} \tau_{F2} &= \tau_F - \tau_{F1} & \tau_{E2} &= \tau_E - \tau_{E1} \\ \beta_{F1} &= \frac{1}{(1-M_1^2)} \left[ P_1 (1-M_1-M_1^2) + \rho_1 \bar{M}_1 + V_1 \left\{ \frac{1}{2} + \frac{3}{2} \bar{M}_1 - \bar{M}_1^2 \left[ 1 + (1+\bar{M}_1) \frac{\gamma}{2} \right] \right\} \right] \\ \beta_{F2} &= \frac{1}{(1-M_2^2)} \left[ P_2 (1-M_2-M_2^2) + \rho_2 \bar{M}_2 + V_2 \left\{ \frac{1}{2} + \frac{3}{2} \bar{M}_2 - \bar{M}_2^2 \left[ 1 + (1+\bar{M}_2) \frac{\gamma}{2} \right] \right\} \right] \\ \beta_{G1} &= \frac{1}{(1-M_1^2)} \left[ P_1 (1+M_1-M_1^2) - \rho_1 \bar{M}_1 + V_1 \left\{ \frac{1}{2} - \frac{3}{2} \bar{M}_1 - \bar{M}_1^2 \left[ 1 + (1-\bar{M}_1) \frac{\gamma}{2} \right] \right\} \right] \\ \beta_{G2} &= \frac{1}{(1-M_2^2)} \left[ P_2 (1+M_2-M_2^2) - \rho_2 \bar{M}_2 + V_2 \left\{ \frac{1}{2} - \frac{3}{2} \bar{M}_2 - \bar{M}_2^2 \left[ 1 + (1-\bar{M}_2) \frac{\gamma}{2} \right] \right\} \right] \\ \beta_{F1} &= P_1 + V_1 \\ \beta_{F2} &= P_2 + V_2 \end{aligned}$$

(13)

For convenience in programming equations (11) on the computer, the following identity substitutions were made:

$$\begin{aligned} \beta_{F1} &= PF_1 P'_1 + RF_1 \rho'_1 + VF_1 V'_1 \\ \beta_{F2} &= PF_2 P'_2 + RF_2 \rho'_2 + VF_2 V'_2 \\ \beta_{G1} &= PG_1 P'_1 + RG_1 \rho'_1 + VG_1 V'_1 \\ \beta_{G2} &= PG_2 P'_2 + RG_2 \rho'_2 + VG_2 V'_2 \end{aligned}$$

(14)

where by definition:

$$\begin{aligned}
 PF_1 &= \frac{1}{(1-\bar{M}_1^2)} [1 - \bar{M}_1 - \bar{M}_1^2] \\
 RF_1 &= \frac{\bar{M}_1}{(1-\bar{M}_1^2)} \\
 VF_1 &= \frac{1}{(1-\bar{M}_1^2)} \left\{ \frac{1}{2} + \frac{3}{2} \bar{M}_1 - \bar{M}_1^2 \left[ 1 + (1+\bar{M}_1) \frac{\gamma}{2} \right] \right\} \\
 PF_2 &= \frac{1}{(1-\bar{M}_2^2)} [1 - \bar{M}_2 - \bar{M}_2^2] \\
 RF_2 &= \frac{\bar{M}_2}{(1-\bar{M}_2^2)} \\
 VF_2 &= \frac{1}{(1-\bar{M}_2^2)} \left\{ \frac{1}{2} + \frac{3}{2} \bar{M}_2 - \bar{M}_2^2 \left[ 1 + (1+\bar{M}_2) \frac{\gamma}{2} \right] \right\} \\
 PG_1 &= \frac{1}{(1-\bar{M}_1^2)} [1 - \bar{M}_1 - \bar{M}_1^2] \\
 RG_1 &= \frac{-\bar{M}_1}{(1-\bar{M}_1^2)} \\
 VG_1 &= \frac{1}{(1-\bar{M}_1^2)} \left\{ \frac{1}{2} - \frac{3}{2} \bar{M}_1 - \bar{M}_1^2 \left[ 1 + (1-\bar{M}_1) \frac{\gamma}{2} \right] \right\} \\
 PG_2 &= \frac{1}{(1-\bar{M}_2^2)} [1 + \bar{M}_2 - \bar{M}_2^2] \\
 RG_2 &= \frac{-\bar{M}_2}{(1-\bar{M}_2^2)} \\
 VG_2 &= \frac{1}{(1-\bar{M}_2^2)} \left\{ \frac{1}{2} - \frac{3}{2} \bar{M}_2 - \bar{M}_2^2 \left[ 1 + (1-\bar{M}_2) \frac{\gamma}{2} \right] \right\}
 \end{aligned} \tag{15}$$

The time constants in equations (12) were evaluated based upon the steady-state through-flow and sonic speed profiles created by the linear temperature gradient.

$$\begin{aligned}
 V(x) &= V_1 \left[ 1 + \left( \frac{T_2}{T_1} - 1 \right) \frac{x}{l} \right] \\
 C(x) &= C_1 \sqrt{1 + \left( \frac{T_2 - T_1}{T_1} \right) \frac{x}{l}}
 \end{aligned} \tag{16}$$

Then the time constants in equations (12) become:

$$\begin{aligned}
 \tau_F &= \frac{l/C_1}{\left(\frac{T_2}{T_1} - 1\right)} \frac{2}{M_1} \ln \left[ \frac{1 + M_1 \sqrt{T_2/T_1}}{1 + M_1} \right] \\
 \tau_G &= \frac{l/C_1}{\left(\frac{T_2}{T_1} - 1\right)} \frac{2}{M_1} \ln \left[ \frac{1 - M_1}{1 - M_1 \sqrt{T_2/T_1}} \right] \\
 \tau_H &= \frac{l/C_1}{\left(\frac{T_2}{T_1} - 1\right)} \frac{1}{M_1} \ln \left[ \frac{T_2}{T_1} \right] \\
 \tau_{F_1} &= \frac{l/C_1}{\left(\frac{T_2}{T_1} - 1\right)} \frac{2}{M_1} \ln \left[ \frac{1 + M_1 \sqrt{1/2 (1 + T_2/T_1)}}{1 + M_1} \right] \\
 \tau_{G_1} &= \frac{l/C_1}{\left(\frac{T_2}{T_1} - 1\right)} \frac{2}{M_1} \ln \left[ \frac{1 - M_1}{1 - M_1 \sqrt{1/2 (1 + T_2/T_1)}} \right] \\
 \tau_{F_1} &= \frac{l/C_1}{\left(\frac{T_2}{T_1} - 1\right)} \frac{1}{M_1} \ln [1/2 (1 + T_2/T_1)]
 \end{aligned} \tag{17}$$

This completes the development of the wave equations.

Equations (11) are applied throughout the augmentor between any two stations between which there is no discontinuity. In applying the equations, the general subscripts 1 and 2 are replaced by the actual upstream and downstream station numbers, respectively. Referring to Figure 33, they are applied between stations (1) - (2), (2) - (3), (4) - (5), (5) - (10) and (10) - (11). Between stations (1) through (5) and between stations (10) - (11) there is no heat addition, and so the heat addition terms  $\bar{q}/\bar{P}$  are set to zero. The heat addition terms for the combustion zone, stations (5) - (10), are discussed in paragraph 2 of this appendix.

Discontinuities occur at the pressure drop locations, stations (2) and (3). These are modeled as small incompressible resistive pressure drops of zero length. The continuity and energy equations are also applied. Referring to Figure 33, across a pressure drop:

$$\begin{aligned}
 P_2 - P_3 &\approx \frac{\rho_2 V_2^2}{2} \\
 W_2 &= W_3 \\
 T_2 &= T_3
 \end{aligned} \tag{18}$$

The equations are linearized and normalized as before to yield:

$$P_i' - \left[ 1 - \left( \frac{P_2 - P_1}{P_2} \right) \right] P_i' = \left( \frac{P_2 - P_1}{P_2} \right) (\rho_i' + 2V_i') \quad (19)$$

$$\rho_i' + V_i' = \rho_i' + V_i'$$

$$P_i' - \rho_i' = P_i' - \rho_i'$$

In applying equations (19) to a given pressure drop, the general subscripts 2 and 3 are replaced by the actual upstream and downstream station numbers, respectively. For convenience in programming, equations (19) were combined with the wave equations (11) to eliminate the need for two stations at each pressure drop. It is the combined equations which appear in the rumble model listing.

A junction occurs where the core stream and fan stream enter the augmentor and form the overall augmentor stream (stations (3), (3H) and (4)). Again applying continuity, momentum and energy:

$$W_3 + W_{3H} = W_4$$

$$\left( \frac{P - P_4}{P} \right) \begin{matrix} \text{FAN SIDE} \\ \text{OR} \\ \text{CORE SIDE} \end{matrix} \approx \left( \frac{W\sqrt{T}}{P} \right)^2 \begin{matrix} \text{FAN SIDE} \\ \text{OR} \\ \text{CORE SIDE} \end{matrix} \quad (20)$$

$$W_3 T_3 + W_{3H} T_{3H} = W_4 T_4$$

The linearized and normalized versions become:

$$\rho_i' + V_i' = \left( \frac{BPR}{1+BPR} \right) \rho_i' + \left( \frac{BPR}{1+BPR} \right) V_i' + \left( \frac{1}{1+BPR} \right) \rho_{3H}' + \left( \frac{1}{1+BPR} \right) V_{3H}'$$

$$P_i' - \left[ 1 - \left( \frac{P_2 - P_1}{P_2} \right) \right] P_i' = 2 \left( \frac{P_2 - P_1}{P_2} \right) \left( \frac{BPR}{1+BPR} \right) V_i'$$

$$+ \left( \frac{P_2 - P_1}{P_2} \right) \left( \frac{BPR}{1+BPR} \right) \rho_i' + 2 \left( \frac{P_2 - P_1}{P_2} \right) \left( \frac{1}{1+BPR} \right) V_{3H}'$$

$$+ \left( \frac{P_2 - P_1}{P_2} \right) \left( \frac{1}{1+BPR} \right) \rho_{3H}' \quad (21)$$

$$P_{3H}' - \left[ 1 - \left( \frac{P_2 - P_1}{P_2} \right) \right] P_i' = 2 \left( \frac{P_2 - P_1}{P_2} \right) \left( \frac{BPR}{1+BPR} \right) V_i'$$

$$+ \left( \frac{P_2 - P_1}{P_2} \right) \left( \frac{BPR}{1+BPR} \right) \rho_i' + 2 \left( \frac{P_2 - P_1}{P_2} \right) \left( \frac{1}{1+BPR} \right) V_{3H}'$$

$$+ \left( \frac{P_2 - P_1}{P_2} \right) \left( \frac{1}{1+BPR} \right) \rho_{3H}'$$

$$V_i' + P_i' = \left[ \frac{BPR (T_3/T_H)}{1 + BPR (T_3/T_H)} \right] P_i' + \left[ \frac{BPR (T_3/T_H)}{1 + BPR (T_3/T_H)} \right]$$

$$= \left[ \frac{1}{1 + BPR (T_3/T_H)} \right] P_{3H}' + \left[ \frac{1}{1 + BPR (T_3/T_H)} \right]$$



For the Swirl augmentor, the momentum equations at stations (3) - (4) and (3H) - (4) are modified to account for the possibility of different pressure drops across the fan and core swirl vanes. The linearized version of the momentum equations for the Swirl augmentor becomes:

$$\begin{aligned} P_3 - \left[ 1 - \left( \frac{P_3 - P_4}{P_3} \right) \right] P_4 &= 2 \left( \frac{P_3 - P_4}{P_3} \right) V_3 + \left( \frac{P_3 - P_4}{P_3} \right) \rho_3 \\ P_{3H} - \left[ 1 - \left( \frac{P_{3H} - P_4}{P_{3H}} \right) \right] P_4 &= 2 \left( \frac{P_{3H} - P_4}{P_{3H}} \right) V_{3H} + \left( \frac{P_{3H} - P_4}{P_{3H}} \right) \rho_{3H} \end{aligned} \quad (22)$$

Definition of the upstream and downstream boundary conditions, at the fan and at the nozzle, respectively, will complete the acoustic equations. The fan was assumed to be delivering a constant mass flowrate through the fan OD (defined as that portion of the fan between the fan splitter and fan tip) and through the fan ID (defined as that portion of the fan between the centerline and the fan splitter). It was also assumed that the temperature of the fan discharge flow could be taken as time invariant (also, because of the low Mach number at fan discharge, total and static temperatures can be used interchangeably). To account for the presence of a core engine, and explore any possible attendant interaction with fan duct acoustics, a simple first order lag representation of the core engine was incorporated into the rumble model. The core engine was represented as a compressor delivering constant corrected air flow (corrected to compressor face conditions) into a lumped volume. Flow out of the volume exited through a choked turbine to emerge at station (3H). The resulting transfer function for the core engine is:

$$\frac{W_{3H}}{P_C} = \frac{1}{1 + \tau_{CORE} S} \quad (23)$$

Where:

$$\begin{aligned} W_{3H} &= \text{mass flowrate at station (3H)} \\ P_C &= \text{static pressure at the compressor face} \\ \tau_{CORE} &= \text{core engine time constant} \end{aligned}$$

A default value of  $\tau_{CORE} = .005$  seconds is built into the rumble model. A different value can be input by the user, and is calculated as the mass of air in the core engine volume divided by the mass flowrate of air through the core engine. Proximity of the fan splitter to fan discharge also affects the boundary condition at the fan. Two cases were considered and are built into the rumble model (see NFSOP). In the first case, called the "proximate" splitter configuration, the fan splitter is assumed to be so close to fan discharge that no communication can occur between the fan duct and the core engine across the fan splitter. For this case, the boundary condition at the fan becomes:

$$\begin{aligned} P_4 &= W_{3H} = 0 \\ W_1 &= \rho_1 + V_1 = 0 \\ T_1 &= P_1 - \rho_1 = 0 \end{aligned} \quad (24)$$

In the second case, called the "remote" splitter configuration, the fan splitter is assumed to be sufficiently remote from fan discharge to allow perfect communication between the fan duct and the core engine across the fan splitter. For this case, the boundary condition at the fan becomes:

$$\begin{aligned}
 P_c &= P_i' \\
 W_i' &= \rho_i' + V_i' = -\frac{P_i'}{BPR} \\
 T_i' &= P_i' - \rho_i' = 0 \\
 W_{sH} &= \frac{P_i'}{1 + \tau_{CORE} S}
 \end{aligned}
 \tag{25}$$

This completes the definition of the upstream boundary condition. It is of interest to note that entropy waves are created by sonic wave reflections at the upstream boundary. Since an entropy perturbation is  $S_1' = P_1' - \gamma \rho_1'$ , and at the boundary  $\rho_1' = P_1'$ , then  $S_1' = (1 - \gamma) P_1'$ . A similar argument will show that entropy waves are also created at the pressure drops (stations (2) and (3)). These are automatically accounted for in the rumble model, but are of minor importance compared to the entropy waves created in the combustion zone by combustion disturbances.

The downstream boundary condition is based upon the presence of a "short" nozzle just downstream of station (11), for which:

$$\frac{W \sqrt{T_o R}}{A P_o} = \phi(P_R)
 \tag{26}$$

where:

$$\phi = \frac{\left[ \left( P_R^{\frac{\gamma-1}{\gamma}} - 1 \right) \left( \frac{2}{\gamma-1} \right) \right]^{\frac{\gamma}{\gamma-1}}}{P_R^{\frac{\gamma+1}{2\gamma}}}$$

$P_R = P_o$  /nozzle throat static pressure

$$P_R \leq \left( \frac{\gamma+1}{2} \right)^{\frac{\gamma}{\gamma-1}}$$

When linearized, the downstream boundary condition becomes:

$$V_{ii}' = \frac{1}{2} (P_{ii}' - \rho_{ii}') + (KNOZ) P_{ii}' \quad (27)$$

where:

$$KNOZ = \frac{\left[ 1 + \left( \frac{\gamma+1}{2} \right) \bar{M}_{ii} \right] \left( \frac{P_R}{\phi} \frac{\partial \phi}{\partial P_R} \right)}{[1 - \bar{M}_{ii}^2 (1+\gamma)] \left( \frac{P_R}{\phi} \frac{\partial \phi}{\partial P_R} \right)}$$

$$\frac{P_R}{\phi} \frac{\partial \phi}{\partial P_R} = \left[ \frac{P_R \frac{\gamma-1}{\gamma}}{2 \left( P_R \frac{\gamma-1}{\gamma} - 1 \right)} - \frac{\gamma+1}{2(\gamma-1)} \right] \left( \frac{\gamma-1}{\gamma} \right)$$

It is also of interest to note that for choked flow,

$$P_R \geq \left( \frac{\gamma+1}{2} \right)^{\frac{\gamma}{\gamma-1}},$$

then  $KNOZ = 0$  and:

$$V_{ii}' = \frac{1}{2} (P_{ii}' - \rho_{ii}') = \frac{1}{2} T_{ii}' \quad (28)$$

substituting from equation (16):

$$V_{ii}' = \frac{1}{2\gamma} S_{ii}' + \frac{(\gamma-1)}{2\gamma} P_{ii}' \quad (29)$$

This equation directly relates how entropy waves, as well as pressure disturbances, striking a choked nozzle will produce a velocity disturbance.

This completes the acoustic equation development. These equations describe the response of pressure, velocity and density throughout the augmentor to a disturbance in combustion. Development of the corresponding combustion equations, which describe how combustion throughout the augmentor will respond to disturbances in pressure, velocity and density, is presented in the following section.

## 2. DEVELOPMENT OF COMBUSTION EQUATIONS

Development of the combustion equations for the V-gutter flameholder augmentor is presented first. Then the combustion equations for Vorbix and Swirl augmentors are presented.

For the V-gutter flameholder augmentor two combustion streams, the fan stream and the core stream, are treated. This is necessary to be able to account for the different combustion characteristics of the fan and core streams. The two streams can have different flameholder designs and fuel-air ratios as well as different flameholder approach temperatures and velocities, causing the two streams to have different efficiency vs. fuel-air ratio characteristics. In addition, the fan stream is preceded by a long fan duct which can exhibit longitudinal resonance at the low frequencies associated with rumble. The core stream is preceded by a short section terminating at turbine discharge, which is much less responsive at low frequencies.

The basic approach taken for the rumble model was to model combustion disturbances in the fan and core streams independently, accounting for the individual properties of each stream. The resulting two combustion disturbances (calculated as volumetric heat release rate disturbances) were then simply added to form a single overall disturbance. The overall disturbance was then distributed evenly over the total cross-sectional area of the augmentor, which was taken to consist of a single overall stream with mean mixed properties. This approach accounts for the different combustion characteristics of the fan and core streams, while avoiding the complexities associated with a rigorous treatment of the radial as well as the axial distribution of combustion throughout the augmentor.

Experience with modeling the combustion process as a plane heat addition with all combustion taking place in zero length, had shown that the resulting predictions of rumble were sensitive to the axial location chosen for the plane. Since combustion actually takes place over a distance of 30 to 60 inches, it was decided that the axially distributed nature of the burning should be accounted for. This was accomplished by dividing the combustion zone into a number of axial sections, each of length  $\ell$ , as explained in part 1, "Development of Acoustic Equations".

Combustion equations used in the rumble model are based upon an extension of empirical steady-state processes to the case of time variant flow. A schematic of the steady-state processes is shown in Figure 30. Consider first that the augmentor contains only the fan stream. An identical set of equations will exist for the parallel core stream. Following a particle of air as it moves through the augmentor, the following steps will occur:

- Particle of air picks up fuel as it crosses the spraybar.
- Particle drifts at through-flow velocity to the flameholder, station (4).
- Particle is ignited by the flameholder wake as it drifts from the flameholder, to the beginning of the combustion zone, station (5) (defined as the location where the bulk fluid temperature begins to rise sharply).
- Particle drifts and burns from station (5) to the end of the combustion zone, station (10) (defined as the location where bulk fluid temperature ceases its sharp rise).

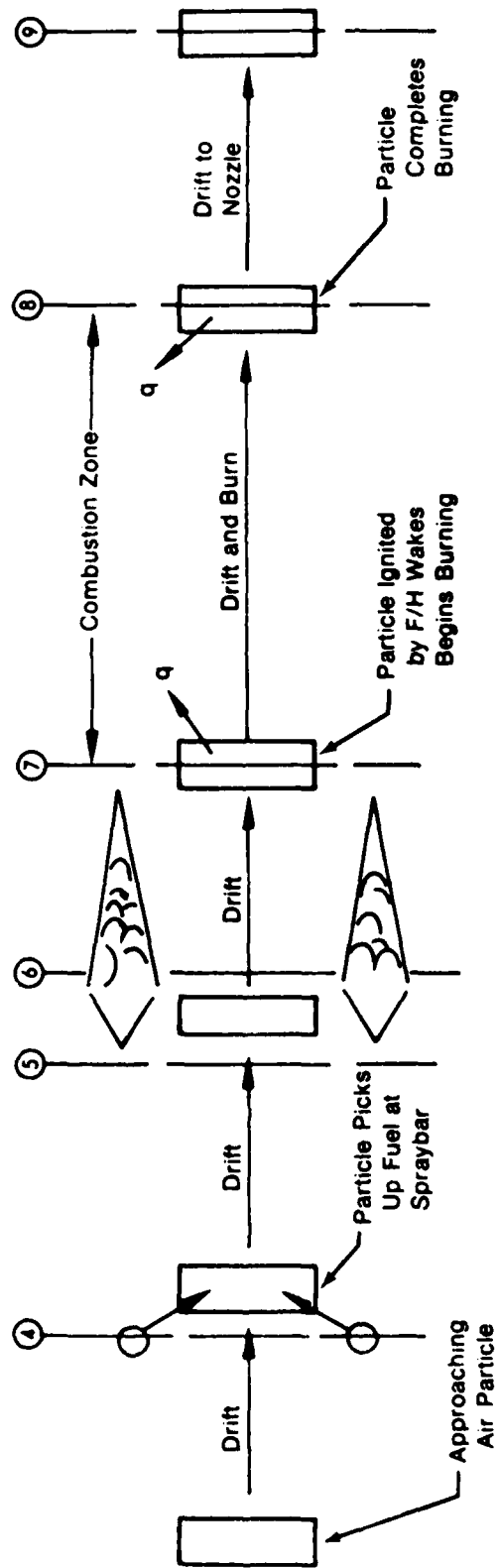


Figure 30. Steps in Augmentor Combustion Process

FD 144860

It was determined (see equation (10)) that for a linear temperature gradient, the steady-state volumetric heat release in a section of length  $l$  in the augmentor could be taken as independent of axial position. This implies that at steady-state a particle of fuel-air mixture, drifting and burning through the combustion zone, has a volumetric heat release rate that is independent of axial position. The rate can be computed directly from the flowrate, ideal temperature rise, efficiency and combustion zone volume of the augmentor.

$$q = \frac{C_p}{V} W T_i \eta \quad (30)$$

For small perturbations, it was assumed that transiently the volumetric heat release rate of a particle could still be taken as independent of axial position, and that equation (30) could be used to compute the rate when  $W$ ,  $T_i$  and  $\eta$  are referenced to instantaneous approach conditions. The resulting equation will model combustion as though it behaves in a quasi-steady manner. The volumetric heat release rate at any location in the combustion zone will reach the steady-state value corresponding to instantaneous conditions at the flameholder and at the spraybar after a delay. The delay is the time required to purge the old combustion gases and refill with new combustion gases traveling at through flow velocity.

For the fan stream, instantaneous approach conditions are taken to be the instantaneous conditions at station (3). Because of the large pressure drop in the fuel spraybar injector, changes in fuel flow in response to augmentor pressure at the spraybar are small compared to changes in air flow. Consequently, fuel flow can be considered constant, and the fuel-air ratio of the particle as it crosses the spraybar is determined by changes in air flow only.

$$FA_{S/B} = \frac{\text{constant}}{W_s} \quad (31)$$

A period of time  $\tau_{DC} = LSC/\bar{V}_3$  is required for the particle to drift from the spraybar to the flameholder. Therefore, the fuel-air ratio of the particle when it reaches the flameholder can be expressed as:

$$FA_c(t) = FA_{S/B} (t - \tau_{DC}) \quad (32)$$

At the ignition plane (flameholder) the particle has a "potential" volumetric heat release rate of:

$$q_c = \frac{C_p}{V_c} W_s T_{ic} \eta_c \quad (33)$$

The ideal temperature rise is a function of the fuel-air ratio of the particle (effects of approach temperature and pressure are negligible). The efficiency is assumed to be a function of the fuel-air ratio and the approach pressure, temperature and velocity.

$$T_{ic} = fcn(FA_c) \quad (34)$$

$$\eta_c = V fcn(FA_c, P_s, T_s, V_s) \quad (35)$$

The particle crossing the flameholder will begin burning after a time  $\ell_4/\bar{V}_4$ , which is the time required to drift from Station (4) to (5) while being ignited. When it begins burning at Station (5), the heat release rate of the particle will be ( $X = 0$  at Station (5)):

$$q(0,t) = q_c(t - \ell_4/\bar{V}_4) \quad (36)$$

At some station,  $X$  distance downstream of Station (5), the local heat release rate will become that of the particle after an additional time delay,

$$\tau_E = \int_0^X dx/\bar{V}(x),$$

which is the time required to drift from Station (5) a distance  $X$  at through-flow velocity  $\bar{V}(X)$ . Then, at a location  $X$  in the combustion zone, the heat release rate will be:

$$q(x,t) = q(0,t - \tau_E) \quad (37)$$

The linearized versions of equations (31) through (35), written in terms of the Laplace transform of the normalized variables are:

$$\begin{aligned} FA'_{sH} &= -W'_s \\ FA'_c &= FA'_{sH} e^{-\tau_{DC} S} \\ q'_c &= W'_s + T'_i + \eta' \\ T'_{ic} &= \left[ \frac{FA}{T_i} \frac{\partial T_i}{\partial FA} \right]_c FA'_c \\ \eta'_c &= \left[ \frac{FA}{\eta} \frac{\partial \eta}{\partial FA} \right]_c FA'_c + \left[ \frac{P}{\eta} \frac{\partial \eta}{\partial P} \right]_c P'_s + \left[ \frac{T}{\eta} \frac{\partial \eta}{\partial T} \right]_c T'_s + \left[ \frac{V}{\eta} \frac{\partial \eta}{\partial V} \right]_c V'_s \end{aligned} \quad (38)$$

solving for  $q'_c$ :

$$\begin{aligned} q'_c &= \left[ 1 - \left\{ \left[ \frac{FA}{T_i} \frac{\partial T_i}{\partial FA} \right]_c + \left[ \frac{FA}{\eta} \frac{\partial \eta}{\partial FA} \right]_c \right\} e^{-\tau_{DC} S} \right] W'_s \\ &+ \left[ \frac{P}{\eta} \frac{\partial \eta}{\partial P} \right]_c P'_s + \left[ \frac{T}{\eta} \frac{\partial \eta}{\partial T} \right]_c T'_s + \left[ \frac{V}{\eta} \frac{\partial \eta}{\partial V} \right]_c V'_s \end{aligned} \quad (39)$$

A corresponding equation for the core stream can be directly written by changing subscript "C" to subscript "H", and changing the reference approach station from (3) to (3H).

$$\begin{aligned} q'_{sH} &= \left[ 1 - \left\{ \left[ \frac{FA}{T_i} \frac{\partial T_i}{\partial FA} \right]_H + \left[ \frac{FA}{\eta} \frac{\partial \eta}{\partial FA} \right]_H \right\} e^{-\tau_{DH} S} \right] W'_{sH} \\ &+ \left[ \frac{P}{\eta} \frac{\partial \eta}{\partial P} \right]_H P'_{sH} + \left[ \frac{T}{\eta} \frac{\partial \eta}{\partial T} \right]_H T'_{sH} + \left[ \frac{V}{\eta} \frac{\partial \eta}{\partial V} \right]_H V'_{sH} \end{aligned} \quad (40)$$

The total volumetric heat release rate (subscript "T") is formed by adding the heat release rates of the fan and core streams:

$$q_t v_T = Q_t = Q_c + Q_H = q_c v_c + q_H v_H \quad (41)$$

or, in normalized form:

$$q_t = \left[ \frac{Q_c}{Q_t} \right] q_c + \left[ \frac{Q_H}{Q_t} \right] q_H \quad (42)$$

Equation (42) computes the instantaneous volumetric heat release rate of a particle of combined fan stream and core stream fuel-air ratio mixture when the particle reaches the flameholder. The term "potential" is applied because the particle has not yet been ignited. The particle is ignited by the flameholder wake as it drifts a distance  $\ell_4$  at velocity  $\bar{V}_4$ . The particle begins releasing the "potential" heat at station (5), as defined by equation (36). To account for adding the core stream to the augmentor flow (originally only the fan stream was considered), equation (36) was rewritten to include the heat release of both the core and fan streams and emerges as:

$$q(o,t) = q_t (t - \ell_4 / \bar{V}_4) \quad (43)$$

Linearized:

$$q'(o,t) = q_t' (t - \ell_4 / \bar{V}_4) \quad (44)$$

Equation (44) simply adds a delay into the system which allows tailoring the axial location of the beginning of the combustion zone. For convenience in programming the equations, this delay is added to the drift delay in the combustion zone ( $\tau_E$ ) to form an overall particle drift delay from the flameholder.

$$\tau_Q = \ell_4 / \bar{V}_4 + \tau_E \quad (45)$$

The particle then releases heat throughout the combustion zone as defined by equation (37), the linearized version of which is:

$$q'(x,t) = q'(o, t - \tau_E) \quad (46)$$

This equation represents the augmentor heat release based on steady-state conditions. To accurately model the combustion process in the augmentor the dynamics of the flameholder wake must be included. These dynamics were incorporated into the heat release term as a first order lag:

$$q_{out/dynamic} = \frac{q_{out/steady-state}}{1 + \tau S}$$

The dynamics involved in calculating the flameholder wake time constant T are discussed in Section II-3.



Equation (45) was presented in part 1, "Development of Acoustic Equations", and used to evaluate integrals in equation (7). The combustion equations require that the following information about the steady-state operating point:

$$\left[ \frac{Q_C}{Q_T} \right], \left[ \frac{Q_H}{Q_T} \right], \left[ \frac{FA}{T_i} \frac{\partial T_i}{\partial FA} \right]_{C,H}, \left[ \frac{FA}{\eta} \frac{\partial \eta}{\partial FA} \right]_{C,H},$$

$$\left[ \frac{P}{\eta} \frac{\partial \eta}{\partial P} \right]_{C,H}, \left[ \frac{T}{\eta} \frac{\partial \eta}{\partial T} \right]_{C,H}, \text{ and } \left[ \frac{V}{\eta} \frac{\partial \eta}{\partial V} \right]_{C,H}$$

The heat release rate ratios  $Q_C/Q_T$  and  $Q_H/Q_T$  are computed in the program from conditions known about each augmentor stream:

$$\frac{Q_C}{Q_T} = \frac{(BPR T_{ic} \eta_C)}{(BPR T_{ic} \eta_C) + (T_{iH} \eta_H)} \quad (47)$$

$$\frac{Q_H}{Q_T} = \frac{(T_{iH} \eta_H)}{(BPR T_{ic} \eta_C) + (T_{iH} \eta_H)}$$

The partial derivative terms  $\left[ \frac{FA}{T_i} \frac{\partial T_i}{\partial FA} \right]_{C,H}$  are computed in the program from a

subroutine curvefit of the ideal temperature rise curve. A graphical definition of the term is supplied in Figure 31. The partial derivative terms involving efficiency are computed in the flameholder combustion model and supplied directly to the rumble model. Alternately, they may be computed from empirical data and be input by the user. The graphical definition of terms is similar to that of Figure 31.

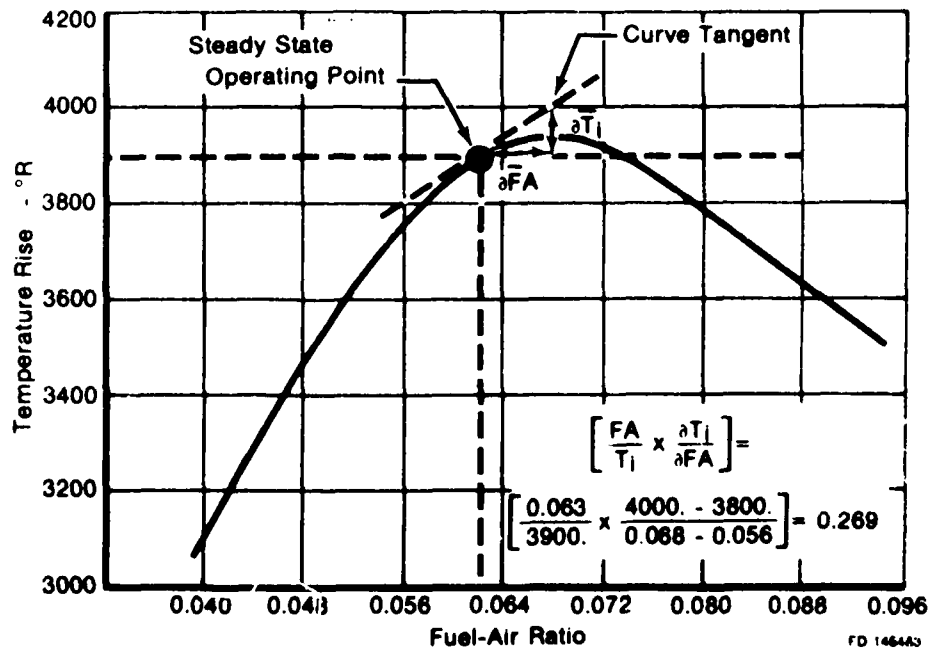


Figure 31. Ideal Temperature Rise for Constant Pressure Combustion of Hydrocarbon Fuels

This completes the combustion equation development for the V-gutter flameholder model. All of the above equations apply to the Vorbix and Swirl augmentors except as noted below.

For the Vorbix and Swirl augmentors, independent heat release rates for the fan and core streams cannot be identified because of the flow mixing. In addition, the effects of pilot fuel-air ratio on augmentor combustion efficiency must be accounted for. Equation (3) is again applied, but on an overall basis only.

$$q_t = \frac{C_p}{v} W_4 T_1 \eta \quad (48)$$

The overall fuel-air ratio is computed from total mixed air flow at station (4).

$$FA = \frac{\text{constant}}{W_4} \quad (49)$$

The overall ideal temperature rise is a function of overall fuel-air ratio. The efficiency is assumed to be a function of overall fuel-air ratio, pilot fuel-air ratio and pressure at station (4).

$$T_1 = fch(FA) \quad (50)$$

$$\eta = fch(FA, FAP, P_4) \quad (51)$$

Then for the Vorbix and Swirl augmentors, the instantaneous "potential" volumetric heat release rate of a particle of mixture when the particle reaches station (4) is:

$$q_t = \left[ 1 - \left[ \frac{FA}{T_1} \frac{\partial T_1}{\partial FA} \right] - \left[ \frac{FA}{\eta} \frac{\partial \eta}{\partial FA} \right] \right] W_4 + \left[ \frac{FAP}{\eta} \frac{\partial \eta}{\partial FAP} \right] FAP + \left[ \frac{P}{\eta} \frac{\partial \eta}{\partial P} \right] P_4 \quad (52)$$

Equation (52) applies to both the Vorbix and Swirl augmentors, and is equivalent to equation (42) for the V-gutter augmentor. The Vorbix and Swirl augmentors differ in pilot location. The Swirl has the pilot at fan duct exit, so that air flow through the Swirl pilot is proportional to fan duct exit flow,  $W_3$ . The Vorbix has the pilot near midspan, radially, and slightly aft of stations (3) and (3H), so that air flow through the Vorbix pilot is proportional to total flow,  $W_4$ . Then, since fuel flow into both pilots is constant:

$$\begin{aligned} \text{Swirl: } FAP &= W_3 \\ \text{Vorbix: } FAP &= W_4 \end{aligned} \quad (53)$$

For convenience in programming,  $W_4$  can be replaced by:

$$\begin{aligned} W_4 &= W_3 + W_{3H} \\ W_4 &= \left[ \frac{BPR}{1 + BPR} \right] W_3 + \left[ \frac{1}{1 + BPR} \right] W_{3H} \end{aligned} \quad (54)$$

AD-A117 749

PRATT AND WHITNEY AIRCRAFT GROUP WEST PALM BEACH FL 0--ETC F/G 21/2  
AUGMENTOR STABILITY MANAGEMENT PROGRAM USER'S MANUAL.(U)  
NOV 81 R C ERNST F33615-79-C-2059

UNCLASSIFIED

PWA-FR-15323

AFWAL-TR-81-2113

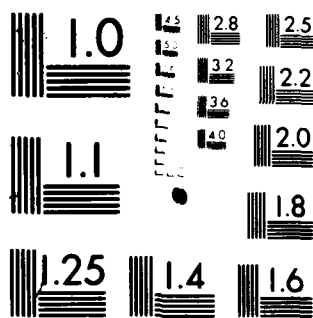
NL

2 of 2

AD-A117 749



END  
DATE  
FILMED  
81-82  
DTIC



MICROCOPY RESOLUTION TEST CHART  
NATIONAL BUREAU OF STANDARDS 1963-A

Substituting (53) and (54) into (52):

$$\begin{aligned} \text{Swirl: } q_i = & \left\{ \left( 1 - \left[ \frac{FA}{T_i} \frac{\partial T_i}{\partial FA} \right] - \left[ \frac{FA}{\eta} \frac{\partial \eta}{\partial FA} \right] \right) \left( \frac{BPR}{1 + BPR} \right) - \left( \frac{FAP}{\eta} \frac{\partial \eta}{\partial FAP} \right) \right\} W_i \\ & + \left\{ \left( 1 - \left[ \frac{FA}{T_i} \frac{\partial T_i}{\partial FA} \right] - \left[ \frac{FA}{\eta} \frac{\partial \eta}{\partial FA} \right] \right) \left( \frac{1}{1 + BPR} \right) \right\} W_{sh} \\ & + \left[ \frac{P}{\eta} \frac{\partial \eta}{\partial P} \right] P_i \end{aligned} \quad (55)$$

$$\begin{aligned} \text{Vorbix: } q_i = & \left\{ \left( 1 - \left[ \frac{FA}{T_i} \frac{\partial T_i}{\partial FA} \right] - \left[ \frac{FA}{\eta} \frac{\partial \eta}{\partial FA} \right] - \left[ \frac{FAP}{\eta} \frac{\partial \eta}{\partial FAP} \right] \right) \left( \frac{BPR}{1 + BPR} \right) \right\} W_i \\ & + \left\{ \left( 1 - \left[ \frac{FA}{T_i} \frac{\partial T_i}{\partial FA} \right] - \left[ \frac{FA}{\eta} \frac{\partial \eta}{\partial FA} \right] - \left[ \frac{FAP}{\eta} \frac{\partial \eta}{\partial FAP} \right] \right) \left( \frac{1}{1 + BPR} \right) \right\} W_{sh} \\ & + \left[ \frac{P}{\eta} \frac{\partial \eta}{\partial P} \right] P_i \end{aligned} \quad (56)$$

Equations (55) and (56) replace equation (42). All other combustion equations are identical to those developed for the V-gutter flameholder augmentor. The partial derivatives in equations (55) and (56) must be computed from empirical data and be input by the user.

This completes development of the combustion equations. For the solution technique, based upon applying the Nyquist criterion to the open loop transfer function (OLTF), the OLTF is formed by renaming  $q_T$  to  $q_{IN}$  in equation (44) and by renaming  $q_T$  to  $q_{OLTF}$  in equations (42), (55) and (56).

## APPENDIX B

### DEVELOPMENT OF FLAMEHOLDER COMBUSTION MODEL EQUATIONS

#### 1. DEVELOPMENT OF THE FAN DUCT COMBUSTION EQUATIONS

The equations which are used in the fan duct combustion analysis are highlighted in this section. The reader is referred to the AFWAL-TR-81-2113 (Contract F33615-79-C-2059) for full details of the analytical development.

The program utilizes the input to set-up and analyze each streamtube as a separate entity. The results are stored for final summation at the completion of the fan duct analysis.

The flow field is first developed from the input:

$$\rho_a = \frac{P_a}{RT_a} \quad (57)$$

$$V_a = M \sqrt{\gamma RT_a} \quad (58)$$

$$W = N/T \quad (59)$$

$$\dot{m}_a = \rho_a V_a W \quad (60)$$

The streamtube width has been set from the flameholder width and the blockage ratio. Note that the streamtube is assumed to be 1-in. deep. The total flowrates are thus per unit depth. If true total flowrates are desired, the number of streamtubes of each type must be set to reflect the total true depth of that type. For example, if 5 streamtubes, of 4 inches depth each, are input as one type, then set the input number of this type equal to 20.

To account for the removal of air from the streamtube for liner cooling, the input fuel-air ratio is adjusted by:

$$(FA)_{\text{effective}} = (FA)_{\text{input}} \frac{1}{1 - WCOOL \left( \frac{1 + BPR}{BPR} \right)} \quad (61)$$

This increases the fuel-air ratio to reflect the air removal when:

$$WCOOL = \dot{m}_{\text{cooling}} / \dot{m}_{\text{engine}} \quad (62)$$

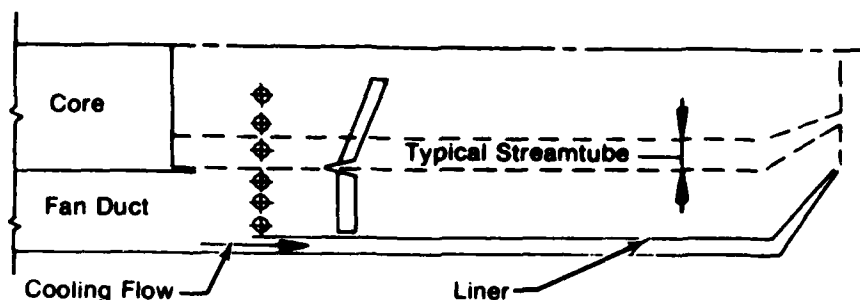
$$BPR = \dot{m}_{\text{duct}} / \dot{m}_{\text{core}} \quad (63)$$

$$\dot{m}_{\text{engine}} = \dot{m}_{\text{duct}} + \dot{m}_{\text{core}} \quad (64)$$

Then

$$\dot{m}_f = \dot{m}_a (FA)_{\text{effective}} \quad (65)$$

This is required since fuel-air ratios are usually based on the total fan duct air flowrates. If true values are known or if no cooling air is used, set WCOOL = 0.0. Refer to Figure 32 for details.



$$BPR = W_{Duct}/W_{Core} \quad ; \quad W_{COOL} = W_{Cooling}/W_{Total}$$

FD 146484

Figure 32. Location of a Core Streamtube in a Turbofan Engine Augmentor

The injection subroutine divides the fuel into 5 droplet size groups which represent the droplet size vs. volume distribution. The curve used is for a variable area pintle injection. The sizes used are:

<u>Group</u>	<u>% Covered</u>	<u>Mean Value</u>
1	0-20	$d_{10}$
2	20-40	$d_{30}$
3	40-60	$d_{50}$
4	60-80	$d_{70}$
5	80-100	$d_{90}$

The curve is a function of the injection pressure drop where:

$$\Delta P_{inj} = PFSR - P_s \quad (66)$$

Any flash vaporization is evaluated from the fuel enthalpy chart assuming adiabatic injection, i.e.,  $\Delta H = 0$

$$H_1 = \text{fcn}(PFSR, TFSR) \quad (67)$$

$$H_2 = \text{fcn}(\% \text{ vaporized}, P_s) \quad (68)$$

The droplet vaporization and acceleration are evaluated by a small time step integration between the spraying and flameholder. The equations are:

$$\frac{dV_l}{dt} = \frac{3}{4} \frac{C_d}{d_l} \frac{\rho_a}{\rho_l} (V_a - V_l)^2 \quad (69)$$

for acceleration, and:

$$\dot{m}_{\text{vaporized}} = KA_s P_s \ln \left( \frac{P_s}{P_s - P_v} \right) \quad (70)$$

$$K = \frac{N_u D_v MW}{R d_l T_s} \quad (71)$$

$$N_u = 2 + 0.6 Re^{1/2} Pr^{1/3} \quad (72)$$

for vaporization.

The evaluation of the liquid temperature follows:

$$h_r = k N_u / d_l \quad (73)$$

$$\dot{q} = h_r A_s (T_s - T_l) \beta \quad (74)$$

$$\beta = \frac{z}{e^z - 1} \quad (75)$$

$$z = Cp_v \dot{m}_v / \pi k d_l N_u \quad (76)$$

$$\Delta \dot{q} = \dot{q} - \dot{m}_v \lambda \quad (77)$$

$$\frac{dT_l}{dt} = \frac{\Delta \dot{q}}{m_l Cp_l} \quad (78)$$

$$m_l = \rho_l \frac{4}{3} \pi \left( \frac{d_l}{2} \right)^3 \quad (79)$$

$$Re = \frac{\rho_a d_l (V_a - V_l)}{\mu_a} \quad (80)$$

This procedure is done for each size group until the flameholder is reached and the net fraction vaporized is evaluated.

$$\beta_1 = 1 - \left( \frac{\dot{m}_v}{\dot{m}_l} \right)_{\text{at F/H}} \quad (81)$$

The impingement of liquid fuel into the flameholder is evaluated by use of a term  $\beta_2$  where:

$$\beta_2 = \frac{\dot{m}_{lc}}{\dot{m}_l \cdot \Gamma} \quad (82)$$



This evaluates the percentage of the liquid fuel exposed to the flameholder which actually collects into its surface. The evaluation procedure is done for each size droplet group by a correlation of  $\beta_2$  vs. flameholder size, apex angle, flow velocity and droplet diameter. The correlation is based on evaluations performed by droplet trajectory analysis using the potential flow field aerodynamics. The total impingement flowrate is thus:

$$\beta_2 = \frac{1}{\dot{m}} \sum_{i=1}^i \dot{m}(i) \beta_2(i) \quad (83)$$

or:

$$\dot{m}_{t_c} = \beta_2 (1 - \beta_1) \Gamma \dot{m}_f \quad (84)$$

The liquid film vaporization rate is evaluated from the equations for the surface film vaporization caused by heat transfer from the flameholder wake. The surface is broken into ten elements and the vaporization and liquid temperature rise in each is calculated from:

$$\dot{m}_v = C_1 A_s P_s \ln \left( \frac{P_s}{P_s - P_v} \right) \quad (85)$$

$$C_1 = \frac{N_u D_v MW}{R \Delta x T_s} \quad (86)$$

$$N_u = 0.33 R_e^{0.5} P_r^{0.33} \quad (87)$$

$$P_v = \text{fcn}(T) \quad (88)$$

$$\dot{q} = \dot{m}_{t_c} C_p \Delta T_f + \lambda \left( \frac{N_u D_v MW}{R \Delta x T_s} \right) P_s A_s \ln \left( \frac{P_s}{P_s - P_v} \right) \quad (89)$$

$$\dot{q} = h_r A_s (T_w - T_{f/H}) \quad (90)$$

$$h_r = N_{u_w} \frac{k}{N} \quad (91)$$

$$N_{u_w} = 0.99 R_e^{0.5} P_r^{0.33} \quad (92)$$

The solution procedure for  $\beta_3$  breaks the flameholder surface into 10 equally spaced increments. The length of each is:

$$\Delta x = \frac{1}{10} \frac{N/2}{\sin(\alpha/2)} \quad (93)$$

The fuel collected by the surface is equally divided into the 10 elements on each face of the flameholder:

$$\dot{m}_c(i) = \frac{1}{20} \beta_2 (1 - \beta_1) \Gamma \dot{m}_f \quad (94)$$

Equations 29 to 36 are used for element  $i = 1$  on the surface with  $\dot{m}_f = \dot{m}_c(i)$  and the fuel temperature is assumed to be the same as the droplet liquid temperature at the flameholder. The fraction vaporized is calculated and the liquid temperature use evaluated. The procedure is repeated using fuel properties evaluated at:

$$T_l(i) = T_l(i)_o + \frac{1}{2} \Delta T_l(i) \quad (95)$$

This procedure continues until convergence, i.e.,  $\Delta T_l$  varies less than 1% between passes. Into the next element,  $i = 2$ , the flowrate is set equal to the unvaporized portion of the  $i = 1$  flow and the collection fraction per equation (94).

$$\dot{m}(2) = \dot{m}_c(2) + \dot{m}_c(1) - \dot{m}_v(1) \quad (96)$$

This flowrate initial temperature is set equal to the mass average of the exit temperature from  $i = 1$  and the droplet liquid collection temperature:

$$T_{li}(2) = \frac{\dot{m}_c(2) T_{lc} + [\dot{m}_c(1) - \dot{m}_v(1)] T_{li}(1)}{\dot{m}_c(2) + \dot{m}_c(1) - \dot{m}_v(1)} \quad (97)$$

The solution procedure is separated until all 10 segments are finished. The vaporized flowrate is the sum of all 10 in both sides of the flameholder:

$$\dot{m}_v = 2 \times \sum_{i=1}^{10} \dot{m}_v(i) \quad (98)$$

The fraction vaporized,  $\beta_3$ , is:

$$\beta_3 = \frac{\dot{m}_v}{\dot{m}_c} = \frac{\dot{m}_v}{(1 - \beta_1) \Gamma \beta_2 \dot{m}_r} \quad (99)$$

All of the vaporized fuel is assumed to enter the recirculation zone.

From these equations,  $\beta_3$  is a function of the wake temperature. The temperature is a function of the wake fuel-air ratio and recirculation rate. Since  $\beta_3$  strongly influences the wake fuel-air ratio, the solution for wake composition and efficiency becomes a curve intersection procedure.

First we define the recirculation and wake kinetics equations and then the solution procedure.

#### a. Recirculation

The wake recirculation flowrate coefficient is defined as:

$$K_1 = \dot{m}_r / \Gamma \dot{m}_a \quad (100)$$

$$\dot{m}_r = \rho_a V_a N K_1 \quad (101)$$

For mass transfer across the recirculation zone boundaries and a homogeneous wake:

$$\dot{m}_r = \frac{\rho_a V_a}{\tau} \quad (102)$$

The wake volume is evaluated as a function of blockage, apex angle, and flow Mach number from literature references as shown in the flameholder Final Report, AFAPL TR-81-. From this:

$$V_w = C_v (L/D)(B/D)N^2 \quad (103)$$

We set:

$$\tau' = \frac{\tau V_a}{N} \quad (104)$$

$$m_r = \frac{V_a}{N} \frac{\rho_a V_w}{\tau'} \quad (105)$$

Thus:

$$m_r = \frac{\rho_a V_a C_v (L/D)(B/D)N}{\tau'}$$

and

$$K_1 = C_v (L/D)(B/D)(\tau')^{-1} \quad (106)$$

By curve fits of  $L/D$ ,  $B/D$  and  $\tau'$  vs.  $\alpha$ ,  $N$ ,  $V_a$ , and  $T_a$ , we find the recirculation rate  $K_1$ .

#### b. Wake Reaction Kinetics

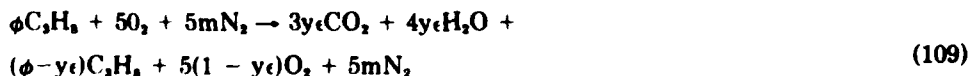
The wake reaction is assumed to be a single step, second order reactive controlled as follows:

$$\frac{dm}{dt} = \frac{k}{R^n} x_o^a x_r^{n-a} \frac{e^{-C/T}}{T^{n-0.5}} \quad (107)$$

For a well stirred reactor (wake is assumed to behave as one):

$$\frac{A}{V_o P^n} = \frac{k(m+1)}{R^n y_e} x_o^a x_r^{n-a} \frac{e^{-C/T}}{T^{n-0.5}} \quad (108)$$

For the assumed single-step reaction process postulated here, the reaction mass balance is (for propane fuel):



Also, a linear efficiency vs. temperature function is assumed:

$$T = T_a + \epsilon \Delta T_{ideal} \quad (110)$$

From these equations, the stirred reactor loading capability may be written as:

$$\frac{A}{V_o P^n} = \frac{k(m+1)[5(1-y_e)]^a [\phi - y_e]^{n-a} e^{-C/(T_1 + \epsilon \Delta T)}}{R^n y_e [5(m+1) + \phi + y_e]^n [T_1 + \epsilon \Delta T]^{n-0.5}} \quad (111)$$

Based on comparison of predicted results with available stirred reactor data, we use the following values for this reaction:

- n: for  $\phi < 1$ ,  $n = 2\phi$   
for  $\phi > 1$ ,  $n = 2/\phi$
- a:  $a = n/2$
- C:  $C = E/R$ , see Figure 33

This yields:

$$\frac{A}{V_o P_o^{2a}} = \frac{1.29 \times 10^{10} (m+1) [5(1-y\epsilon)]^a (\phi - y\epsilon)^a e^{-C/(T_1 + \epsilon \Delta T)}}{(0.08206)^{2a} y\epsilon [5(m+1) + \phi + y\epsilon]^{2a} [T_1 + \epsilon \Delta T]} \quad (112)$$

for lean mixtures.

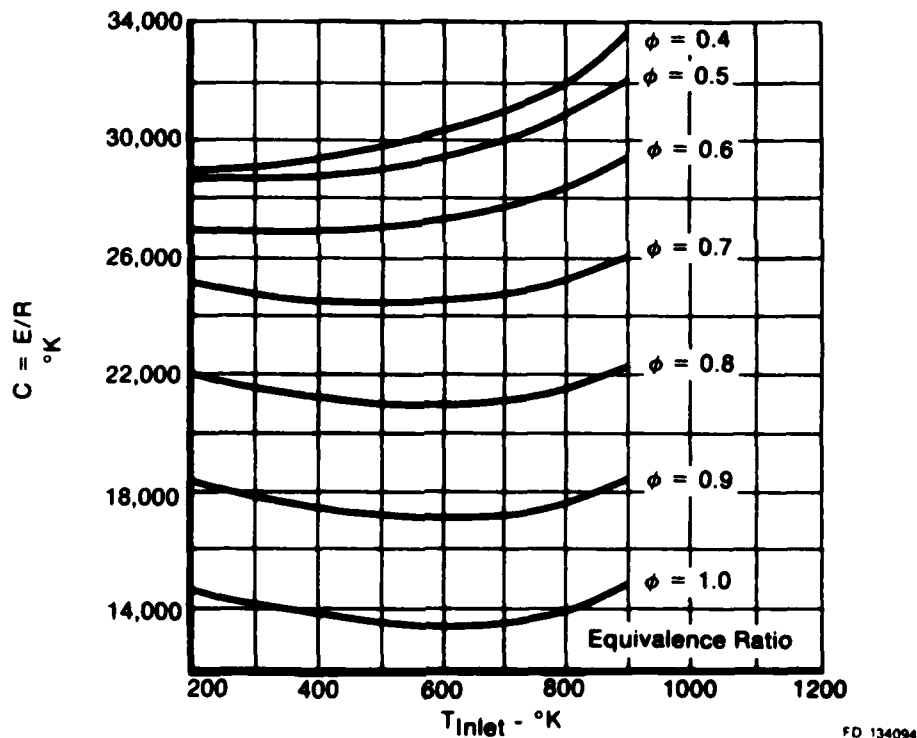


Figure 33. Variation in Activation Energy With Inlet Temperature and Equivalence Ratio

The kinetics solution proceeds by successive iteration between  $\epsilon = .999$  and  $0.70$  to find the wake efficiency where:

$$\frac{A}{V_o P_o^{2a}} = \frac{K_1 \Gamma m_a}{V_o P_o^{2a}} \quad (113)$$

at a given fuel-air ratio in the wake.

The solution procedure for the wake composition and reaction efficiency proceeds as follows:

- (1) The wake temperature is varied in steps from 1000° F to 5000° F and calculated at each wake.
- (2) The wake fuel-air ratio is varied from 0.02 to 0.20 and the wake temperature calculated at each fuel-air ratio.

The results of (1) are used in the wake fuel-air ratio equation:

$$FA)_{wake} = FA)_{total} \left\{ \beta_1 + (1 - \beta_1) \frac{\beta_2 \beta_3}{K_1} \right\} \quad (114)$$

This results in two curves, which define the wake fuel-air ratio vs. wake temperature and wake temperature vs. wake fuel-air ratio. A solution technique looks for the intersection of these curves, if it exists. This then defines the stable wake composition solution.

The fan duct gutter wakes may be supplied with hot gases from an external (to the wake) source such as a pilot region, see Figure 34. If this occurs, the external thermal source is assumed to effectively increase the inlet temperature of the recirculated air-fuel flowrate, i.e.,:

$$\dot{m}_r = K_1 \rho_a V_a \Gamma + \dot{m}_{ext} \quad (115)$$

$$T_a = \frac{T_a K_1 \rho_a V_a \Gamma + T_{ext} \dot{m}_{ext}}{\dot{m}_r} \quad (116)$$

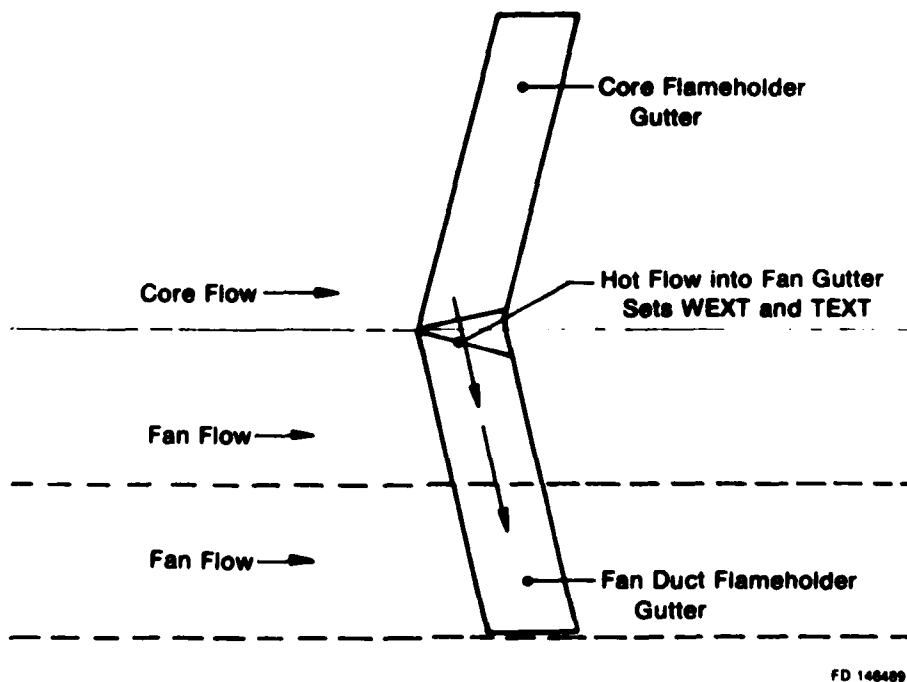


Figure 34. External Heat Addition to Fan Duct Gutters

The program then analyzes the behavior at these new conditions as if they were input.

After the wake has been analyzed, the turbulent flame penetration into the free-stream is analyzed.

The turbulent flame propagation into the unreacted free-stream is initiated in the shear layers of the wake. The model used relates the local turbulent flame speed to the local aerothermodynamic conditions and performs a finite difference integration of the flame front penetration starting in the wake and proceeding to the exhaust nozzle.

For the purposes of current analysis, the following assumptions were made:

- Uniform air flow profiles
- Uniform fuel-air ratio
- Incompressible acceleration of free air velocity by the flameholder blockage with no induced profile
- Known wake size and reaction efficiency
- Two-dimensional ducted flame.

The schematic of the situation which is analyzed is shown in Figure 35.

The approach flow, at known levels of pressure, temperature, velocity and fuel-air ratio, is accelerated by the blockage of the flameholder to velocity  $U$ , where:

$$U = \frac{V_a}{(1 - \Gamma)}$$

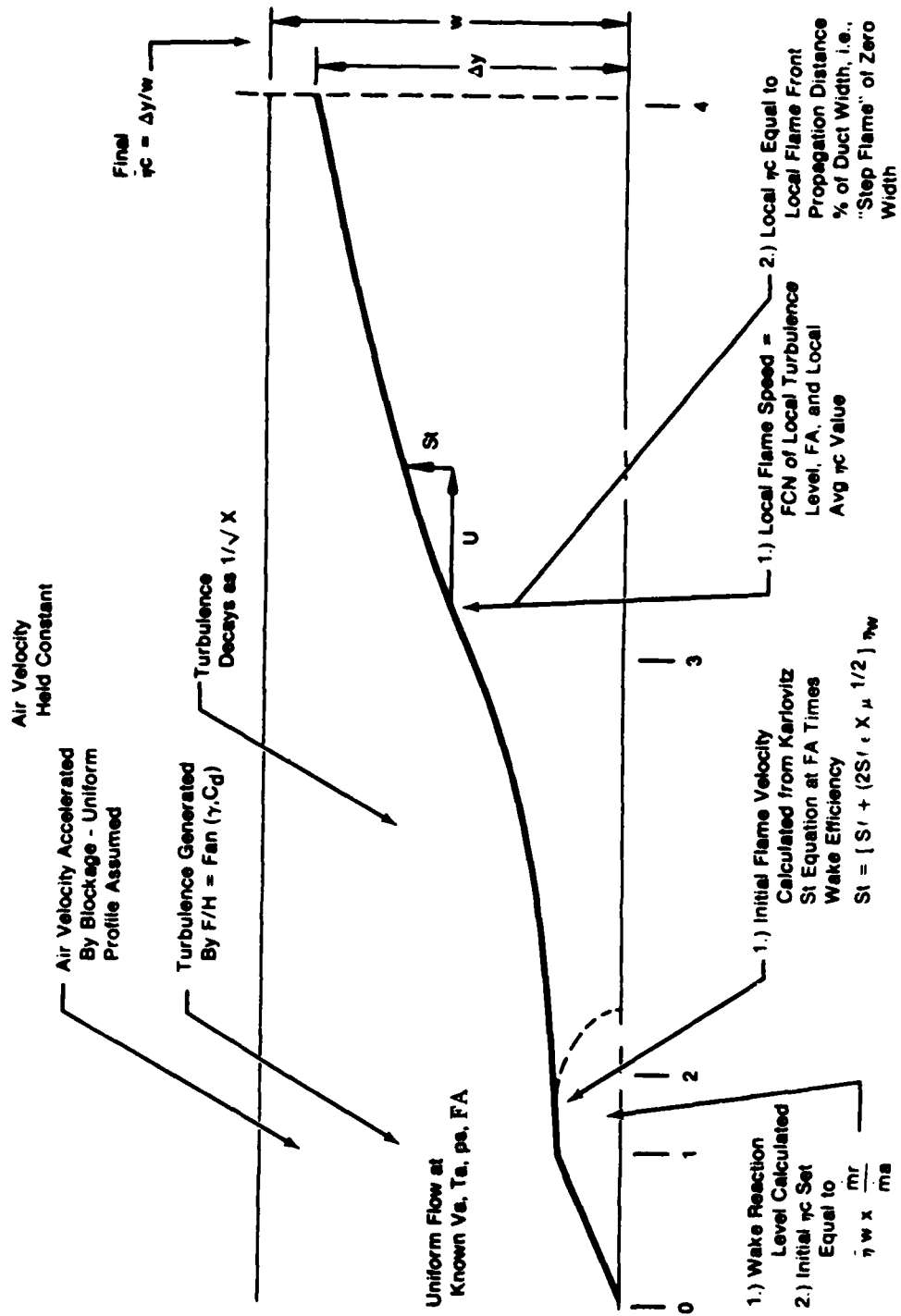
Where:

- $U$  = Velocity at flameholder tip
- $V_a$  = Approach velocity
- $\Gamma$  = Blockage ratio.

At this point, Station 1, an induced turbulence level is calculated from:

$$\epsilon_o = \left[ \left\{ C_d \Gamma + \left( \frac{\Gamma}{1 - \Gamma} \right)^2 \right\} \frac{1}{6} \right]^{1/2}$$

This equation relates the turbulence intensity,  $\epsilon_o$ , to the blockage ratio and the flameholder zero blockage drag coefficient,  $C_d$ .



FD 134097

Figure 35. Schematic of Flame Spreading Analysis

At this location, the turbulent flame velocity calculations are initiated. The equation used for the local flame speed is the Karlovitz equation:

$$St = St_l + (2u St_l)^n$$

Where:

$$\begin{aligned} St &\sim \text{Turbulent flame speed, ft/sec} \\ St_l &\sim \text{Laminar flame speed, ft/sec} \\ u &\sim \text{RMS turbulence velocity, ft/sec.} \end{aligned}$$

The value of  $u'$  is:

$$u' = \epsilon_o U \quad (117)$$

Additionally, the turbulent flame speed initial value is related to the degree of initiation of the flame speed initial value is related to the degree of initiation of the flame front by the wake by the following:

$$St' = St \times \eta_w \quad (118)$$

This generates an effective turbulent flame speed which completely fills the depth of the duct and propagates at the same transverse rate as the full flame speed which does not fill the duct. This arises from the fact that the inefficiencies of the wake reaction generate localized regions where flame front ignition does not occur. This use of a reduced value effective flame speed accounts for this in a two-dimensional model.

The initial value for the augmentor efficiency is the wake reaction level on a mass weighted basis, expressed as an equation this is:

$$\eta_{c_o} = \eta_w \frac{\dot{m}_r}{\dot{m}_a} \quad (119)$$

Where:

$$\begin{aligned} \eta_{c_o} &\sim \text{Initial efficiency} \\ \eta_w &\sim \text{Wake efficiency} \\ \dot{m}_r &\sim \text{Wake mass flowrate} \\ \dot{m}_a &\sim \text{Total duct flowrate.} \end{aligned}$$

The type of flame utilized in this model is a zero thickness flame which separates a region of unreacted propellants from a region of completely reacted products. From this setup, the average local augmentor efficiency is simply the ratio of the transverse flame penetration,  $\Delta y$ , to the duct width,  $w$ .

To be consistent, the transverse location of the flame front at the initial calculation station is taken to be:

$$\Delta y_o = \eta_{c_o} \cdot w \quad (120)$$



This value is assigned to the first axial station. This is assumed to occur halfway down the length of the recirculation zone. From visual observations of wake stabilized flames, this is the approximate location of transverse flame initiation.

From this location downstream to the exhaust nozzle, the flame front transverse location is calculated by a finite difference integration of the local flame speed. Several axial profiles are introduced as the integration proceeds. These are:

- (1) The turbulence intensity is decayed from the value generated at the aft flameholder lip at a rate inversely proportional to the square root of axial distance over an effective jet length. The final value is set at the initial turbulence level. The effective jet length is set at  $10 L/D$  where the  $D$  is the open area distance between adjacent flameholders.
- (2) The velocity of the unreacted fuel-air mixture is retained at the level generated at the flameholder lip. Measured profiles from several ducted flame test rigs support this assumption.
- (3) A term is introduced which relates the local flame speed to the local average duct combustion efficiency, peaking at 50%. This treats the counteracting influences of reduced heat loss as efficiency increases and reduces the free oxygen concentration. Local rates which roughly follow a sine wave function have been reported from duct data.

An additional term is added to account for the reduction in flame speed of a fuel spray compared to a premixed flame. This term relates the ratio of effective flame speed to premixed laminar flame speed. It accounts for the complicated interactions during flame spreading in an evaporating spray in a simplified manner. The effect of the liquid droplet diameter is shown in Figure 36. The droplet diameter utilized in the analysis will be the mean diameter as it exists at the flameholder trailing edge.

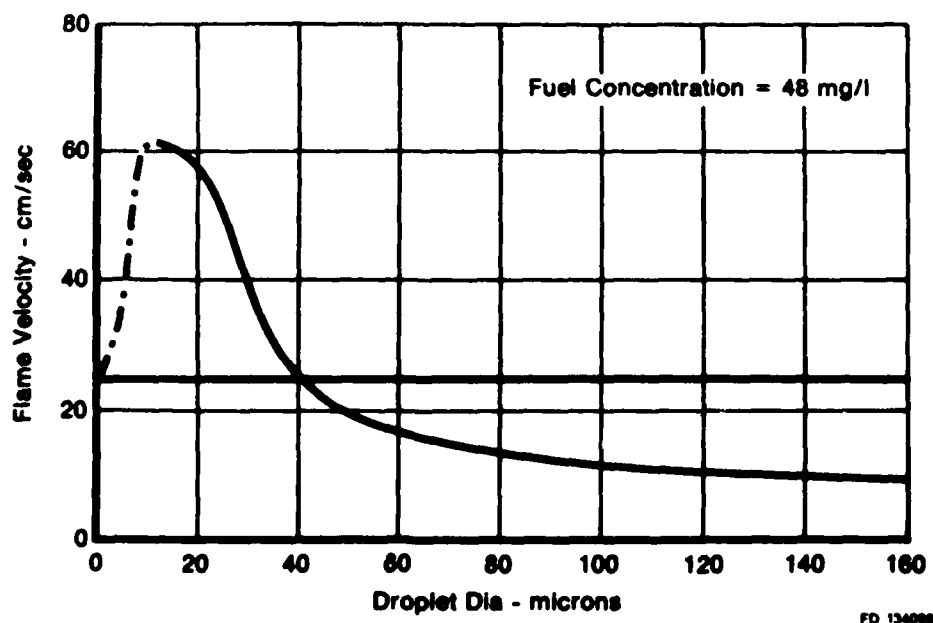


Figure 36. Flame Speed for Monodisperse Tetralin Spray

Analysis of the terms utilized for evaluation of the laminar flame speed term,  $S_L$ , has resulted in the following:

$$S_L = S_L(\phi) \left( \frac{T_a}{540} \right)^{1.5} \left( \frac{\chi_{O_2}}{0.21} \right)^2 \quad (121)$$

Where:

$S_L$  = laminar flame speed at 1 atm and 540°R

$\phi$  = equivalence ratio

$T_a$  = air temperature, °F

$\chi_{O_2}$  = oxygen mole fraction.

The influence of pressure is indeterminate at this time and has been incorporated as  $\sqrt{P_s}$  for subatmospheric data and no influence for pressures above 1 atmosphere.

The finite difference solution uses 1 in. increments in axial length as the stepping variable. This sets a time interval:

$$\Delta t = 0.0833/V. \quad (122)$$

The transverse flame penetration distance is thus:

$$\Delta y = St \Delta t = y(i+1) - y(i) \quad (123)$$

where  $St$  is evaluated at the conditions of  $x = x(i)$ .

The stepping procedure terminates when either:

(1)  $x(i+1) = \text{augmentor length}$

(2)  $y(i+1) = w$ .

The first defines  $\eta_c$  at the exhaust nozzle, the second defines 100%  $\eta_c$  before the nozzle. This defines one fan streamtube. The exit temperature is thus:

$$T_{ex}(i) = T_a(i) + \eta_c(i) \Delta T_1(i) \quad (124)$$

$$\Delta T_1(i) = \text{fcn}(T_a(i), FA(i)_{\text{effective}}).$$

This represents the actual combustion efficiency based on the true fuel-air ratio in the streamtube.

For multi-streamtube cases, the exit and inlet conditions are mass averaged using the general equation:

$$Z = \frac{\sum_{i=1}^n m(i) Z(i)}{\sum_{i=1}^n m(i)} \quad (125)$$

The average input fuel-air ratio and average inlet temperature combine to yield the average ideal temperature rise. The average inlet and exit temperatures yield the average actual temperature use. Thus:

$$\bar{\eta}_c = \frac{\Delta T_{\text{actual}}}{\Delta T_{\text{ideal}}} \quad (126)$$

This is the chemical efficiency. The thermal exit efficiency assumes that the augmentor liner cooling air flow is included in the average exit temperature:

$$T_{\text{exit}} = \frac{\sum_{i=1}^n \dot{m}(i) T_{\text{ex}}(i) + \dot{m}_{\text{cool}} T_a}{\sum_{i=1}^n \dot{m}(i) + \dot{m}_{\text{cool}}} \quad (127)$$

This reduces the average exit temperature and yields the lower value for thermal combustive efficiency. This value for  $\eta_c$  reflects the average exit temperature based on the average input fuel-air ratio and based on total fan duct air flow and fuel flow.

Before execution of the core streamtube analyses, the influence coefficients which are required are evaluated. These are of the form:

$$\frac{\partial \eta}{\partial A} \frac{\Delta}{\eta} = Z(\Delta) \quad (128)$$

Where:

$$A = V_a, p_a, T_a, \text{ and } FA.$$

They are calculated from a 1% change in the variables and the linear form:

$$\frac{\Delta \eta}{\Delta A} \frac{\bar{A}}{\bar{\eta}} = \frac{\eta_2 - \eta_1}{A_2 - A_1} \cdot \frac{(A_1 + A_2)}{(\eta_1 + \eta_2)} \quad (129)$$

Where:

$$A_2 = 1.01 A_1. \quad (130)$$

The value of  $\eta_2$  is obtained by execution of the analysis at all the same input as  $\eta_1$ , except  $A_1$  is replaced with  $A_2$ . Thus, the analysis is done once for base and four more times for the Z factors.

## 2. DEVELOPMENT OF THE CORE STREAM COMBUSTION EQUATIONS

The same basic analysis procedure as accomplished in the duct is used in the core with several major operational differences:

- a. There is no cooling air removal from the core streamtubes. Thus, the input fuel-air ratios are used in the analysis.
- b. The droplet vaporization rate is so rapid that the fuel exists only as a vapor after a couple of inches from the spraybar. This removes the requirement to solve for the wake compositive since it is the same as the input fuel-air ratio.
- c. The wake reaction efficiency is solved directly at the input fuel-air ratio and recirculation rates which are calculated the same as the fan duct.
- d. There is no droplet size effect in the turbulent flame speed model. The rapid droplet vaporization results in gaseous phase turbulent flame penetration.

The solution for a core streamtube proceeds as follows:

- (1) The set-up equations are the same as the fan streamtubes.
- (2) The recirculation coefficient,  $K_1$ , is calculated the same way as done in the fan stream. This generates the value of  $A/V_o P^2$  required for the kinetics solution.
- (3) The wake reaction kinetics solution is performed at the same value of fuel-air ratio as input for the streamtube.
- (4) The turbulent flame penetration solution is the same as for the fan stream except that the droplet correction term is absent. The equation introduces a value for the oxygen concentration,  $x_{O_2}$ .

This value is less than the fan duct due to the removal of oxygen by the mainburner combustion process. This vitiation yields:

$$x_{O_2} = 0.21 \frac{(FA)_{mB}}{(FA)_{stoch}} \quad (131)$$

The analysis produces a value of  $\eta_c$  for each streamtube,  $i$ , by the same equation as used in the fan:

$$\eta_c(i) = \frac{Y(i)}{w(i)} \quad (132)$$

where  $Y(i)$  is the penetration distance transverse to the flow and  $w(i)$  is the streamtube width.

The exit temperature calculation is different from the fan duct due to the vitiation of the approach air flow and the temperature removal in the turbine between the main combustor and the augmentor inlet.

The ideal temperature rise for each streamtube is evaluated by generating a fictitious main combustor inlet temperature. The procedure is as follows:

- (1) For known main burner FA and streamtube inlet temperature,  $T_a(i)$ , a fictitious  $\Delta T$  is read from a curve as in Figure 37.

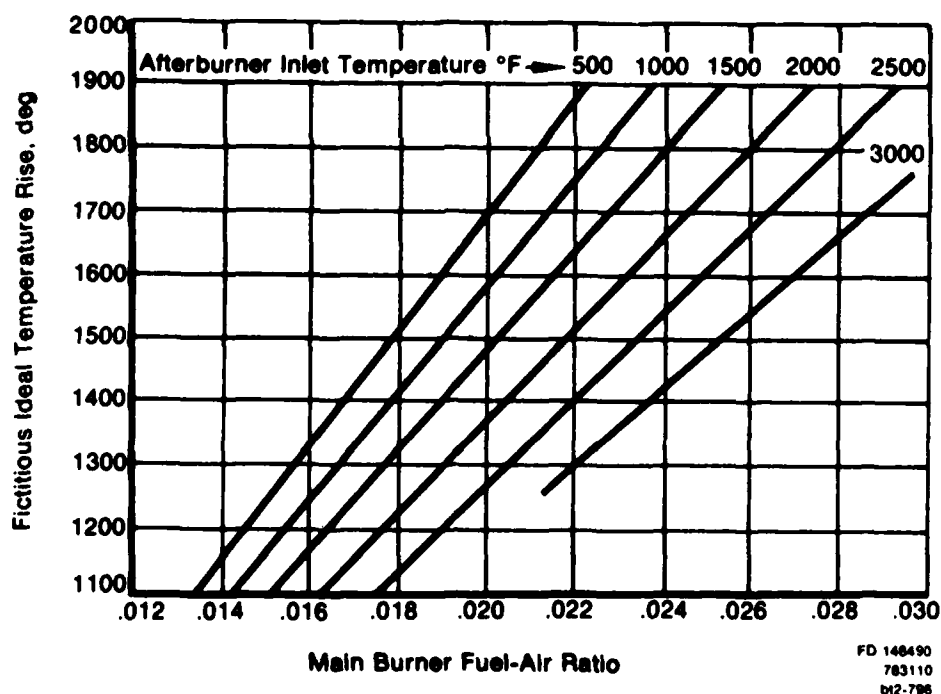


Figure 37. Fictitious Temperature Rise vs Main Burner Fuel-Air Ratio

(2) A fictitious main burner inlet temperature is calculated:

$$T_{mB}(i) = T_a(i) - \Delta T_{fict}(i) \quad (133)$$

(3) An overall fuel-air ratio is calculated:

$$FA_{oa}(i) = FA_{mB} + FA(i) \quad (134)$$

(4) With  $FA = (FA)_{oa}(i)$  and  $T = T_{mB}(i)$ , the overall effective temperature rise is read from the ideal temperature rise curve.

(5) The streamtube exit temperature is:

$$T_{ex}(i) = \Delta T_i(i) + T_{mB}(i) \quad (135)$$

(6) The streamtube net ideal temperature rise is thus:

$$\Delta T_i(i) = T_{ex}(i) - T_a(i) \quad (136)$$

This value is calculated for each streamtube and used exactly as the ideal  $\Delta T$  curve is used in the fan streams. The streamtube exit temperature is:

$$T_{ex \text{ actual}}(i) = T_a(i) + \eta_c \Delta T_i(i) \quad (137)$$

The inlet temperatures and fuel-air ratios are mass averaged as is the exit temperature, using equation (125).

The overall core efficiency is calculated from steps (1) to (6) using average inlet conditions to yield the average ideal  $\Delta T$  and equations (137) and (125) for the average exit temperature:

$$\bar{\Delta T}_{actual} = T_{exit} - T_a \quad (138)$$

$$\bar{\eta}_c = \frac{\bar{\Delta T}_{actual}}{\bar{\Delta T}_i} \quad (139)$$

The influence coefficients are shown in equations (128) to (132) are evaluated as was done in the fan.

